The role of extracellular histones in critical illness and their application in acute pancreatitis

Thesis submitted in accordance with the requirements of the University of Liverpool for the degree of Doctor of Philosophy

By

Tingting Liu

April, 2017

UNIVERSITY OF LIVERPOOL

Abstract

Histones are basic nuclear proteins that bind to genomic DNA. There are five subclasses: core histones H2A, H2B, H3 and H4, and linker histone H1. Release of extracellular histones has been shown in a range of critical illness animal models and human patients including sepsis and acute pancreatitis. Extracellular histones act as damage-associated molecular pattern molecules (DAMPs) on parenchymal epithelial and endothelial cells, cardiomyocytes, immune cells (neutrophils, monocytes, macrophages, dendritic cells and lymphocytes) and platelets to activate Toll-like receptors (TLRs; TLR2 and TLR4) and/or NLR Family Pyrin Domain Containing 3 (NLPR3) inflammasome as well as induce calcium influx, proinflammatory cytokine production, thrombin generation and cell death. Anti-histone strategies such as anti-histone antibodies or pharmacological neutralisers alleviate histone-induced toxicity.

To progress the translational relevance of histones in circulation, this thesis explores the development of xMAP technology based assay for measuring relevant toxic histones and also the significance of histone determination in animal models and patients with acute pancreatitis.

Truncated histones were generated by recombinant DNA technology and the purity was 75.6-95.1%, except for histone H2A C-terminal (35.5%). Anti-histone single chain variable fragment (ahscFv) was also generated (purity > 95%) and shown to bind to histone subclasses by Western blot and IAsys resonant biosensor. Fluorescein isothiocyanate (FITC)-full length and FITC-truncated histones (H1.1 C-, H2A N-, H3.1 N-terminal) bound to the cell membrane and induced calcium influx in EA.hy926 cells, while other truncated histones did not. ahscFv significantly prevented histone-induced cell death. To measure all toxic histones in one assay, Luminex xMAP multiplex technology was developed. Standard curves of both singleplex and multiplex assays were developed and used to measure the levels of circulating histones in plasma of patients with severe trauma, sepsis and pancreatitis. However, the recovery ratio in spiked plasma was low and the assay failed to detect histones in patient plasma which were detectable by Western blot.

Release of circulating histones were investigated in mice with acute pancreatitis induced by either 4 or 12 injection of caerulein (50 µg/kg/h; CER-AP) or by infusion of pancreatic duct with sodium taurocholate (3.5%, 1 ml/kg; NaTC-AP). Four and 12 injections of caerulein resulted in oedematous and necrotising CER-AP, respectively, with marked systemic inflammation and multiple organ injury observed in the necrotising CER-AP. NaTC-AP caused more diffuse pancreatic necrosis, systemic inflammation and multiple organ injury. Circulating histones, as measured by Western blots, were elevated early with further increases in necrotising CER-AP (peak > 100 µg/ml) and NaTC-AP (peak > 140 µg/ml) as disease progressed but not in oedematous CER-AP which were comparable to saline controls. The levels of circulating histones were significantly associated with pancreatic necrosis and multiple organ injury parameters.

Circulating histones were then measured from healthy volunteers and a consecutive cohort of acute pancreatitis patients admitted to Royal Liverpool University Hospital (RLUH) within 48 h of disease onset. The predictive values of circulating histones for persistent organ failure (POF), major infection and mortality were compared with

biochemical markers and clinical scores. A total of 236 patients (mild 156, moderate 57, severe 23 as per Revised Atlanta Classification) and 47 heathy volunteers were included. The median histone level in severe acute pancreatitis was 18.8 μg/ml (interquartile range: 5.9-33.8), significantly higher than mild 1.1 μg/ml (0.6-2.1) or moderate 1.3 μg/ml (0.5-2.8) category which was comparable with heathy volunteers 1.0 μg/ml (0.5-1.6). The area under the receiver-operating characteristic (AUC) curve of histones for predicting POF and mortality was 0.92 (95% confidence interval [CI]: 0.85-0.99) and 0.96 (0.92-1.00) respectively, which was as or more accurate than tested biomarkers or clinical scores. For infected pancreatic necrosis and/or sepsis, the AUC of histones was 0.78 (0.62-0.94). Histones did not predict or correlate with local pancreatic complications and transient organ failure, but negatively correlated with leucocyte cell viability (r = -0.511, P < 0.01).

A study of consecutive acute pancreatitis patients with primary admission to RLUH (n = 260, blood sampling < 24 h) or referred (n = 52) from other hospitals and healthy controls (n = 47) were recruited. Referred patients had POF > 48 h (blood sampling < 24 h of admission to ICU of the RLUH then daily for one week) within 3 weeks of disease onset. Histones, cytokines and routine biochemical markers were measured. Multivariable analyses determined associations between circulating histone levels and variables. There were 235 patients in Group 1 (no POF), 25 in Group 2 (POF < 24 h) and 52 in Group 3 (POF > 48 h). Circulating histones were significantly correlated with tested proinflammatory cytokines, clinical severity scores and individual organ injury parameters. Circulating histones were significantly more elevated in Group 3 compared to Group 2 but both were higher than in Group 1 or healthy volunteers. Multivariable analyses revealed that it was POF, but not pancreatic necrosis or other variables that most significantly associated with elevated circulating histones (odds ratio: 98.1, 95% CI: 14.4-669.0, P < 0.001).

Acknowledgment

I wholeheartedly thank my primary supervisor Professor Cheng-Hock Toh for his excellent supervision and help through my PhD. Specific thanks are given to my secondary supervisor Dr Guozheng Wang who has been supervising me on a daily basis, taught various useful techniques in molecular biology. I appreciate that Dr Ingeborg Welters, my third supervisor, who has trained me for creating clinical database. Without the close supervisions from my 3 supervisors my PhD project would not have been possible.

I wish to give my sincere thanks to Dr Simon T. Abrams who taught me a range of good laboratory and presentation skills, and without whom my NIHR BRC Fellowship would not been possible. I wish to thank Drs Yasir Alhamdi and Dunhao Su for their daily support and comfortable way of discussing science.

I would like to thank Dr Adam Lightfoot for providing me training on luminex xMAP and Mr Zhengxing Cheng for providing me *in vivo* samples of acute pancreatitis.

Great thanks to Dr Wei Huang, Mr Peter Szatmary and Professor Robert Sutton for their strong support on clinical acute pancreatitis. I would also thank all the members from the NIHR Liverpool Pancreas Biomedical Research Unit for their hospitality.

I would like to acknowledge the financial support from my NIHR BRC Fellowship.

Finally many thanks to my parents, husband and daughter, without their support I would not have finalised my thesis in time.

Abbreviations

ACD	accidental cell death
ACS	abdominal compartment syndrome
ahscFv	anti-histone single chain variable fragment
ALT	alanine transaminase
ANOVA	analysis of variance
APACHE II	Acute Physiology and Chronic Health Examination II
APC	activated protein C
APFC	acute peripancreatic fluid collection
aPTT	activated partial thromboplastin time
ARDS	acute respiratory distress syndrome
AUC	area under curve
BISAP	Bedside Index for Severity in Acute Pancreatitis
BUN	blood urea nitrogen
C1INH	C1 esterase inhibitor
CDRs	complementarity-determining regions
CECT	enhanced computerised tomography
CER	caerulein
CER-AP	caerulein-induced acute pancreatitis
CGD	chronic granulomatous disease
CI	confidence intervals
CRP	C-reactive protein
cscFv	control single chain variable fragment
CT	computerised tomographic
DAMPs	damage-associated molecular patterns
DIC	disseminated intravascular coagulation
DMEM	Dulbecco's Modified Eagle's Medium
DPI	diphenylene iodonium
EDTA	ethylenediaminetetraacetic acid
ELISA	enzyme-linked immunosorbent assay
ESPEN	European Society for Clinical Nutrition and Metabolism
FI	fluorescence intensities
FITC	fluorescein isothiocyanate
GCLP	Good Clinical Laboratory Practice
GCS	Glasgow Coma Scale
H&E	hematoxylin and eosin
HMGB1	high mobility group box protein 1
IAP	intra-abdominal pressure
ICU	Intensive Care Unit
IL	interleukin
IL-1Ra	IL-1 receptor antagonist
IPTG	isopropyl β-D-1-thiogalactopyranoside
IQR	interquartile range
ISTH	International Society on Thrombosis and Haemostasis
JAAM	Japanese Association for Acute Medicine
JMHW	Japanese Ministry of Health and Welfare
LB	Luria-Bertani
MCP-1	monocyte chemoattractant protein-1

MCTSI	worst modified CT severity index
MFI	mean FI
MODS	multiple organ dysfunction syndrome
MPT-RN	mitochondrial permeability transition-medicated regulated necrosis
NADPH	nicotinamide adenine dinucleotide phosphate
NaTC	sodium taurocholate
NaTC-AP	sodium taurocholate-induced acute pancreatitis
NCCD	Nomenclature Committee on Cell Death
NETs	neutrophil extracellular traps
Ni-NTA	Nikeli-Nitrilotriacetic acid
NLPR3	NLR Family Pyrin Domain Containing 3
NLR	negative likelihood ratio
NPV	negative predictive value
OR	odds ratio
PAMPs	pathogen-associated molecular patterns
PaO_2/FiO_2	partial pressure arterial oxygen and fraction of inspired oxygen
PCD	programmed cell death
PCR	polymerase chain reaction
PE	phycoerythrin
PEEP	positive end expiratory pressure
PI	propidium iodide
PLR	positive likelihood ratio
PMA	phorbol myristate acetate
PMT	photomultiplier tubes
POF	persistent organ failure
PPACK	d-phenylalanyl-l-prolyl-l-arginyl chloromethylketone
PPV	positive predictive value
PRRs	pathogen recognition receptors
PT	prothrombin time
PVDF	polyvinylidene difluoride
RAC	Revised Atlanta Classification
RCD	regulated cell death
RLUH	Royal Liverpool University Hospital
ROC	receiver operating characteristics
ROS	reactive oxygen species
SDS-PAGE	sodium dodecyl sulfate polyacrylamide gel electrophoresis
SEM	standard errors of means
SIRS	systemic inflammatory response syndrome
SOFA	Sequential Organ Failure Assessment
SOPs	standard operating procedures
TLRs	Toll-like receptors
TNF	tumour necrosis factor
VDAC	voltage dependent anion-selective
WBC	white blood cells
WSACS	World Society of the Abdominal Compartment Syndrome

Table of contents

Chapter 1– General introduction

1.1 General introduction of critical illness

1.1.1 Burdens of critical illness

Critical illness is a condition describing patients with acute organ failure (e.g. sepsis, septic shock, severe acute pancreatitis, drug-induced liver failure, etc.), undergoing major surgical procedures, severe traumatic injuries, and end-stage life support who need admission to Intensive Care Unit (ICU)[1]. Critical illness is the predominant factor of deaths in adults and affects > 20 million world population annually, causing dramatic economic and social burdens[1]. Moreover, patients who survived from critical illness usually have significantly impaired quality of life as compared with general population[2, 3], and post-hospitalisation complications further increase expenses. In the USA, the direct critical care costs are approximately $3500 per each day (up to $263 billion annually) which accounts for 13-39% of total hospital costs[4, 5]. This figure represents up to 11.2% of total USA healthcare expenditure[5]. In the UK, the NHS report reveals that a Level 2 High Dependency bed costs £857 and a Level 3 Intensive Care bed costs £1932 per day[6], and the average ICU stay is 5.7 days with a mortality rate of 32.4%[7].

The management of critically ill patients usually include treatment for aetiology factors, fluid resuscitation[8, 9], anaesthesia[10], pain relief[11], nutritional support[12], antibiotics[10], and appropriate organ support and monitoring[1]. Despite the improvement of organ support modalities, the overall mortality of critically ill patients remains about 25% due to multiple organ dysfunction syndrome (MODS)[13] and the mortality rate reaches 40%-100% when ≥ 3 affected organs fail[14]. Therefore, understanding the pathogenesis and effective targeting MODS/organ failure are fundamental for breakthroughs in critical illness.

1.1.2 Organ or system dysfunction/failure

The most leading cause for critical illness and ICU admission is sepsis[15], a condition defined as life-threatening organ dysfunction/failure caused by a dysregulated host response to infection[16]. However, there are substantial amounts of patients also admitted to ICU due to acute organ failure induced by sterile inflammation from diseases such as severe acute pancreatitis[17-19] and drug-induced liver failure[20, 21]. Regardless of aetiology and risk factors, these initial sterile local inflammations can cause systemic inflammation and sequential failure of distant organs without pre-existing advanced comorbidities. The affected organs/systems include pulmonary, cardiovascular, renal, haematological, central nervous as well as liver and gut.

1.1.2.1 Acute respiratory distress syndrome (ARDS)

ARDS is one of the most common reasons for ICU admission[22]. In 1967, Ashbaugh *et al.*[23] first introduced this syndrome manifesting as cyanosis refractory to oxygen therapy, reduced lung compliance, diffuse infiltration changes on the chest X-ray. Since then, over the last 50 years the definition alterations were suggested in 1988[24], 1994[25], 2005[26] and 2012[27] (also reviewed in ref[22]). The newly proposed Berlin definition[27] categories ARDS into 3 classes according to partial pressure arterial oxygen and fraction of inspired oxygen (PaO_2/FiO_2, mmHg) on a basis of positive end expiratory pressure (PEEP, minimum 5 cmH_2O): mild, PaO_2/FiO_2 200-300; moderate, PaO_2/FiO_2, 100-199; severe, $PaO_2/FiO_2 < 100$. In a study[28] of 127 ARDS secondary to acute pancreatitis, the mortality rates of mild, moderate and severe ARDS were 0%, 9.4% and 15.8%, respectively. The most recent multicentre study[29] demonstrates that the period prevalence of ARDS is 10.4% (3022/29144) in the ICU, with mortality of mild, moderate and severe is 34.9%, 40.3% and 46.1%, respectively. Current treatment for ARDS includes ventilation (non-invasive[30, 31] and mechanical[22, 29]), fluid balance

restoration, neuromuscular blockade, prone positioning and referral to extracorporeal membrane oxygenation centre depends on individual condition[22].

1.1.2.2 Circulatory shock

Circulatory shock, or failure, is featured as systematic inadequate cellular oxygen supply caused by hypotension and hypoperfusion typically with hyperlactatemia, a sign of abnormal cellular oxygen metabolism[32]. It affects about 1/3 patients in the ICU[33] and sepsis-induced acute circulatory failure remains more than half of the cases[34]; hypovolaemia and cardiogenic factors are also common and are not mutually exclusive[32].

Circulatory shock is clinically diagnosed either by lack of fluid response or acidaemia on the basis of hypotension (systolic blood pressure < 90 mmHg, mean blood pressure < 70 mmHg, or need for vasoactive agents)[32]. It is distinctly different from acute decompensated heart failure which normally has advanced pre-existing comorbidities such as atrial fibrillation, coronary artery diseases, myocardial infarction and chronic pulmonary diseases[35]. However, myocardial injury as evidenced by elevated cardiac troponin (both I and T isoforms) levels can occur in both circulatory injury[36, 37] and heart failure[35]. The initial treatment of circulatory shock is fluid resuscitation[32, 38-40]. Recently, early goal-directed fluid resuscitation has not been shown to be superior to conventional protocol in 3 multicentre randomised, controlled trials in septic patients[38-40]. However, the role of early-goal directed fluid resuscitation remains controversial in severe acute pancreatitis, better designed trials are warranted to address the type of fluid, the rate of administration, and how fluid therapy should be guided[41]. When fluid resuscitation fails to restore hypoperfusion, vasoactive agents are needed[32, 42-44].

1.1.2.3 Acute renal failure

Acute renal failure and its less severe form, acute renal injury, are characterised by rapid loss of renal function, resulting in an impaired ability to excrete metabolic waste (increased nitrogen products and/or decreased urine output) and maintain fluid and electrodes balance[45, 46]. This accounts for substantial amount of ICU admissions as a primary reason[47-49] or develops as one of the secondary complications. Pre-existing chronic kidney diseases are most dominate risk factors for developing of acute renal failure[50]. Acute renal failure is classified as prerenal (e.g. hypovolaemia or hypotension), intrinsic renal (typically acute tubular necrosis) and postrenal (obstructive) categories according to the causing factors[51]. It is diagnosed by a combination of disease history, clinical presentations, physical examinations, blood nitrogen/creatinine ratio, urinalysis (sediment, protein, sodium and osmolality)[45, 46, 51]. According to different aetiologies and risk factors, the treatment of acute renal failure is composed of non-dialysis (volume expansion, use of diuretics and dopamine, N-acetylcysteine and calcium-channel blockers), supportive (correction of hyperkalaemia, sodium retention, hyperglycaemia, acidosis, provision of nutritional support and control of infection) and renal replacement therapy[51]. A continuous strategy is not superior to intermittent haemodialysis[52, 53] and neither early is better than the delayed approach[54].

1.1.2.4 Acute liver failure

Acute liver failure is characterised by a sudden onset of altered mental status and development of coagulopathy due to severe injury of hepatocytes or extensive necrosis[55, 56], typically without pre-existing end stage liver diseases[57]. It is an uncommon but not rare cause for ICU admission, resulting in high short-term morbidity and mortality[58, 59].

In the developed countries, the most common aetiology for acute liver failure is drug-induced, e.g. acetaminophen accounts for > 57% acute liver failure in the UK annually[58]; while in the developing countries virus-induced prevails[58, 59]. Depending on weeks from jaundice to encephalopathy, there are three most noticeable systems to classify acute liver failure. The O'Grady system classifies acute liver injury to hyperacute (0-1 week), acute (1-4 weeks) and subacute (4-12 weeks) and the survival rate without emergency liver transplantation is good, moderate and poor, respectively[58]. The Bernuau system divides acute liver failure into fulminant (0-2 weeks) and subfulminant (2-12 weeks) subtypes[59]. The Japanese system dissects the disease into fulminant (0-8 weeks) and late-onset (> 8 week) stages, and the fulminant stage is further separated into acute (0-10 days) and subacute (10 days-8 weeks) subclasses. The management of acute liver failure is challenging which requires multidisciplinary approach to deal with MODS and arrange liver transplantations in selected cases[59].

1.1.2.5 Haemostatic dysfunction

Coagulation abnormalities are frequently observed in critically ill patients[60]. It is caused by the loss of haemostasis between coagulation and the fibrinolytic system and manifests as thrombocytopenia (platelet count < 150 $\times 10^9$/L), prolonged global clotting times [prothrombin time (PT), activated partial thromboplastin time (aPPT)], reduced levels of coagulation inhibitors (antithrombin III, protein C, and protein S), or increased levels of fibrin degradation products (D-dimer and soluble fibrin monomer)[61]. The most common aetiology factor of thrombocytopenia is sepsis which accounts for 52% of cases, followed by disseminated intravascular coagulation (DIC), drug-induced, trauma and others[60]. DIC represents the most severe form of coagulopathy and is characterised by the widespread activation of coagulation proteases which result in endothelial dysfunction, intravascular fibrin formation, thrombotic occlusion, and eventually organ

failure[61-64]. Deranged coagulation status has also been evidenced in acute pancreatitis and is related to its severity[65-67]. DIC secondary to acute pancreatitis is reported in case studies[68-71] and is associated extremely high mortality.

Apart from risk factors, clinical presentations, physical examinations, the diagnosis of DIC involves laboratory analysing a plethora of coagulative and anti-coagulative related parameters including the platelet count, PT, aPTT, antithrombin, protein C, D-dimer and increasing extracellular DNA and DNA-binding proteins such as histones[64, 72]. In 1983, the Japanese Ministry of Health and Welfare (JMHW) proposed a graded scoring criteria for diagnosis of DIC[73]. The JMHW DIC criteria include SIRS components, platelet counts, PT, aPTT, fibrinogen, fibrin/fibrinogen degradation products with five points or more for the establishment of DIC. In 2006, these criteria have been revised subsequently by the Japanese Association for Acute Medicine (JAAM) by removing fibrinogen components from the JMHW criteria after a multicentre study[74]. Basic on a similar concept, the International Society on Thrombosis and Haemostasis (ISTH) introduced a novel scoring criteria for DIC[75]. The ISTH criteria include points for each components including platelet counts, increased fibrin marker levels and fibrinogen level, a score of ≥ 5 indicates overt DIC while < 5 is suggestive non-overt DIC. Compared with the JAAM criteria, the ISTH criteria abandon the Systemic Inflammatory Response Syndrome (SIRS) score element which is considered to be non-specific for DIC and therefore are more stringent to diagnose DIC[64]. Not surprisingly, the mortality rate of DIC is doubled using the ISTH criteria when compared to the JAAM criteria (46% *versus* 22%)[76, 77]. The ISTH recommends that current management of DIC should include removal of aetiological factors, using prothrombin complex concentrate and anticoagulants (unfractionated heparin or low-molecular-weight

heparin for thrombotic phenotype), and initiating antifibrinolytic treatment when appropriate[64, 78, 79].

1.1.2.6 Neurological dysfunction

Mental disorders, displaying as coma or impaired consciousness, can be caused directly by trauma, vascular and infective lesion of the brain, or indirectly by metabolic catastrophes such as organ failure(s), hypoglycaemia, diabetic ketosis, and drug intoxication[80]. There was lack of methodology to standardise assessing coma and impaired consciousness in traumatic head injury historically until the introduction of Glasgow Coma Scale (GCS) by Teasdale and Jennett in 1974[81]. The GCS includes detailed measurement of motor responses, verbal responses and eye opening. Since its first introduction, it has been widely applied in daily clinical practice and research in the neurological or ICU settings over more than last 40 years[82]. However, recent studies show that scoring agreement between observers is only 32%[83] or the diagnostic error rate of GCS is around 10%[84]. Some researchers raised concerns that the GCS does not incorporate brain reflexes, clinical signs of bad prognosis, or to measure verbal component in incubated patients and therefore it needs critical reappraisal again[85].

1.1.2.7 Gut dysfunction and abdominal compartment syndrome (ACS)

Due to lack of generalised biochemical markers, gut dysfunction has been overlooked in the settings of critical care. In critical illness, the most common type of gut dysfunction is acute intestinal failure. Over the last 25 years, the definitions of intestinal failure have been changing constantly. Recently, The European Society for Clinical Nutrition and Metabolism (ESPEN)[86] has defined acute intestine failure as type II functional classification: “prolonged acute condition, often in metabolically unstable patients, requiring complex multidisciplinary care and intravenous supplementation over periods of weeks or months”. ACS is diagnosed as intra-abdominal pressure (IAP)

> 20 mmHg with or without an abdominal perfusion pressure < 60 mmHg that is associated with new organ dysfunction/failure by World Society of the Abdominal Compartment Syndrome (WSACS)[87]. Prevention of excessive fluid resuscitation, monitoring IAP, analgesia, correct body positioning, evacuation of intra-luminal contents by gastroprokinetics, coloprokinetics, and enemas are critical factors[88]. If all these fail, then surgical decompression will be the last resort to treat ACS[88, 89].

1.1.3 Organ failure scores

MODS, or organ failure(s), was systematically described and the severity of each organ failure was graded in 1990s. In 1995, Marshall et al.[90] first reported a MODS score that is composed by 6 items including: respiratory (PaO_2/FiO_2 ratio), cardiovascular (heart rate and the ratio of central venous pressure to mean arterial pressure), renal (serum creatinine level), hepatic (serum bilirubin level), haematological (platelet count) and central nervous (GCS). Each system scores 0-4 depends on the respectively cut-off values. The same group then used hypotension and acidaemia to replace the original definition of cardiovascular dysfunction in the new scoring system (Brussels score). Based on similar idea, in 1996, Le Gall *et al.*[91] proposed and validated a Logistic Organ Dysfunction System score to assess organ dysfunction status on the day of ICU admission. In the same year, Vincent *et al.*[92] proposed a Sepsis-related Organ Failure Assessment (SOFA) score aiming to dynamically minor organ failure severity in the ICU settings. This score is fundamentally similar to the Marshall and Brussels scores, but several changes have been made: hypotension and acidaemia are replaced by use of inotropes to define cardiovascular dysfunction; respiratory support is also added to indicate respiratory dysfunction; oliguria is further supplemented to determine renal dysfunction. As the SOFA score is not specific to only sepsis but can represent whole

range of critical illnesses with organ failure, it is thereafter also called Sequential Organ Failure Assessment (SOFA) score (Table 1.1). In 1998, the SOFA score was validated in a multicentre study, showing that SOFA score was significantly higher in more severe organ failure and was strongly associated with mortality[93]. Since then, the SOFA score has been extensively employed by the ICU settings for daily evaluating severity and estimating prognosis[94-96].

Table 1.1 The Sequential Organ Failure Assessment (SOFA) score

	SOFA score				
Varibles	**0**	**1**	**2**	**3**	**4**
Respiratory (PaO_2/FiO_2 mmHg)	> 400	≤ 400	≤ 300	≤ 200*	≤ 100*
Cardiovascular (hypotension)	No hypotension	MAP < 70 mmHg	Dop ≤ 5 or dob (any dose)†	Dop > 5, epi ≤ 0.1, or nore ≤ 0.1†	Dop > 15, epi > 0.1, or nore > 0.1†
Renal (creatine, mmol/l; urine, ml/d)	110	110-170	171-299	300-440 or < 500	> 440 or < 200
Liver (bilirubin, μmol/l)	20	20-32	33-101	102-204	> 204
Coagulation (platelets, $\times 10^9$/l)	> 150	≤ 150	≤ 100	≤ 50	≤ 20
Central nervous system (GCS)	15	13-14	10-12	6-9	< 6

PaO_2/FiO_2, partial pressure arterial oxygen and fraction of inspired oxygen; MAP, mean arterial blood pressure; Dop, dopamine; Dob, dobutamine; Epi, epinephrine; Nore, norepinephrine; GCS, Glasgow Coma Scale.
*Values are with respiratory support.
†Adrenergic agents administered for at least 1 hour (doses given are in μg/kg per minute).

1.2 Pathophysiology of organ failure

1.2.1 Inflammatory cells and mediators

1.2.1.1 Macrophages, dendritic cells and neutrophils

Tissue resident macrophage and dendritic cells can phagocytose the cell debris and simultaneously secret pro-inflammatory cytokines to recruit circulating neutrophils and monocytes/macrophages. Meanwhile, chemicals released by these tissue resident cells can increase the vasodilatation and epithelium permeability resulting in phagocytes migration, blood proteins leakage to tissue and circulation. The conventional role of neutrophils in the pathogenesis of organ failure has been well recognised and characterised in diseases such as sepsis[97], severe acute pancreatitis[98], acute liver failure[99] and acute glomerulonephritis[100]. The role of neutrophils at least include degranulation and phagocytosis[101-103]. Although neutrophils defend host prominently, it is one of the major culprits in causing collateral cell damage by passively releasing damage-associated molecular patterns (DAMPs) including reactive oxygen species, sodium hypochlorite, neutrophil elastase, high mobility group box protein 1 (HMGB1), histones, etc. and forming neutrophil extracellular traps (NETs)[104, 105].

1.2.1.2 NETs

In 2004, a novel mechanism of neutrophils has been discovered by Brinkmann and colleagues[106]. They described a phenomena that includes vacuolisation, relaxation of chromatin, rupture of nuclear membrane, mixing up of chromatic and granular components and release of the chromatic-granular components to form the nets-like extracellular structure, which is called NETs[106]. As it is distinctly different from those of neutrophil apoptosis and necroptosis, a term of NETosis is coined to describe this phenomena by Steinberg and Grinstein in 2007[107]. NETs formation is released by the activated neutrophils triggered by the pathogens like bacteria and fungi[108], or DAMPs[104,

[109], the cellular breakdown products including components from nucleus, mitochondria, cytosol and cell membrane that are immunogenic[110]. DNA consists the backbone of NETs, which is decorated by chromatic and granular proteins and peptides. As histones are abundant in the NETs components, the backbone DNA is mostly from nuclei instead of mitochondria which contain histone-like proteins rather than histones.

It is believed that the main role of NETosis is to trap, kill and lyse the pathogens in a higher concentration of granular antimicrobial components, resulting in the enforcement of their microbicidal effects. The conduct of undergo phagocytosis or NETosis might depends on the size of pathogens. During counteracting larger size of bacteria or fungi, activated neutrophils cannot engulf the pathogens by phagocytosis. Instead, they process NETosis, then the lysed pathogens and debris of NETs can be cleared by macrophages. However, NETosis also can be triggered in inflammation and worsen the diseases.

Reactive oxygen species (ROS) generation and autophagy are essential for undergo NETosis[104]. NETosis can be triggered by live bacteria, phorbol myristate acetate (PMA) or IL-8, but NETs formation is absent in stimulated neutrophils from patients with chronic granulomatous disease (CGD)[104]. CGD patients have the mutations in the phagocyte NADPH (nicotinamide adenine dinucleotide phosphate) oxidase, resulting in lack of ROS generation which is essential in the antimicrobials[111]. This scenario highly indicated that ROS generation is required for the NETosis. Fuchs and co-workers used diphenylene iodonium (an inhibitor of NADPH oxidase) to block NETosis which further confirmed the essential role of ROS generation in NETosis[112]. However, ROS alone is not sufficient to induce NETosis. Remijsen and colleagues used PMA to stimulate neutrophils which were pre-treated with wortmanin which inhibits autophagy

via inhibition of PI3K[113]. These pre-treated neutrophils did not show massive vacuolisation but remained the superoxide production, implying although ROS oxidase remains active when autophagy is pharmacologically inhibited, PMA is unable to induce NETosis. Instead, block either ROS oxidase or autophagy can led to activation of caspases and apoptosis. Therefore, NETosis requires both ROS generation and autophagy and apoptosis might function as a backup program when NETosis is inhibited.

Beside the function of microbicide, NETs and its components can initiate inflammatory response[102, 114, 115], cytokine release[102, 114, 115], thrombin generation[116-119], platelet aggregation[119, 120], etc. Except infectious disease, excessive NETs formation has been found in patients with non-infectious diseases such as systemic lupus erythematous[121, 122], cystic fibrosis[123, 124], depth vein thrombosis[119], pancreatitis[125-127], etc and impairs wound healing in diabetics[128]. In contrary, aggregated NETs have been shown to limit inflammation by degrading cytokines and chemokines in gout[129]. These paradox findings indicate that NETosis is a double-edged sword in immunity. Therefore, it is essential to understand the mechanisms of inducing and regulating NETosis, which might provide a potential therapeutic target.

1.2.1.3 Cytokines and chemokines

Cytokines are the small proteins secreted by cells with the functions of regulation of transcription, translation, healing, inflammation, etc[130]. The term ‘cytokine storm’ vividly described the image of an immune system gone awry and the systemic inflammatory response flaring out of control and cytokines including tumour necrosis factor (TNF) superfamilies[131, 132,133, 134], interleukin (IL)-1 families[135], IL-6 families[136-138], and chemokine families[139] are well studied. In systemic inflammation such as

observed in sepsis[140, 141] or severe acute pancreatitis, the cytokine storm is driven by TNF, IL-1, IL-2, IL-6, reactive oxygen species and arachidonic metabolites which are counteracted by anti-inflammatory mediators IL-10, IL-4 and IL-1 receptor antagonist (IL-1Ra)[142]. Chemokines such as IL-8 and monocyte chemoattractant protein-1 (MCP-1) are also released to enhance the recruitment of inflammatory cells to the primary injury site[140-142].

IL-1 family contains 11 members including IL-1α, IL-β, IL-18, IL-33 and IL-1Ra[135, 143]. Both IL-1α and IL-1β are pro-inflammatory cytokines which have functions of increasing acute-phase signalling, trafficking immune cells to the local infection site, activing epithelial cells and inducing more cytokine release. Caspase-1 inflammasome regulates the maturation and secretion of IL-1β, IL-18 and IL-33 in inflammatory responses. However, in sterile inflammation IL-1β and IL-18 is processed by neutrophil proteinase-3 and neutrophils are a major source of these pro-inflammatory cytokines.

Elevated IL-1β has been reported lethal as blockage of IL-1R decreased mortality in experimental models[144]. IL-1 possess the capability of secondary production of IL-1 and TNF-α, but this inflammatory cascade can be regulated by IL-1Ra and IL-6. IL-1Ra is upregulated and competitively bind to IL-1R1 to the blockage of transduction of IL-1 signalling[145]. Simultaneously, IL-6 secreted majorly from mononuclear phagocytic cells can inhibit IL-1 and TNF synthesis and stimulate synthesis of IL-1Ra, resulting in anti-inflammatory response[138]. The other role of IL-6 is pro-inflammatory mediator by effect on B cell maturation and secretion of immunoglobulins, activation of T cells and induction of hepatocyte of acute phase proteins[137, 138].

Chemokines are another group of cytokines that have a hallmark feature of recruiting immune cells into the injured site by induction of chemotaxis[139, 146-149]. IL-8 (also termed CXCL8) is secreted from variable cells triggered by stimulates especially IL-1 and TNF[150, 151]. The essential role of IL-8 is the traits of chemoattractant and degranulation of neutrophils[148]. MCP-1 (also known as CCL2) majorly regulates the migration and infiltration of monocytes, as well as T lymphocyte and natural killer cells[152, 153]. The recruited monocyte convert to macrophage to be involved in the battle with infection and inflammation[154].

Collectively, cytokines and chemokines released by the primary injured parenchymal cells and residential immune cells trigger a chain of responses to recruit migration of immune cells (neutrophils[101, 103, 155, 156], dendritic cells[157, 158], monocytes/macrophages[159-162], mast cells[163, 164] and other granulocytes) involved in innate immunity to the injured site[165]. The principle function of innate immune responses is to 1) bring phagocytes to the injured area to isolate, destroy and inactivate the invaders and/or remove the debris of cell death; 2) prepare subsequent healing.

1.2.2 Cell death, DAMPs and DAMP receptors

Scientists have been trying to define the classifications of different types of cell death since 19th century. The definitions are variable from morphology to immunological characteristics. Since 2005, Nomenclature Committee on Cell Death (NCCD)[166] has been working on unifying criteria for the definition of cell death. Recently, NCCD in 2015[167] classified cell death into two broad categories: accidental cell death and regulated cell death (RCD), which contains programmed cell death. In contrary to ACD, RCD can be initiated by a genetically encoded molecular machinery, and the

course of RCD can be altered by application of specific pharmacologic and/or genetic modulations at least to some extent. The types of cell death including apoptosis[168-172], autophagic cell death[173-177], autosis[178], necroptosis[179-185], mitochondrial permeability transition-medicated regulated necrosis[186-189], pyroptosis[190], parthanatos[191] and ferroptosis[192-194] have been summarised in excellent reviews.

A concept of Danger Model was proposed by Polly Matzinger in 1994[195], which described that the immune system together with an extended network of other host tissue cells is capable of discriminate dangerous signals rather than only distinguishing self and non-self. The dangerous signals can be elicited by pathogens, injured, infected and necrotic tissues, or cells under non-physiological death which release dangerous molecules with the capability to stimulate pro-inflammation. The Danger Model is the fundamental theory of DAMPs and in 2004 the concept of DAMPs was formally composed by Seong and Matzinger[110]. During tissue injury, the intracellular molecules or their derivatives are positively (secretion) or negatively released into the extracellular space or exposure on the outer leaflet of plasma membrane. The extracellular matrix is the source of DAMPs as well. Similar to pathogen-associated molecular patterns (PAMPs), DAMPs can elicit and modulate the immune system by effecting on the function of antigen-presenting cells (like macrophages and dendritic cells) and other cell types (like mast cells and neutrophils).

Up to date, few membrane-bound or cytoplasmic pathogen recognition receptors (PRRs; also referred as pattern recognition receptors) have been provide to recognise DAMPs, including Toll-like receptors (TLRs), NLR Family Pyrin Domain Containing 3 (NLPR3), RIG-I-like receptors, receptor for advanced glycation end products and

purinergic receptors, which shows that PAMPs and DAMPs share some receptors and indicate infection (pathogen-induced) and sterile inflammation have some similarities. Sepsis is initiated by the recognition of classical PAMPs via the PRRs[196] which may induce uncontrolled inflammatory response, immunosuppression and thus successive organ failure(s)[197]. In non-infectious conditions such as during early phase of acute pancreatitis, acetaminophen-induced liver injury, myocardial infarction, ischaemia-reperfusion-induced brain injury and blunt trauma, extensive cell death may occur which leads to profound cytokine/chemokines[139, 198] and cellular contents release[199-201]. The source of DAMPs is principally from primary and secondary necrotic cell death[202, 203], a process occurs in apoptotic cells that are not removed by phagocytic cells timely and sufficiently. DAMPs can also be recognised by the PRRs and non-PRR receptors expressed by the residential immune cells (e.g. macrophages and dendritic cells) to initiate pro-inflammatory responses (Figure 1.1 and 1.2)[203]. Based on the location of DAMPs derived from, DAMPs are mainly classified into three groups: extracellular matrix, cytosol and organelle, the latter includes mitochondrion, endoplasmic reticulum, granule and nucleus. The classification of DAMPs has been summarised in Table 1.2.

1.2.3 Others

Besides aforementioned themes, coagulation[204], microcirculatory[205], gut (bacterial translation[206] or gut-lymph theory[207, 208]) and two-hit phenomenon[209] have been proposed to play a role in the pathogenesis of organ failure. In summary, regardless of the aetiology, the initial injury has been converted to systemic inflammation, if persists, resulting in multiple organ failure. Systemic inflammation and organ failure then further promote local injury and immune cells to trigger synchronised RCD, a vicious cycle begins (Figure 1.3).

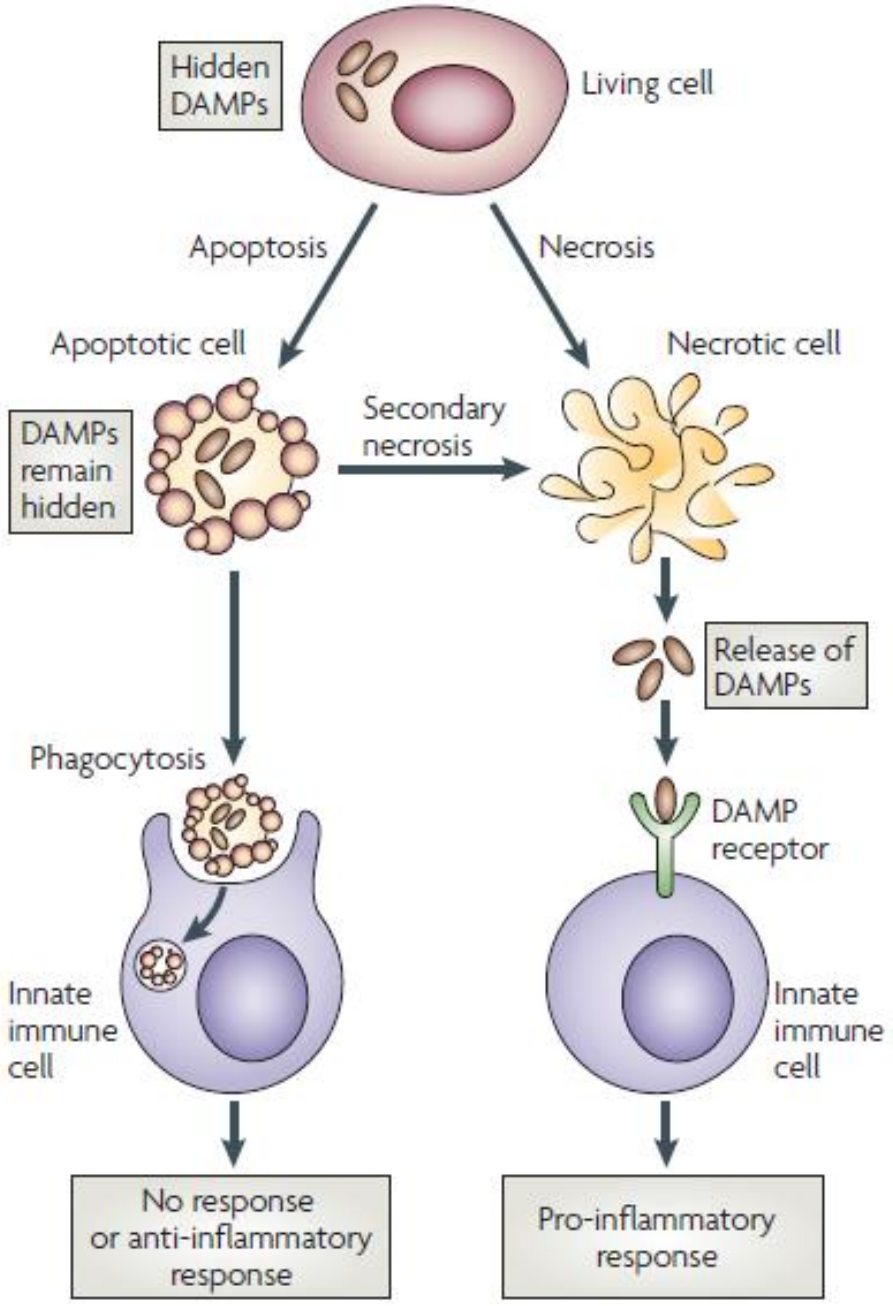

Figure 1.1 DAMPs from primary and secondary necrosis that trigger pro-inflammatory response. Intracellular molecules that are normally hidden in the interior of the cells. In stressed conditions, if apoptotic cells are engulfed by phagocytic cells timely and efficiently, there will be no discernible immune response from the host; while primary necrotic or secondary necrotic cells (uncleared apoptotic cells) release their cellular contents which are recognised by DAMP receptors, initiating the pro-inflammatory response (from Kono *et al.*[203]).

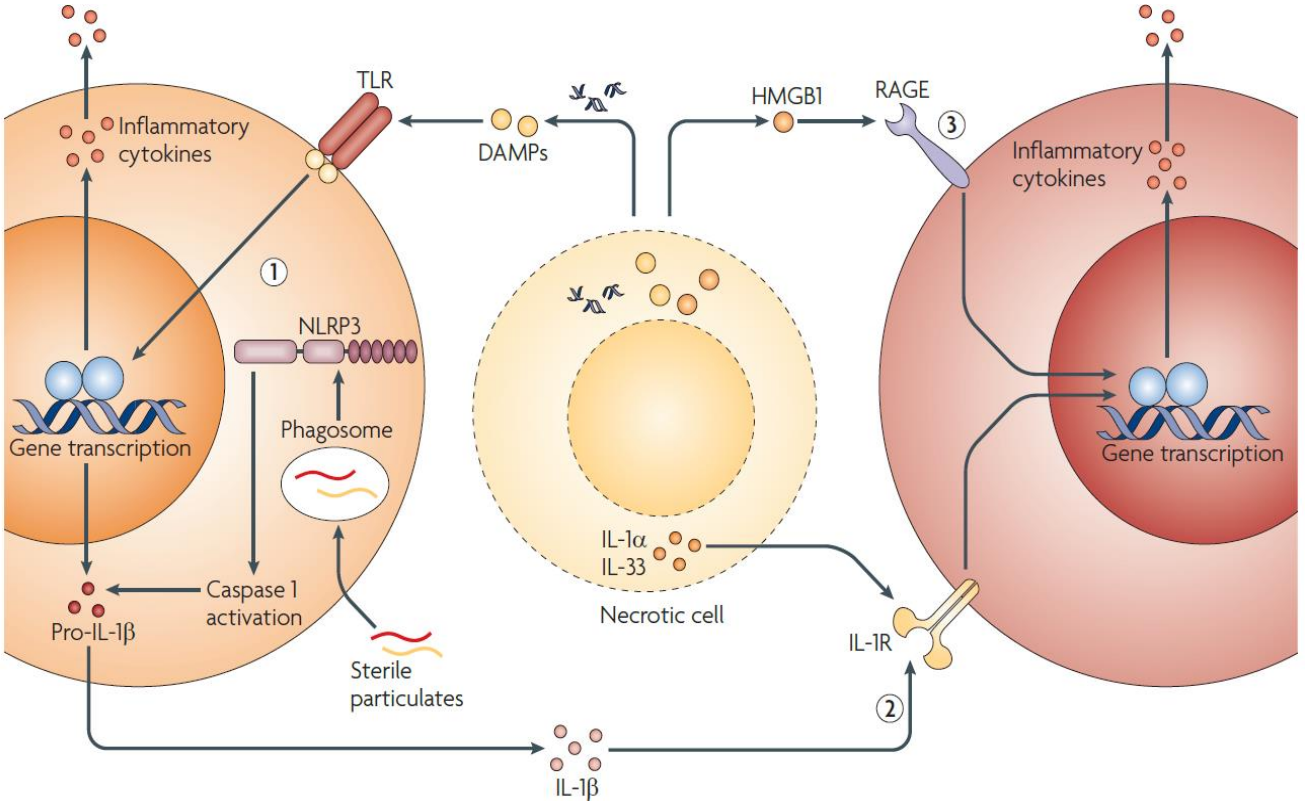

Figure 1.2 Mechanisms for sterile inflammation triggered by necrotic cells. Primary or secondary necrotic cell death lead to release of cellular contents such as DAMPs and intracellular cytokines interleukin (IL)-α and IL-33. DAMPs activate Toll-like receptors (TLRs) and receptor for advanced glycation end products (RAGE) to promote inflammation; activation of TLR also primers the generation of IL-1β via NLRP3 (NOD-, LRR- and pyrin domain-containing 3); IL-1β, IL-α and IL-33 activate IL-1 receptor (IL-R) to further promote inflammation (from Chen *et al.*[165]).

Table 1.2 Classification of DAMPs

DAMPs	**Cell death modality**	**receptors**
Extracellular matrix		
Fibrinogen	-	TLR4
Heparan sulphate fragments	-	TLR4
Hyaluronan	-	TLR2 and TLR4
Cytosol		
S100 proteins	Necrosis	RAGE, TLR4
Heat shock proteins	Apoptosis/secondary necrosis and necrosis	TLR2, TLR4
IL-1α	Necrosis	IL-1R
Galectins	Secondary necrosis and necrosis	CD7, CD43, and CD45
Organelles		
Mitochondrion		
Mitochondrial DNA	Necrosis	TLR9
ATP	Apoptosis/secondary necrosis and necrosis	P_2X_7, P_2Y_2
N-formyl peptides	Necrosis	FPR-1
Cytochrome c	Secondary necrosis and necrosis	LPG?
Cardiolipin	Apoptosis	?
Carbamoyl phosphate synthase-1	?	?
Endoplasmic reticulum		
Calreticulin	Immunogenic apoptotic cell death	CD91
Granule		
Cathelicidines	Necrosis and NETosis	TLR7, TLR9 and RAGE
Myeloperoxidase	Necrosis and NETosis	?
Neutrophil elastase	Necrosis and NETosis	TLR4?
Defensins	?	TLR4, CCR6
Nucleus		
High-mobility group box 1	Secondary necrosis and necrosis	RAGE, TLR2, TLR4 and TLR9
DNA	Necrosis and NETosis	TLR3
Histone	Necrosis and NETosis	TLR2, TLR4 and TLR9?

TLR, Toll-like receptor; RAGE, receptor for advanced glycation endproducts; FPR-1: Formyl Peptide receptor 1; LPG: leucine-rich alpha-2-glycoprotein-1; CCR, CC chemokine receptors.

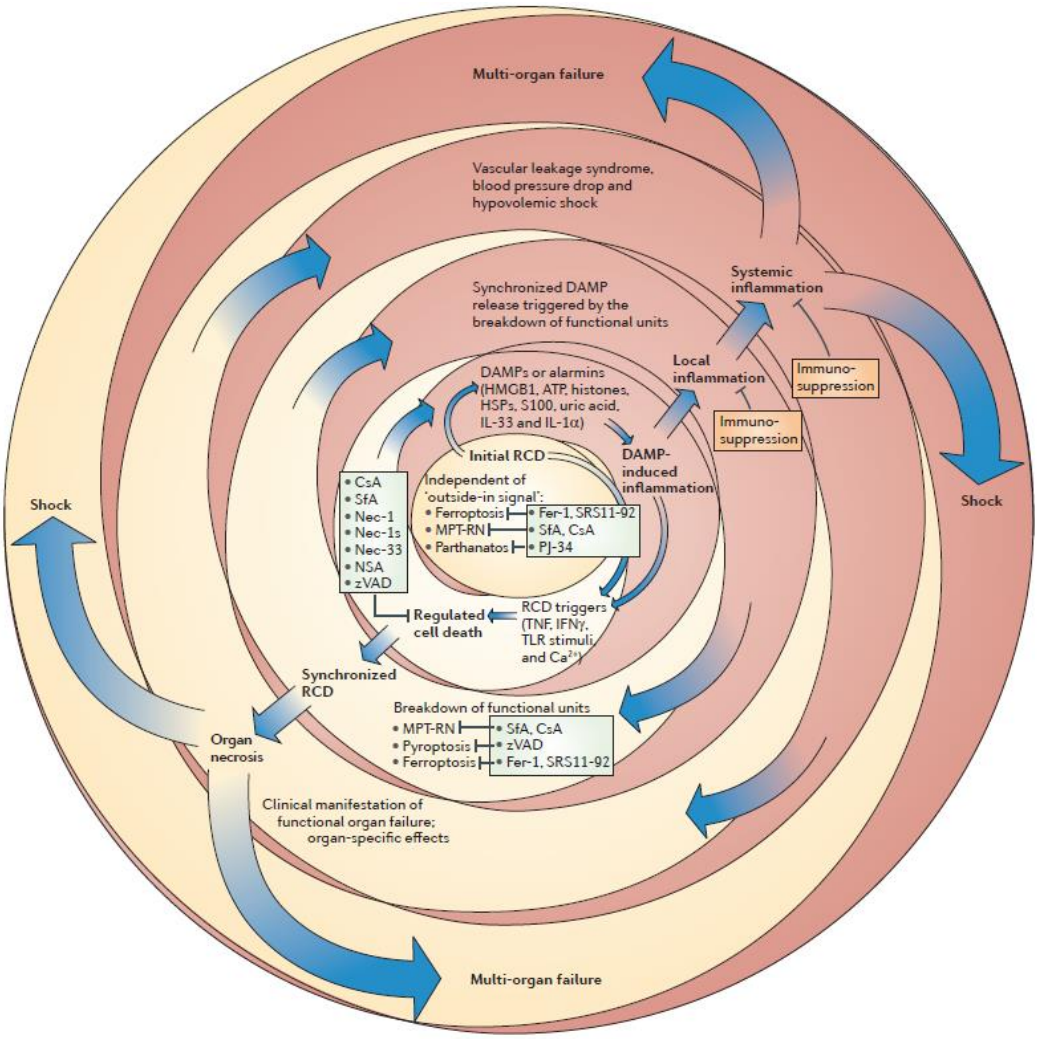

Figure 1.3 Regulated cell death-induced auto-amplification inflammation loop. After the stimulation from primary insults, cells are undergoing accidental (ACD) and regulated cell death (RCD). While ACD is currently unmanageable, the initial RCD can be blocked or alleviated by specific inhibitor depends on the principle RCD pathway, e.g. sanglifehrin A (SfA) and cyclosporin (CsA) are used for targeting mitochondrial permeability transition-mediated RCD (MPT-RN); necrostatin-1 (Nec-1), Nec-1s and Nec-33 are used for RIPK1-mediated cell death. ACD and uncontrolled RCD results in local inflammation, systemic inflammation and multiple organ failure (i.e. shock). Systemic inflammation and organ failure in turn acerbate local injury, leading to synchronised RCD and subsequent release of more DAMPs (from ref[210]).

1.3 The emerging role of extracellular histones in critical illness

1.3.1 Extracellular histones are key inflammatory mediators

Elevated levels of circulating nucleosomes have been observed in acute conditions such as organ failure induced by trauma, stroke and sepsis[211], and are correlated with disease severity[212]. In 2009, a landmark study by Xu *et al.*[213] identified extracellular histones as key inflammatory mediators which caused organ failure and death in animal models of sepsis. Thereafter, the mechanisms of how extracellular histones cause tissue injury and organ failure begun to be understood.

1.3.2 Histone binding molecules

In 2010, an elegant study by Pemberton *et al.* 2010[214] has shown that histones precipitated a range of proteins include lipoproteins, proteinase inhibitors, competent proteins, coagulation factors, immunoglobulins and others in human plasma (*Supplementary Table 1*). Intravenous injection of radiolabelled calf thymus histones has been shown to be bound to heparin sulphate in the capillary glycocalyx of the lung of rabbit[215]. Also, absorption of histones have been found on natural polysaccharides, especially alginic acid and pectin[216]. Recently, novel molecules that bind to histones have been identified (*Supplementary Table 2*), these include TLRs (TLR2 and TLR4; TLR9 involvement is controversial), C-reactive protein (CRP), recombinant thrombomodulin, Mer receptor, αvβ5 integrin, neutralised serum albumin, N-acetyl-heparin, antithrombin activity depleted heparin, inter-α inhibitor protein, high-molecular-weight hyaluronan, MBP-p33, pentraxin 3 and C1 esterase inhibitor (C1INH). All these data greatly contribute to our understandings of histone biodistribution, mechanisms of cytotoxicity and potentially therapeutic targets.

1.3.3 Effects of extracellular histones on different cell types

The effects of extracellular histones *in vitro* and *ex vivo* are summarised in *Supplementary Table 3*. The cytotoxicity extracellular histones have been clearly shown in parenchymal, immune and red blood cells. Data collectively suggest that extracellular histones (normally ≥ 20 μg/ml) were toxic to these cells via TLR2/4 and NLRP3 mediated signalling pathway. At higher concentrations, histones directly caused "pore" on cell membrane thus induce calcium influx and subsequent rapid cell death. Anti-histone treatment generally significantly reduced histone-induced toxicity.

1.3.4 Release of extracellular histones in animal models of critical illness and treatment strategies

The release of extracellular histones in sepsis (*Supplementary Table 4*), acute lung injury (*Supplementary Table 5*), acute liver injury (and ischaemia-reperfusion injury including stoke, myocardial infraction and renal injury; *Supplementary Table 6*), acute pancreatitis (and peritonitis and glomerulonephritis; *Supplementary Table 7*) are systematically summarised. The local and systemic release of circulating histones and NETs have been generally observed. Exogenous administration of non-pathological doses of calf thymus histones converted acerbate local injuries in acute lung injury, liver injury and pancreatitis models. Moreover, the extent of extracellular histone release correlate with proinflammatory cytokines/chemokines, systemic inflammation, organ injury and mortality in critical illness murine models. *In vivo* infusion of fluorescein isothiocyanate (FITC)-labeled calf thymus histones (45 mg/kg) revealed that the lung had the highest accumulation of FITC intensity, followed by spleen, kidney, plasma, liver, heart and brain[217]. The histone-induced haemostatic dysfunction is summarised in *Supplementary Table 8*. Exogenous administration of pathological doses of calf thymus histones

induced thrombocytopenia with elevation of cytokines/chemokines, systemic inflammation, multiple organ injury and mortality.

In all these critical illness models, direct anti-histone treatments, such as anti-histone antibodies, activated protein C (APC), heparin and heparin derivatives, CRP, albumin, etc. reduced local and systemic extracellular histones, alleviated severity and mortality. Targeting histone receptors (TLR2, TLR4, NLRP3 and NLRP3 components) or binding molecules also hold promises for reducing disease severity.

Now we clearly understand histone-induced cytotoxicity at least in large rely on the positively charged amino acids, thus neutralising histones would be an excellent strategy. However, to develop novel anti-histone strategies there are much cautions to be taken. The most studied anti-histone strategy is anti-histone antibody, but using of antibody may lead to autoimmune problems. Heparin may be effective in patients at high doses but may put patients at risk of bleeding due to the small therapeutic window. CRP, an acute phase protein, reduces histone-induced organ injury, but acute phase proteins (i.e. CRP and serum amyloid P) have been shown to delay the clearance of nucleosomes[218] and core histones[219]. Polycations also neutralise histones, but accumulated polycations lead to lung injury. APC fails to show efficacy in critical illness patients. Natural herbal medicine may be a good resource for drug discovery in this regard. The natural polysaccharides alginic acid and pectin absorb histones but do not bind to other plasma proteins[216], minimising the chance of affecting anticoagulation proteins.

1.3.5 Measurement of circulating histones

As the toxicities of circulating histones described above, it is clear that determination and monitoring of the levels of circulating histones in patients or experimental animals can guide clinical therapy and help researches. The current available commercial assay for circulating histones is based on enzyme-linked immunosorbent assay (ELISA) which only measures histone-DNA complexes. Western blot remains to be the only method for the measurement of all circulating histones currently. Western blot is a very common and wildly used method which detects the target protein in a reduced and denatured condition. Proteins are separated by molecular weight using sodium dodecyl sulfate-polyacrylamide gel electrophoresis procedure, followed by transferred to a membrane, typically nitrocellulose or polyvinylidene difluoride (PVDF), where they are stained with the specific antibody to the target protein. Running with a linear range of recombinant target protein (called as standards), we can quantify sample concentration using the equation formed by standard concentration and density.

It has been reported that the toxicity of each monomer is different. Histone H4 is the most toxic one followed by histone H3. If measured by Western blot, it is impossible to determine the exact populations of circulating histones unless doing 5 monomers individually, which requesting much more samples and working time. Therefore, a more comprehensive, robust and convenient method is required.

1.4 Hypotheses of the proposed work

Nowadays, there is an increasing interest to use circulating nucleosomes in diagnosis and prognosis in conditions such as sepsis, stroke and autoimmune diseases as well as in the diagnosis, staging, prognosis, and monitoring of therapy in cancer[211]. In acute inflammation condition (i.e. acute pancreatitis), extensive cell death may occur and lead to release of chromatin components into the extracellular environment. The circulating nucleosomes have marked differences to their breakdown products, circulating histones and cell-free DNA[220]. Circulating histones may present as histone-DNA complexes, free monomers, or degraded forms. The former has been shown to be much less immunogenic than the free histone monomers[220]. However, the issue of whether the degraded histone forms have cytotoxicity have not been systematically addressed, nor there are available assay to quantify their circulating levels. Recently, release of extracellular histones[221] and formation of NETs[125] have been observed in experimental acute pancreatitis[125] and anti-histone antibody rescued mice from death[222]. Furthermore, elevated plasma nucleosomes (histone-DNA complexes) have been demonstrated in acute pancreatitis patients, and their levels correlated with disease severity[125, 223].

We hypothesised that circulating histones would also elevate in experimental acute pancreatitis and correlate with severity parameters. In parallel, we also hypothesised that on admission circulating histone levels can predict persistent organ failure and may further increase with disease progressing.

We also interested to test whether degraded histone forms still carry cytotoxicity effect and we endeavoured to develop an assay to measure all types of circulating histones with xMAP technology.

Chapter 2 – Toxicity of circulating histones

2.1 Introduction

Histones are a family of alkaline proteins which package and order DNA into structural units called nucleosomes (Figure 2.1)[224]. With the feature of positive charge, core histones (histone H2A, H2B, H3 and H4) form an octamer which is wrapped by 147 base pairs negatively charged DNA[225]. The histones H3 and H4 form a stable H3-H4 tetramer, whereas H2A and H2B form two H2A-H2B dimers which are less stable[226]. Histone H1/H5, the linker histone, binds the nucleosome at the entry and exit site of DNA, which is essential for regulating DNA de-condensation during transcription and post-transcriptional modifications[227-231].

In the chapter 1, the extracellular histone-induced cell toxicity and its mechanisms have been introduced in details. Circulating nucleosomes released from nuclear chromatin during extensive tissue injury and cell death are degraded into individual histones in the liver[232] where these histones are also rapidly cleared[218]. These findings demonstrate that the monomer histones can be further cleaved or degraded into N or C terminal histones after release into circulation. It is also well known that enzymes like activated protein C can cleave histones into their truncated forms. Therefore, histones entry into circulation as different complexes including degraded circulating histones. However, whether these circulating histones possess cytotoxicity remains unknown.

In this chapter, we sought to investigate the cytotoxicity of both monomer and truncated histones and further to examine whether anti-histone strategy confers protective effects.

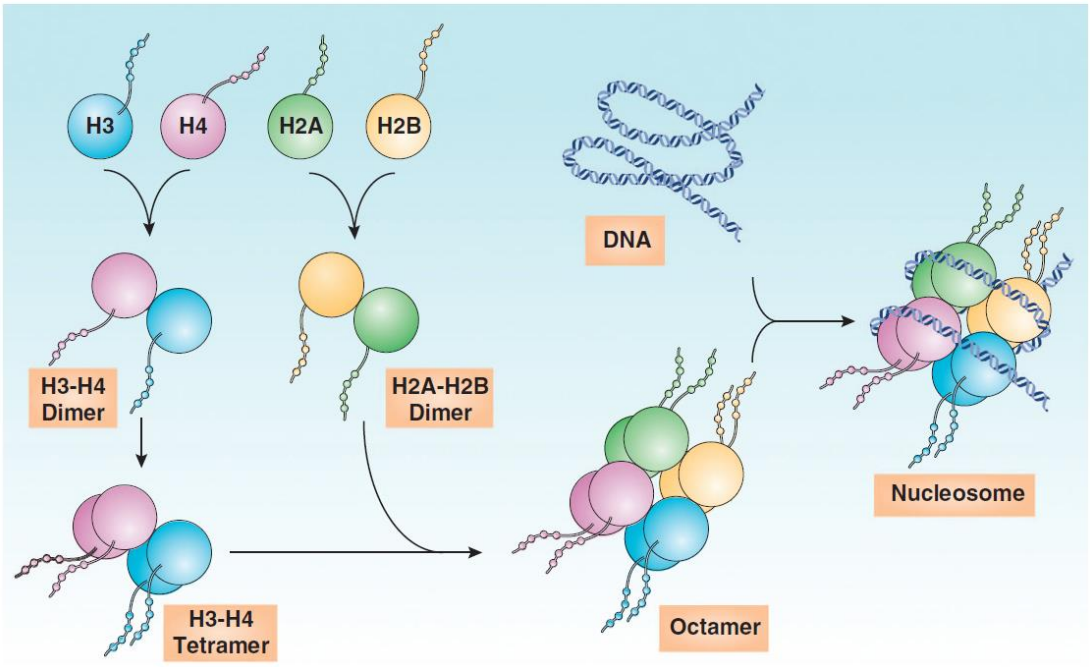

Figure 2.1 Structure of core histones and nucleosome. Two pairs of histones H3 and H4 form a tetramer which is incorporated by 2 dimers composed by histones H2A and H2B to form an octamer. This histone octamer is wrapped up by ~147 bp of DNA to form nucleosome. (From reference Chen *et al.* Cell Death and Diseases 2014[199])

2.2. Martials and Methods

2.2.1 Generation of N and C terminal recombinant histones

2.2.1.1 Sequence design

Histones H1.1 and H1.4 possess most of the identical amino acids sequence in the 11 identified H1 isoforms[233, 234]. H2A and H2B are the most frequent isoforms of their respectively categories[234]. H3.1 is the most ubiquitously expressed among 3 H3 isoforms (H3.1, H3.2 and H3.3)[234]. There is only one H4 isoform, the canonical H4[234]. DNA sequences of H1.1, H2A, H2B, H3.1 and H4 were employed as templates. H1.1 DNA sequence was synthesised by Eurofins MWG Operon and the rest of histone plasmids (pHCE-histone) were a gift from Dr Hitoshi Kurumizaka (RIKEN Genomic Sciences Centre, Yokohama, Japan). All the sequence design related information for truncated histones are summarised (Table 2.1).

2.2.1.2 Generation of pET-16b-N or C terminal histone plasmid

Key steps for generating pET-16b-N or C terminal histone plasmid (Figure 2.2):

A. Amplification of pHCE-histone plasmid: pHCE-H2A, pHCE-H2B, pHCE-H3.1 and pHCE-H4 plasmids were amplified by using the Subcloning Efficiency™ DH5α™ Chemically Competent Cells *Escherichia coli* (Invitrogen, USA). The DH5α 100 µL was thaw on ice and 1 µL of each plasmid was immediately added after thawing, followed by 20 min incubation on ice. Then a heat shock at 42°C for exactly 45 s was applied in water bath and the eppendorf was immediately placed back on ice. The eppendorf was supplemented with 250 µL Luria-Bertani (LB) medium and stood for 20 min to allow the bacteria to recover. Bacteria were incubated at 37°C for 45 min with shaking at 200 rpm, and pelleted by spinning at 12,000 × g for 30 s. After removing 150 µL redundant supernatant, the bacteria were resuspended in the remaining medium and spread homogenously on the LB agar plate containing 100 µg/mL ampicillin (pHCE

vector is ampicillin resistant). An overnight incubation at 37°C was followed. On the second day, a single colony from the agar plate was picked up and cultured in 5 mL LB/ampicillin medium in a 15 mL Falcon tube at 37°C and 200 rpm for overnight. On the third day, bacteria were harvested by spinning at 3,000 × g for 30 min and plasmids were extracted using QIAprep Spin Miniprep Kit (Qiagen, Netherlands) following the manufacturer's protocol and kept in -20°C.

B. Digestion and purification of histone DNA: the purified pHCE-histone plasmids and histone H1.1 synthesised DNA were digested by restriction endonucleases Ndel and BamHI (both from New England Biolabs, USA). The each digested mixtures was loaded into 1% agarose gel to isolate histone DNA from the vector. The lower bands, histones, were cut and extracted using QIAquick Gel Extraction Kit (Qiagen, Netherlands) following the manufacturer's protocol. Histone DNA was eluted in 20 µL H_2O and kept at -20°C.

C. Generation of N or C terminal histone DNA: the purified histone DNA and designed primers N or C terminal of each histones were used to do polymerase chain reaction (PCR) following the manufacturer's protocol (GoTaq® PCR Core Systems, Promega, UK). All of the N or C terminal histone DNA were extracted (1.2% DNA agarose gel was used), digested (Ndel and BamHI), purified and stored as before.

D. Ligation and amplification of pET-16b-N or C terminal histone plasmid: both Ndel and BamHI digested pET-16b vector and N or C terminal histone DNA were mixed (molar ratio: 1:10) for ligation using the Quick Ligation™ Kit (New England Biolabs, USA). Then pET-16b-N or C terminal histone plasmid was transformed to the DH5α bacteria for the amplification.

E. DNA sequencing: the purified plasmids were sequenced by Beckman Coulter Genomics (Takeley, UK) and all the DNA sequences were 100% marched.

Table 2.1 Sequence design information for truncated histones

Name	Gene Bank No.	Residues	5'-primer	3'-primer
H1.1 N ter	NM_005325	1-110	CTAGTTATACATATGTCTGAAACAGTGCCTCCCGC	TTCTAGGATCCCTAGTTGAGCTTGAAGGAACCCGA
H1.1 C ter	NM_005325	111-214	CTAGTTATACATATGAAGAAGGCGTCCTCCGTGGAA	TTCTAGGATCCTACTTTTTCTTGGGTGCCGCTTTC
H2A N ter	NM_003513.2	1-62	CTAGTTATACATATGTCTGGTCGCGGCAAAC	CTAGGATCCCTACTCGGCGGTCAGGTACTCAAGC
H2A C ter	NM_003513.2	63-130	CTAGTTATACATATGATCCTGGAGCTGGCGGGCAATG	CTAGGATCCCTACTTTCCCTTGG
H2B N ter	NM_021058	1-63	CTAGTTATACATATGCCAGAGCCAGCGAAG	CTAGGATCCCTAATTCATGATGCCCATG
H2B C ter	NM_021058	84-126	CTAGTTATACATATGGACATTTTCGAGCGCATC	CTAGGATCCTACTTAGCGCTGGTGTACTT
H3.1 N ter	NM_003537.3	1-74	CTAGTTATACATATGGCTCGTACTAAACAG	CTAGGATCCTATTCTCGCACCAGGCGCTGGAAC
H3.1 C ter	NM_003537.3	75-136	CTAGTTATACATATGATCGCCCAAGACTTCAAGACC	CTAGGATCCTACGCTCTTTCTCC
H4 N ter	NM_003545.3*	1-41	CTAGTTATACATATGGAAACCCGTGGCGTGCTGAA	CTAGGATCCTCATTAACCGCCAAAACCATACAGGGT
H4 C ter	NM_003545.3*	51-103	CTAGTTATACATATGATTTATGAAGAAACCCGTG	CTCTAGGATCCTCATTAACCGCCAAAACC

*Mutated from NM_003545.3 (See reference Tanaka *et al.* Methods 2004[235])

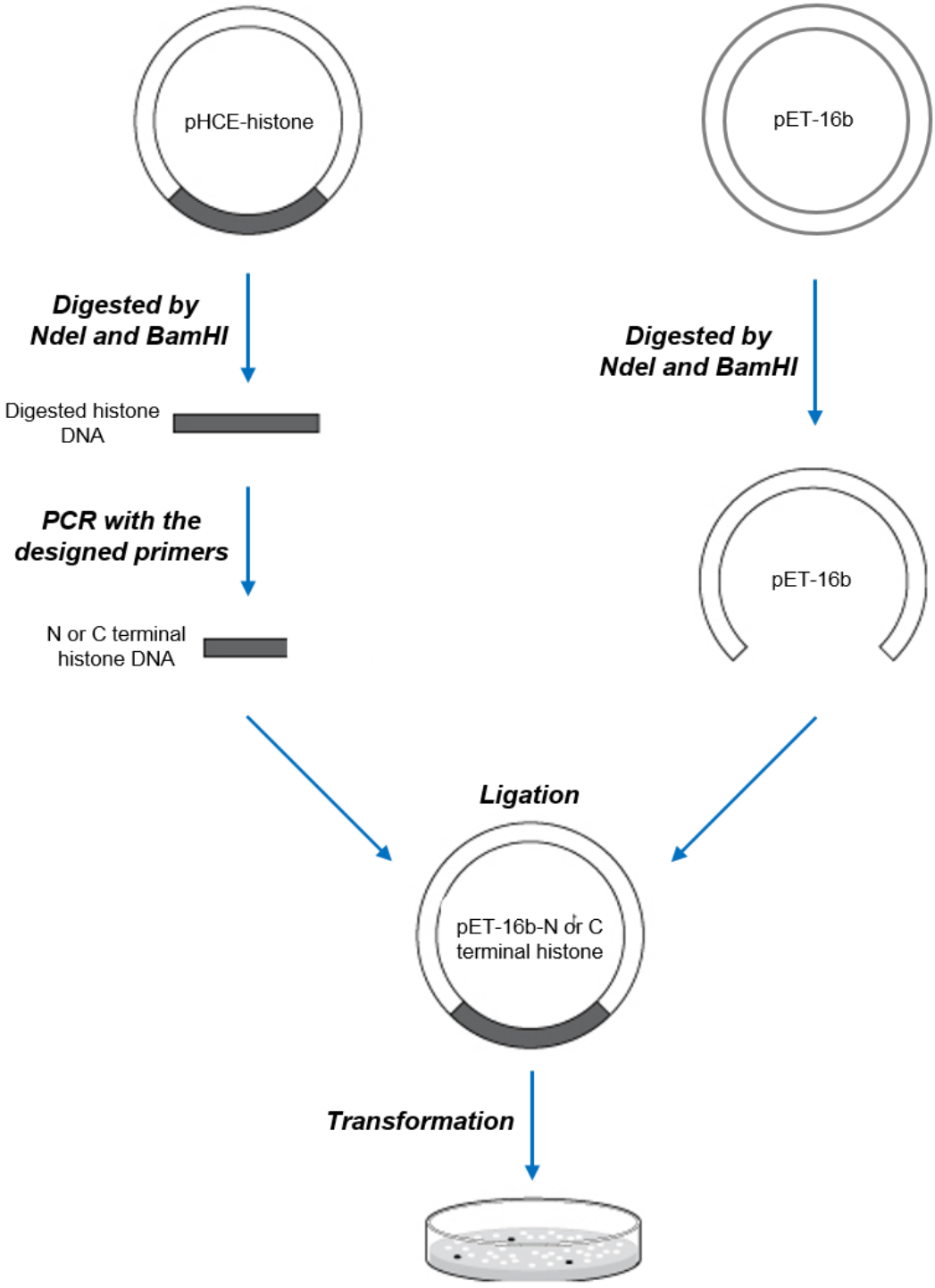

Figure 2.2 Generation of N or C terminal histone plasmid using recombinant DNA technology. The experiment steps involved amplification of pHCE-histone plasmid, digestion and purification of histone DNA, generation of N or C terminal histone DNA, and ligation and amplification of pET-16b-N or C terminal histone plasmid.

2.2.1.3 Expression, extraction and purification of N or C terminal histone proteins

Purified pET-16b-N or C terminal histone plasmid, extracted from DH5α, was transformed into the C41 (DE3) *Escherichia coli* and cultured on agar plate containing 100 µg/mL ampicillin (pET-16b vector is ampicillin resistant). Six single colonies were respectively cultured in 3 mL LB/ampicillin medium in the 15 mL Falcon tubes at 37^{o}C and 200 rpm until the optical density was 0.5 at absorbance of 600 nm. Isopropyl β-D-1-thiogalactopyranoside (IPTG; Melford, UK) of 1 mM was added into 4 tubes while the other 2 tubes without IPTG were used as negative controls. Tubes were incubated for another 4 h. The bacteria of 20 µL in each tube were taken to run a sodium dodecyl sulfate polyacrylamide gel electrophoresis (SDS-PAGE) gel to check the expression of N or C terminal histone. After confirmation of histone protein expression, 1 L bacteria were cultured until the optical density reached 0.5 before adding 1 mM IPTG. After > 4 h incubation with IPTG, bacteria were harvested by centrifugation at 5,000 × g for 10 min at room temperature. Bacteria pellets were resuspended in 20 mL Resuspension Buffer and kept at -80^{o}C overnight. On the next day, bacteria mixture was disrupted by sonication on ice 3 min × 3 at an interval of 3 min. Pellet and supernatant were collected by centrifugation at 15,000 × g for 30 min at 4^{o}C. Pellet was resuspended in 20 mL Binding Buffer followed by sonication and centrifugation as above again. As the pET-16b vector contains the Histidine-tag coding sequences, the expressed N or C terminal histone was purified by the Histidine-tag/Nikeli-Nitrilotriacetic acid (Ni-NTA) system (Qiagen, USA) and assessed by 15% SDS-PAGE gel. First, 1.5 mL Ni-NAT Agarose resin (Qiagen, USA) was poured into a 10 mL purification column. Allow the resin to settle completely by gravity, followed by a wash step with 50 mL H_2O. Equipment Ni-NAT Agarose with 100 mL Resuspension Buffer, then resin was settled by gravity at room temperature. The second supernatant was added into column and passed through

by gravity. Then column was washed with 200 mL Wash Buffer. The wash through was collected for later check. Expressed protein was eluted in 20 mL Elution Buffer. All the steps were performed at 4^{o}C by gravity. Elute was transferred into the dialysis bag with a cut-off 3.5 kD (Spectrum Labs, USA) and dialysed against urea in 2 L Dialysis Buffer for overnight at 4^{o}C (change buffer twice). The pass through, wash through and elution dialysis (10 µL per each collection) was removed for 15% SDS-PAGE gel and Coomassie Brilliant Blue staining. The buffer recipes during this process are summarised in Table 2.2.

Table 2.2 Buffer recipes for expression, extraction and purification of histone proteins

Buffer	**Chemicals**
Resuspension Buffer	150 mM Tris-HCl (pH 7.4) + 50 mM NaCl, 1 mM PMSF (add freshly)
Binding Buffer	Resuspension Buffer + 6 M Urea
Wash Buffer	20 mM Tris-HCl (pH 7.4) + 200 mM NaCl + 50 mM imidazole + 3 M urea
Elution Buffer	20 mM Tris-HCl (pH 7.4) + 200 mM NaCl + 250 mM imidazole + 3 M urea
Dialysis Buffer	20 mM Tris-HCl (pH 7.4) + 200 mM NaCl + 5% glycerol

Tris-HCl, Tris(hydroxymethyl)aminomethane hydrochloride; PMSF, phenylmethane sulfonyl fluoride.

2.2.2 Generation of pan anti-histone ahscFv and cscFv

The anti-histone single chain variable fragment (ahscFv) and its control single chain variable fragment (cscFv) were generated by using the recombinant DNA technology. Their primers were listed (Table 2.3). The details of pan anti-histone ahscFv and cscFv establishment was described in Dr Dunhao Su's PhD thesis entitled "Production, Characterisation and Application of Humanised Anti-Histone Antibodies in Critical Illness" which is available at University of Liverpool library. In brief, ahscFv was designed on the basis of complementarity-determining regions (CDRs) of anti-histone antibodies from human with autoimmune disorders. For the development of cscFv, the CDRs were changed but the rest of sequence of ahscFv was kept. Gene sequences

pCR2.1-ahscFv and pCR2.1-cscFv were synthesised and verified by Eurofins MWG Operon. The function and affinity of ahscFv and cscFv were determined by Western blot and biosensor, respectively.

Table 2.3 The primers for ahscFv and cscFv

Name	**5'-primer**	**3'-primer**
ahscFv	ATGGATTCACCATATGGAAATTCAGCT	TGGCAAGCGGATCCCTAATTATT
cscFv	ATGGATTCACATATGGAAAAC	TGGCAAGCGGATCCTTACTGGCA

2.2.3. Cytotoxicity of histones towards endothelium cells

2.2.3.1 Membrane binding

Human endothelial cell line EA.hy926 were cultured in Dulbecco's Modified Eagle's Medium (DMEM) supplemented with 20% Fetal Calf Serum (FCS). Both human recombinant histone subclasses (New England Biolabs, USA) and house generated truncated histones were conjugated with fluorescein isothiocyanate (FITC, Invitrogen, USA) following the manufacturer's protocol. Cells of 5×10^5 were incubated with 10 μg/mL FITC-histone for 10 min followed by membrane binding observation using confocal microscope (Zeiss LSM510 system, Carl Zeiss Jena GmbH, Germany).

2.2.3.2 Calcium influx

Each histone and trauncated histone-induced calcium influx was reflected as the increase of intracellular calcium concentration ($[Ca^{2+}]_i$). Cells were loaded with 3 μM Fura-2AM for 20 min and washed with Calcium Assay Buffer (pH 7.4) containing 20 mM Hepes, 120 mM NaCl, 4.7 mM KH_2PO_4, 1.2 mM MgCl, 1.25 mM $CaCl_2$, and 10 mM glucose. The Fura-2AM was monitored continuously by a F-7000 fluorescence spectrometer (Hitachi, Japan) at excitation 340 nm and 380 nm and emission at 510 nm as previous decribled[236]. The $[Ca^{2+}]_i$ was calculated using the software provided.

2.2.3.3 Cell viability

Full length, truncated and calf thymus histones as well as serum from acute critical illenss patients (ethical approval obtained) were used. EA.hy926 cells of 1×10^6 were seeded and treated with different types of histone (each 20 µg/mL) or serum. After fixed in 70% ethanol for 30 min at -20^{o}C, the cell viablity was determined by flow cytometry (BD Biosciences, USA) using 10 µg/mL propidium iodide (PI) staining. Viable cells have intacted nuclei with a distinct diploid DNA peak (2N), while damaged nuclei cells have a broad peak of hypodiploid particles (< 2N).

2.3 Results

2.3.1 Generation of truncated histones

Eight out of 10 truncated histones were successfully generated by using the recombinant DNA technology (Table 2.4), while histone H2B C ter and H4 N ter were synthesised peptides (Figure 2.3). The purity of all truncated histones were 75.6-95.1% measured by the histogram density, except histone H2A C (35.5%).

Table 2.4 Expression and purity of truncated histones

Name	Predicted WM (Da)	Actual WM (Da)	Purity (%)	Storage Buffer
His_{10}-H1.1 N ter	10893	13072	90.6	Tris-HCl
H1.1 C ter- His_{10}	10835	14551	80.1	Tris-HCl
His_{10}-H2A N ter	6512	8436	95.1	Tris-HCl
H2A C ter- His_{10}	7509	8489	35.5	Tris-HCl
His_{10}-H2B N ter	6958	9004	92.7	Tris-HCl
H2B C ter peptide	4617	6710	83	H_2O:ACN = 5:1
His_{10}-H3.1 N ter	8266	9733	90.8	Tris-HCl
H3.1 C ter- His_{10}	7024	7912	75.6	Tris-HCl
H4 N ter peptide	4264	7155	94.4	H_2O
H4 C ter- His_{10}	6065	7284	79	Tris-HCl

His_6, Hexahistidine; Tris-HCl, Tris(hydroxymethyl)aminomethane hydrochloride; ACN, acetonitrile.

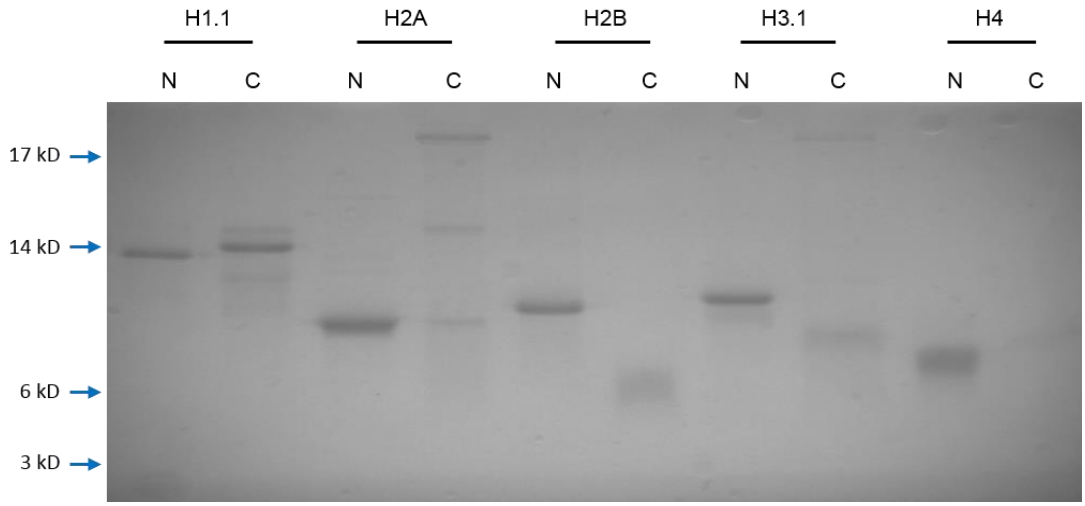

Figure 2.3 Expression and purity of truncated histones. Except histone H2B C and H4 N, all truncated histones were expressed by *E. Coli* using the recombinant DNA technology. Histone H2B C and H4 N were synthesised peptides. Each histone protein (5 µg) was loaded in 18% SDS-PAGE gel and stained by Coomassie Brilliant Blue. N, N-terminal; C, C-terminal.

2.3.2 Generation of ahscFv and cscFv

The molecular weight of expressed ahscFv and cscFv were 27 and 29 kDa respectively, measured by Coomassie Brilliant Blue and their purity were > 95% (Figure 2.4A). Both of them were stored in PBS (+ 5% glycerol). The western blot revealed ahscFv bound to histone H1 and H3 while cscFv did not (Figure 2.4B and C). The ahscFv successfully recognised all the human recombinant histone subclasses and calf thymus histones, as demonstrated by western blot (Figure 2.5A) and biosensor analyses (Figure 2.5B). The western blot demonstrated that ahscFv had higher band density with H1, H2B and H4, followed by H3 and H2A. The biosensor assay showed similar results, albeit a strongest binding of ahscFv to H3 was observed.

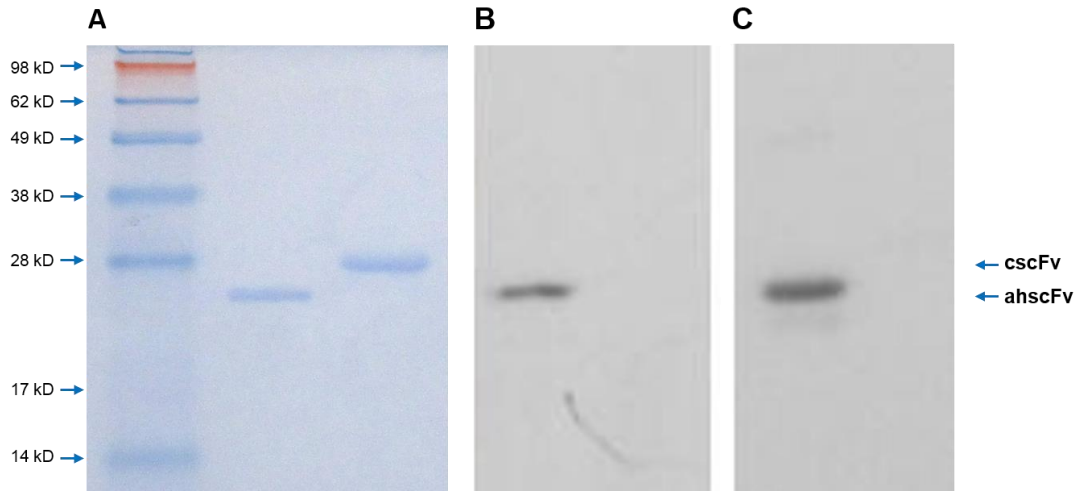

Figure 2.4 ahscFv and cscFv expression and their histone binding capacity. ahscFv and cscFv (each 5 µg) were loaded in 15% SDS-PAGE gel. (A) Stained by Coomassie Brilliant Blue; Probed by (B) Biotin-histone H1, or (C) H3, and streptavidin-HRP after membrane transfer shows that only ahscFv bound but cscFv did not. HRP, horseradish peroxidase.

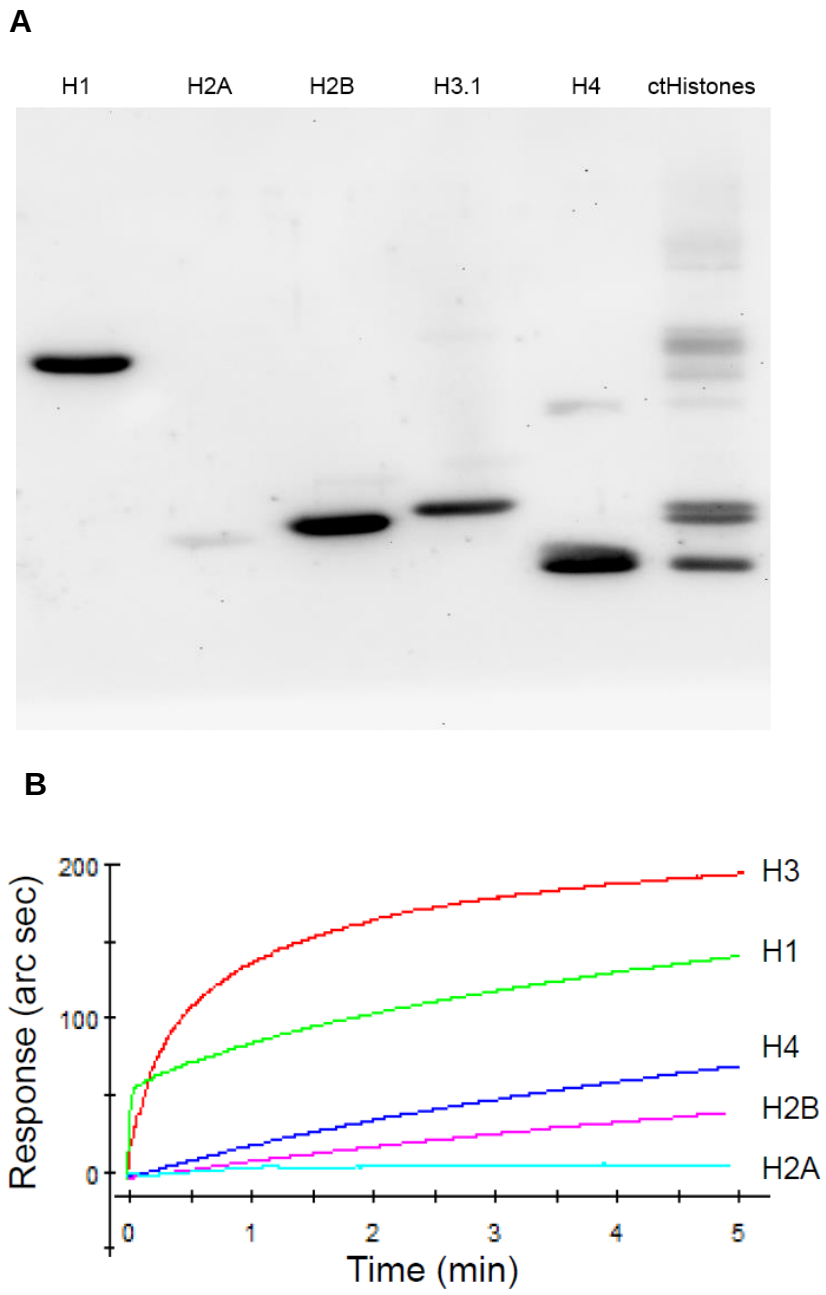

Figure 2.5 ahscFv recognises all the monomer histones. (A) The binding between ahscFv and histones was confirmed by western blot: recombinant histones (5 µg of each) and calf thymus histones (ctHistones, 25 µg) were loaded and transferred to PVDF membrane, then probed by HRP conjugated ahscFv; (B) The binding of recombinant human histone subclasses (each 1 µM concentration) to ahscFv was determined by IAsys resonant biosensor, in which the ahscFv was immobilised on aminosilane surfaces using BS3.

2.3.3 Histones bind to cell membrane and induce calcium influx

The detailed membrane binding by full length and truncated histones in EA.hy926 cells are shown in Table 2.5 and an example is shown in Figure 2.6. All the FITC-full length histones and 3 FITC-truncated histones (H1.1 C, H2A N, H3.1 N) bound to the cell membrane. All the remaining tested FITC-truncated histones were not shown to bind cell membrane.

Table 2.5 Histone membrane binding in EA.hy926 cells

	H1			**H2A**			**H2B**			**H3.1**			**H4**		
Histone	F	N	C	F	N	C	F	N	C	F	N	C	F	N	C
Binding	+	-	+	+	+	-	+	-	-	+	+	-	+	-	-

F, full length; N, N-terminal; C, C-terminal.

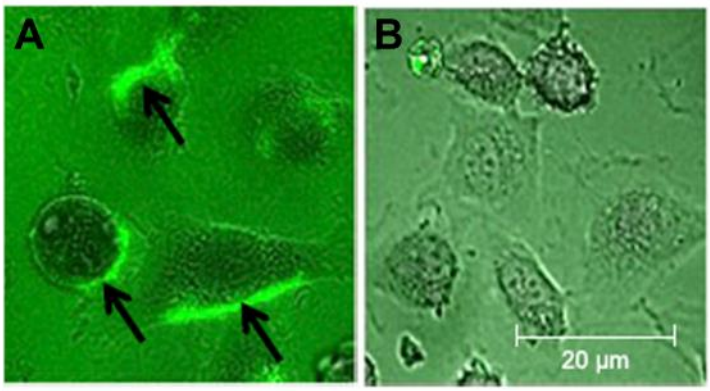

Figure 2.6. Membrane binding of histone in endothelial cells. (A) Confocal images of EA.hy926 cells 10 minutes after incubation with FITC–labelled histones (10 µg/ml) alone (arrows indicate FITC-labeled histones). (B) FITC-labelled histones preincubated with ahscFv (100 µg/ml). Scale bar: 20 mm. FITC, fluorescein isothiocyanate.

The calcium influx induction by full length and truncated histones in EA.hy926 cells are shown in Figure 2.7. The full length and truncated histones which bound to cell membrane also dramatically induced calcium influx as determined by increased $[Ca^{2+}]_i$. The histone H4 induced highest $[Ca^{2+}]_i$ (H4 > H2A N > H3.1 > H2A > H2B > H1.1 C > H1 > H3.1 N).

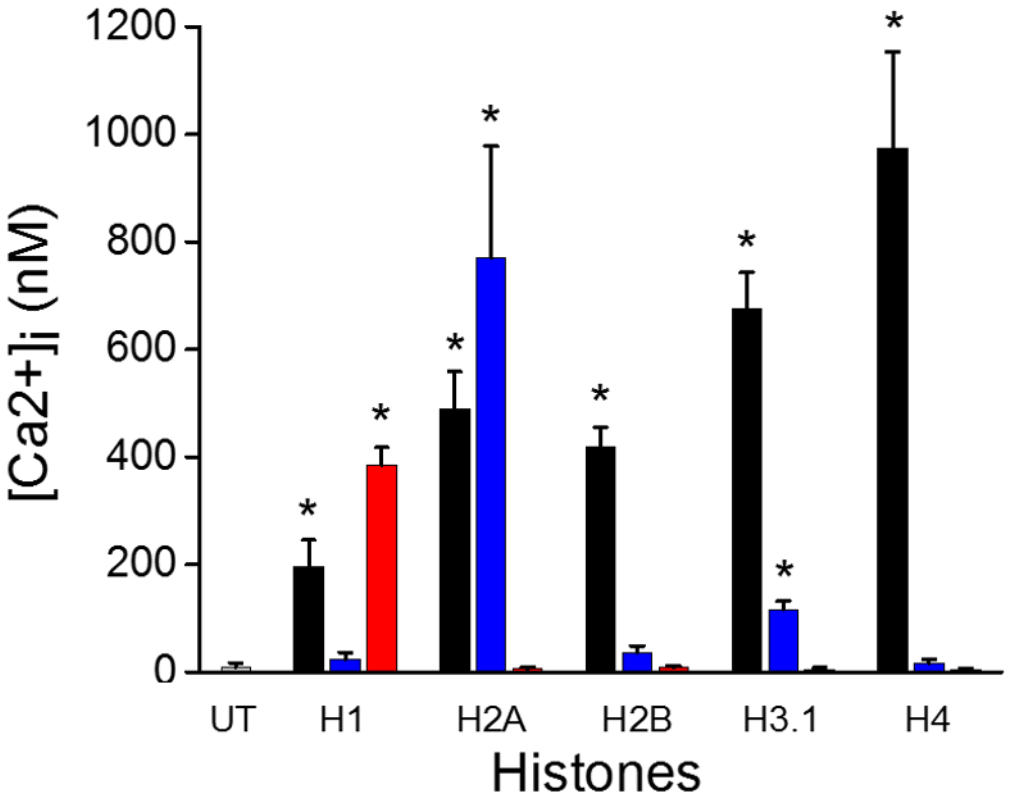

Figure 2.7 Histones induce calcium influx. FITC-labelled histones (each 20 µg/ml) were used to determine histone membrane binding in EA.hy926 cells; Intracellular calcium concentration ($[Ca^{2+}]_i$) was measured by confocal microscopy using fluorescent dye Fluo-2AM. *$P < 0.01$ when compared to the untreated (UT) group, Student's *t* test. Black, full length histone; Blue, histone N terminal; Red, histone C terminal.

2.3.4 Histones induce cytotoxicity

The histone-induced cell viability changes in EA.hy926 cells are demonstrated in Figure 2.8. In line with the findings with cell membrane binding and calcium influx profile, all full length and 3 truncated histones (H1.1 C, H2A N, H3.1 N) also significantly induced cell death (reflected by PI uptake) when each of them (20 µg/mL) were incubated with cells for 1 h. The other truncated histones did not have discernible effects on cell viability.

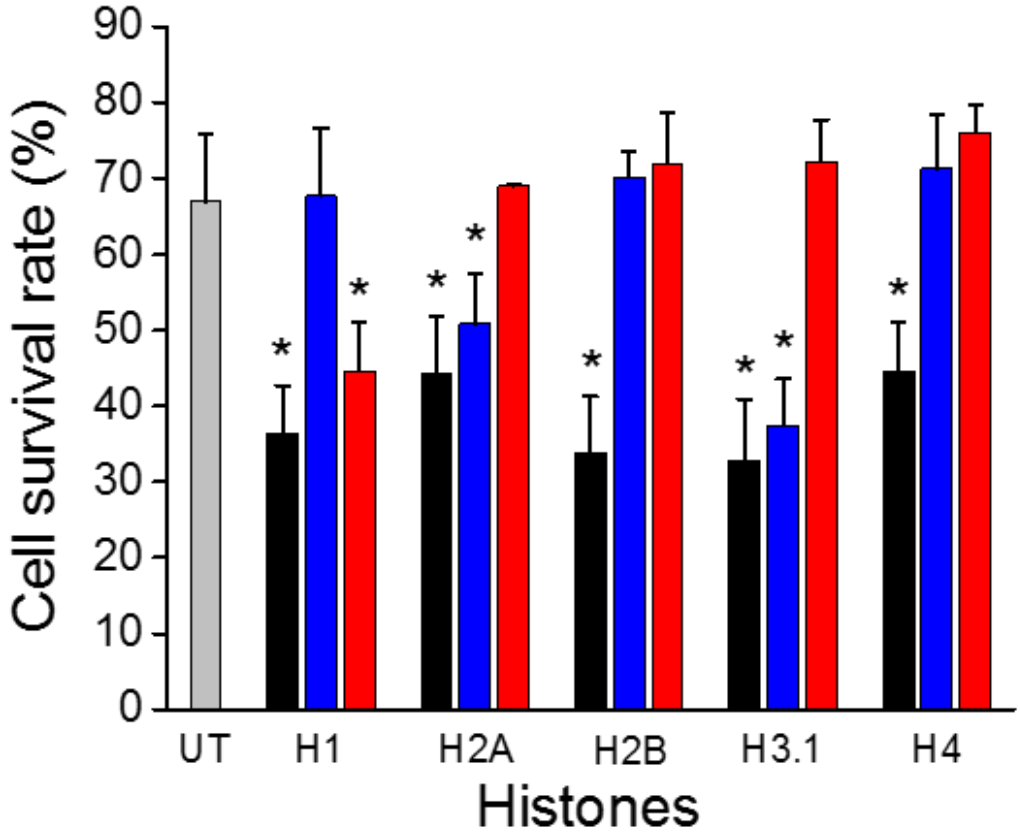

Figure 2.8 Histones induce cytotoxicity. Histone-induced cytotoxicity in EA.hy926 cells were measured by cell uptake of propidium iodide. Each full length and truncated histones (20 µg/mL) was incubated with the cells for 1 h before testing cell viability *$P < 0.05$ when compared to the untreated (UT) group, Student's *t* test. Black, full length histone; Blue, histone N terminal; Red, histone C terminal.

2.3.5 ahscFv prevents against histone-induced cytotoxicity

The cell viability of EA.hy926 cells treated by calf thymus histones or sera from acute critical illness and the effects of ahscFv are shown in Figure 2.9. The cell viability was nearly halved after incubated with histones (20 μg/mL) for 1 h. The histone-induced reduction of cell viability was significantly improved by co-administration of ahscFv (200 μg/mL). Sera from acute critical illness (all had histone levels > 50 μg/mL) also caused markedly decrease of cell viability which was elevated by adding ahscFv.

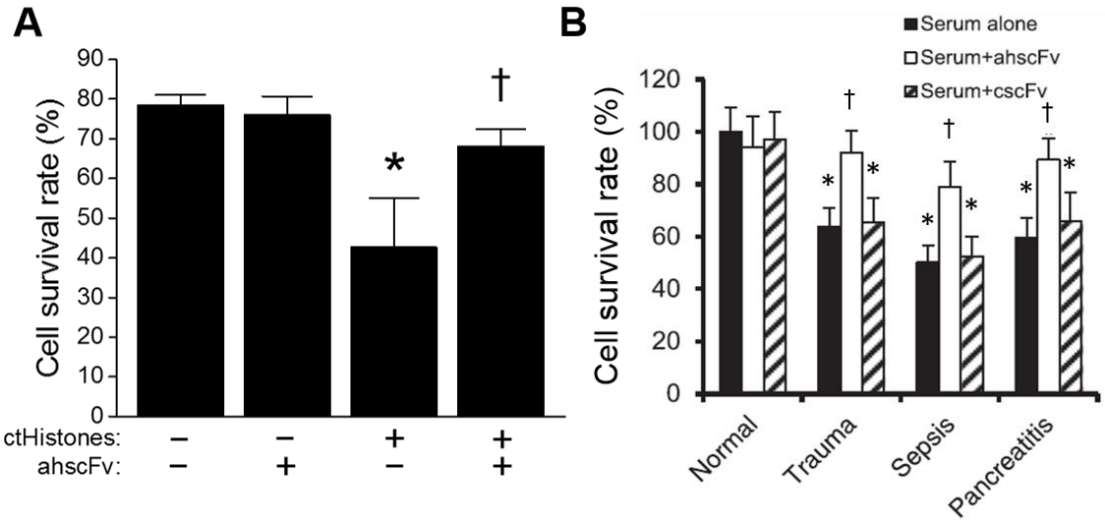

Figure 2.9 ahscFv prevents against histone-induced cytotoxicity. Histone-induced cytotoxicity and the effects of ahscFv and cscFv (each 200 μg/mL) in EA.hy926 cells were measured by cell uptake of propidium iodide. **P* < 0.05 when compared to the untreated group or cscFv group; †*P* < 0.05 when compared to the respective serum treated group or serum + cscFv treated group per each disease category, Student's *t* test. ctHistones, calf thymus histones.

2.4 Discussion

In order to elaborate with current research frontiers about the toxticity of circulating nucelosomes[211] and histones[199], in this chapter, we endeavoured to generate truncated histones that mimicking circulating degradated histones and further systematically assessed the effects of full length and truncated hisotones on cell membrane binding, calcium influx and thus the cytoxticity. To our knowledage, this is the first time to generate 8 truncated histones (H1.1 N, H1.1 C, H2A N, H2A C, H2B N, H3.1 N, H3.1 C, H4 C) using recombinant DNA technology. However, we did not succeed in generatering H2B C and H4 N, thus the syntheic peptides of them were used for subsequent experiments. All 10 tuncated histones were confirmed by the protein dye Coomassie Brilliant Blue which showed the respective molecular weight of individual histone on the SDS-PAGE gel.

Consistent with existing literature, we found that all the full length histones bound to cell membrane, induced calcium influx and reduced cell viability. Histone H4 induced highest $[Ca^{2+}]_i$, which was followed by H3, other core histones and the linker histone. These data provide quantitative evidence that at least partially explained why H4 and H3 are the most toxic monomer histones. This phenomena actually fits into the sequence of how individual histones are released during cell injury: H1 releases first, then H2A and H2B, followed by H3 and finally H4. The latter two histones form the most stable nuceolsome core[237]. Whether the histone releasing sequence correlates with the toxticity of individual histones warrants further investigation. Adding to the above findings, we also unravelled that 3 truncated histones (H1.1 C, H2A N, H3.1 N) possessing membrane binding capacity and thus was able to induce calcium influx. In line with this, the cell viability was greatly reduced by these truncated histones compared to the

untreated group or treated by other truncated histones (H1.1 N, H2A C, H2B N, H2B C, H3.1 C, H4 N, H4 C). The lesser cell toticity of the other truncated histones may be explained by that none of these histone bound to cell membrane nor induced calcium influx. These novel findings highlight the importance of circulating histones as inflammatory mediators as they are still toxic even when degraded. The translational value of these findings are also paramount: (1) developing an assay to determine the ciruclating histone levels has great clincial prospective; (2) degradation of circulating histones may not completely remove the toxticity (e.g. by activated protein C). This translational aspect will be further discussed in the chapter 7, the overview chapter.

In parallel, we also generated pan ahscFv for antagonising the toxticity of cirulating histones. The ahscFv and its control were confirmed by protein dye of their respective molecular weight. The binding capacity of ahscFv was ascertained by the probed biotin-histones, while the cscFv did not bind to any histones. Furthermore, the pan ahscFv identified calf thymus histones and all the 5 monomer histones with a highest binding afinity to H3, followed by H1, H4, H2B and H2A. The ahscFv nearly restored histone-induced decrease of cell viability by either calf thymus histones or circulating histones containing serum from critical illness patients. Further humanisation of ahscFv may have clinical applicability for diseases in which circulating histones play an important role.

Other attempts of neutralising histone action should be centred around the molecular mechanisms of histone toxicity. It is known that polycations are able to form pores in lipids[238], yet according to other reports polycations may use specific transmembrane channels[239] or rely on intracellular signalling molecules[239, 240]. In several cell types the

cytotoxicity of histones was sensitive to lanthanoids, okadaic acid and genistein[241], which points to certain specificity in the mechanism of membrane permeabilisation. If indeed histones open some endogenous large-pore channels, leading to loss of cytosolic constituents, then the candidate list of such channels is about 8-9 member long[242] and includes $P2X_7R$, transient Receptor Potential channels (TRPA1 and TRPV1), maxi anion, plasma voltage dependent anion-selective (VDAC), connexin hemichannel, pannexin hemichannel and maitotoxin-induced pore. Some of these channels (like Pnx1 and $P2X_7$ or maitotoxin- and $P2X_7$, etc.) can work in synergy. $P2X_7$ opening is often a part of anti-microbial response, so that some antimicrobial peptides (such as cathelicidin LL37[243, 244] and human neutrophil peptide-1[245]) can activate this receptor (although it seems that LL37 and defensins may also form pores themselves[242]). LL37 is a positively charged peptide (charge +6, 30 amino acids), and human neutrophil peptide-1 (known also as alpha-defensin) is slightly charged (+3, 30 amino acids). Histone H4 is also a major anti-microbial agent[246], and fetuin-A (structurally related to cathelicidin LL37) is known to complex with H2A[247]. Histone H2A has strong antimicrobial properties itself[248]. $P2X_7$ opening can be amplified by positively charged antibiotic polymixin B[249]. It was suggested that $P2X_7$ pore may be the same as maitotoxin-activated cationic channel[250-252]. Paradoxically, histones H3 and H2B, inhibit perforin- or toxin-mediated cell lysis[253, 254]. As for pannexins, both histone-induced membrane permeabilisation and pannexin1 conductance are inhibited by La3+/Gd3+, while connexins are well known to be sensitive to okadaic acid, just like histone-induced cell death[241].

Thus, testing whether any "professional" large-conductance channels play a role in histone-induced toxicity warrants further investigation. As many of these channels have

specific inhibitors, it may be justified to use such inhibitors in conditions of elevated plasma histones alone or in combination with anti-histone strategies.

Chapter 3 – Develop a rapid, robust and comprehensive assay to monitor the toxic histones in circulation

3.1 Introduction

3.1.1 Toxicity of circulating histones

Extensive cell death occurs in the acute phase of many human diseases and is a common feature observed in many critically ill patients[210, 255, 256]. However, the contribution of this process to the overall progression of the disease has been overlooked until recently. During the cell death, nuclear breakdown products, particularly histones which is one of the damage-associated molecular pattern molecules (DAMPs)[199], are released into the circulation and are rarely detectable unless there is extensive cell death, due to rapid hepatic clearance[218]. Recently, extracellular histones have been shown to induce endothelial damage, cytokine elevation, platelet aggregation and coagulation activation *in vitro* and mortality in mouse models[199]. The toxicity of circulating histones is described in the chapter 1. In chapter 2, we systematically investigated the toxicity of circulating histones in details with a focus on truncated histones (mimicking degraded circulating histones). Despite realising the importance of measuring circulating histones, there is no rapid, robust and comprehensive assay to detect the levels of toxic histones.

3.1.2 History and principle of xMAP technology

3.1.2.1 History

xMAP technology is a microsphere-based immunofluorescence assay. This assay composed of flow cytometer and fluorescence. In 1977, Horan and colleagues[257] reported the first use of flow cytometry for analysis of microsphere-based immunoassays. Because of the ability to distinguish different particles by size and colour, flow cytometer possesses the ability of multiplexed analysis with different

microsphere populations. In the last decade, Luminex Corporation developed a more comprehensive platform by merging flow cytometer with fluorescence, namely FlowMetrix™ which performs multiplexed measurement of up to 64 analytes simultaneously[258]. Later, xMAP technology, with measurement of up to 500 analytes, has been updated (xMAP® Technology Technical Note 2010).

3.1.2.2 The workflow of xMAP technology

xMAP technology contains of sets of carboxylated microspheres which stained with two dyes, red (> 650 nm) and orange (585 nm). The polystyrene microsphere has a diameter of 5.6 μm and bears carboxylate functional group on the surface. Therefore, any amine-containing molecules including antibodies can virtually bind to the microspheres respectively via a two-step carbodiimide reaction. Each microsphere has a sufficient surface for coupling 1-2 × 10^6 molecules. Luminex Corp provides 500 distinct sets of microspheres which can be classified by the unique orange/red emission profile of each set excited by laser. The size of different set of microspheres is uniformed and can be identified by the 90-degree light scatter, also called side-scatter gate, to make sure only the uniform single particles are classified. Microsphere aggregations and other particles within the samples are eliminated. For identification of different bead sets, the feature of the varying amounts of proprietary two dyes emitting fluorochromes allows the classification of the individual sets of microspheres. Using the size and orange/red colour, the xMAP can count the amount of microspheres in different bead sets. Except the orange/red colours, green colour is applied for counting the events captured by the molecules bound to the microspheres. A green colour dye conjugated antibodies, normally Streptavidin-Phycoerythrin (PE), are used. The emission wavelength from microspheres and streptavidin-PE are received and converted into electrical signals by photomultiplier tubes (PMT), then are digitalised, converted and displayed as

fluorescence intensities (FI). The xMAP quantitates the green, orange and red fluorescence of each microsphere using the FL1, FL2 and FL3 detectors, respectively. All the data are collected by the software and analysed based on the internal standards. The workflow is shown in the Figure 3.1.

3.1.2.3 The advantages of xMAP technology

xMAP technology is considered as an alternative to enzyme-linked immunosorbent assay (ELISA). The comparison between them in different analytes, samples time and costing are summarised in Table 3.1[258-260]. The principal advantage of xMAP technology is the multiplexing capability. ELISA immobilises the capture antibody in the surface of microplate well consequently only one analyte can be detected in one kit. Conversely, xMAP technology immobilises antibody on the surface of microsphere, allowing researchers to pool different sets of microspheres into a well for multiplexing analytes testing. Furthermore, a virtue of the suspended microspheres provides a smaller surface area compared to a microplate well, which requiring small sample volume and reducing non-specific binding. Different from ELISA replying on enzyme-mediated amplification of signal, xMAP technology utilises the fluorescence which is more direct, stable and sensitive. Therefore, less volume of sample is required. This character of xMAP assay is essential when working with limited samples (like paediatric samples, cerebrospinal fluid, synovial fluid, mouse serum, etc.). As all the interested analytes are measured in one go, xMAP assay avoids sample frozen-thaw cycles as well.

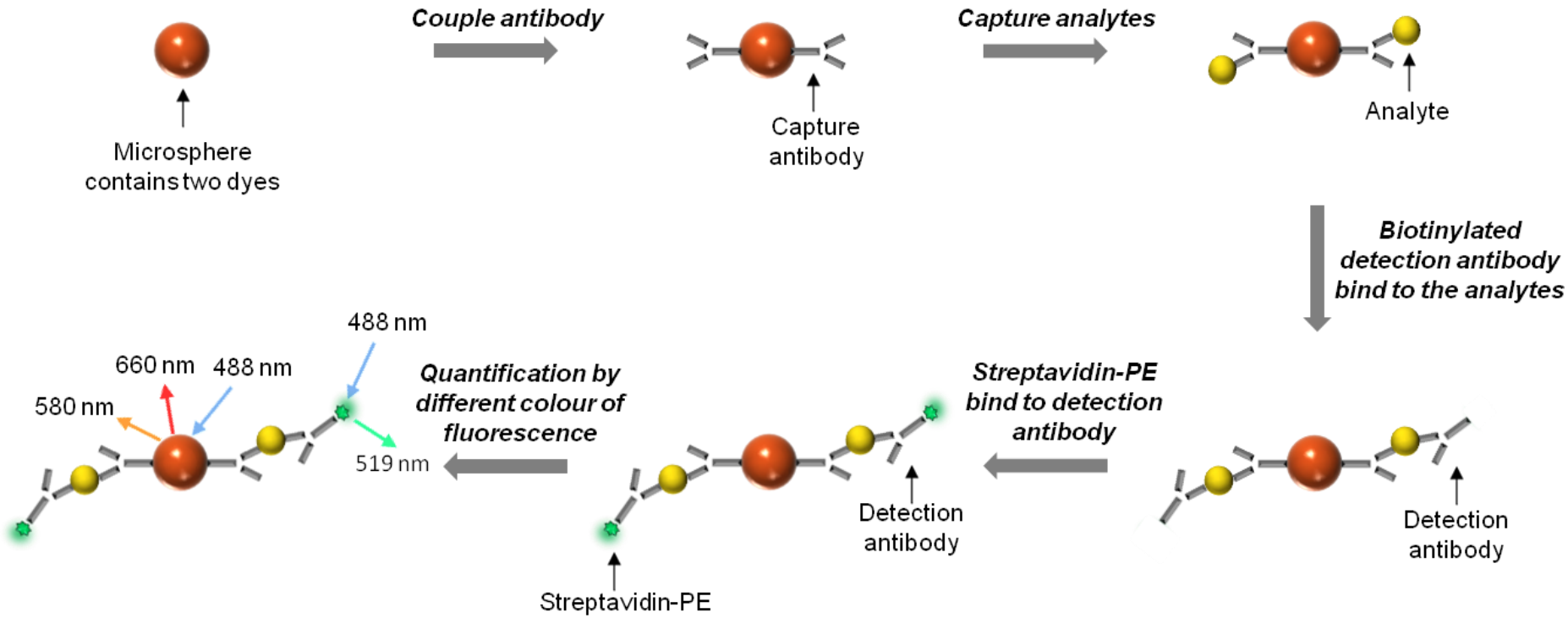

Figure 3.1 The workflow of xMAP technology. (The xMAP workflow is summerised based on references Fulton *et al.* Clinical Chemistry 1997[258] and Vignali Journal of Immunological Methods 2000[259])

Table 3.1 Advantages of xMAP technology compared to ELISA

	xMAP Technology	**ELISA**
Number of analytes	10	10
Number of 96-well plates	1	10
Total sample volume	12.5-25 µL	> 250 µL
Total time required	3 hours	> 30 hours
Assay range	5 to 6 logs dynamic range	3 to 4 logs dynamic range
Cost	< £2,000	> £3,000

3.1.2.4 Why choose this method

After cell death, histones are released into the circulation, decondensed and degraded into dimers (H3/H4 and H2A/H2B), monomer (H1, H2A, H2B, H3 and H4) and truncated histones (N and C terminal of each histone)[232]. In the previous chapters and our previous studies, the toxicity of extracellular histones has been proved both *in vitro* and *in vivo.* Therefore, a multiplexing assay is required to monitor the levels of histones and provide the guidance to clinicians.

3.2 Martials and Methods

3.2.1 Separation and storage of samples

Peripheral blood was collected into S-Monovette sodium citrate 10 mL tube (Sarstedt, Germany) from patients and healthy donors after consenting and with the ethical approval (Liverpool Ethics Committee). Blood was separated by spinning at 2,600 × g for 20 mins at 4^{o}C for 20 min with break off. Plasma was removed without disturbing the white layer and kept at -80^{o}C till using.

3.2.2 Multiplexing assay

3.2.2.1 Carbodiimide coupling

To determine the affinity of anti-histone single chain variable fragments (ahscFv), detection antibody and the specificities of the capture antibodies, the immobilised individual histones were utilised. Also, the capture antibodies were coupled to the microspheres to make the "capture sandwich" assay. The coupling protocol is below.

Five regions (33, 34, 35, 36 and 37) of Luminex MagPlex microspheres were brought from Luminex Corporation (USA). Each microsphere of 200 µL were added into 1.5 mL reaction tube (Protein Lobind, Eppendorf, Germany). Microspheres were fixed by placed in the magnetic separator for 30 s and liquid was removed carefully. Microspheres were washed twice with 200 µL of Activation Buffer (100 mM Na_2HPO_4, Ph 6.2) and incubated in 80 µL Activation Buffer plus 10 µL Sulfo-NHS (50 mg/mL; Pierce, USA) and 10 µL EDC (50 mg/mL; Pierce, USA) for 20 min, 650 rpm, at room temperature on a roll mixer in the dark. Then activated microspheres were washed three times with 500 µL Coupling Buffer (50 mM MES hydrate, Ph 5.0; Pierce, USA). Buffer was removed from last wash. Histone antibodies (each 5 µg) or designed concentrations

of histones in 250 µL Coupling Buffer was mixed with microspheres. The mixture was incubated 2 h, 650 rpm at room temperature on a roll mixer in dark. Microspheres were washed three times with 500 µL Wash Buffer and resuspended in 100 µL Block Store Buffer, then stored at 4°C protecting from the light. Buffer recipes are summarised in Table 3.2. Anti-histone antibodies are summarised in Table 3.3.

Table 3.2 Buffer recipes of carbodiimide coupling

Buffer	**Chemicals**	**Company**
Activation Buffer	100 mM Na_2HPO4, pH 6.2	Sigma, UK
Coupling Buffer	50 mM MES hydrate, pH 5.0	Pierce, USA
Wash Buffer	PBS + 0.05% Tween20	Sigma, UK
Block Store Buffer	PBS + 1% BSA	Sigma, UK

PBS, phosphate buffered saline; BSA, bovine serum albumin.

Table 3.3 Anti-histone capture antibody list

Antibody	**Antigen**	**Catalogue**	**Company**
Anti-histone H1.0	Human histone H1.0 N ter	SAB401366	Sigma, UK
Anti-histone H2A	Human histone H2A C ter	L88A6	Cell Signalling, UK
Anti-histone H2B	Human histone H2B C ter	Ab1790	Abcam, UK
Anti-histone H3.1	Human histone H3.1 N ter	H9289	Sigma, UK
Anti-histone H4	Human histone H4 N ter	Ab70701	Abcam, UK

3.2.2.2 Microspheres recovery counting

After coupling procedure, the microspheres recovery counting is necessary. The stock microsphere was vortexed thoroughly for 20 s. Took 2 µL from the stock and mixed with 998 µL Wash Buffer in a 1.5 mL Eppendorf tube. The tube was vortexed for 1 min. Microspheres solution of 100 µL per well was transferred into a 96-well filter plate (Millipore, UK). Plate was placed on a shaker for 10 min, 900 rpm at room temperature before applying to the Bio-Rad Mutilplex plate reader (USA). Bio-Rad 200 was used to count microspheres. Parameters were set as Sample Size: 50 µL, Time Out: 80 s, Total Beads: 10,000. The number of microspheres in the bead stock was calculated as: Beads per µL stock = counted beads × dilution factor / 30.

3.2.2.3 Biotinylation of antibodies

The ratio of biotin and detection antibody in molar is essential. Ideally, 20 or 50-fold of biotin are used in the biotinylation procedure in many literatures. A 20-fold of biotin was used in this protocol and the mass of biotin was calculated based on the molecular weight of itself and the antibody, M (Sulfo-NHS-LC-LC-Biotin, Pierce): 670 Da (670 g/mol), M (anti-histone antibodies): 150 kDa (150,000 g/mol), M (ahscFv): 27 kDa (27,000 g/mol). Sulfo-NHS-LC-LC-Biotin was dissolved in PBS and calculated volume was incubated with detection antibody in PBS for 2 h on ice. The excessed biotin was removed by the desalt column (Pierce, USA). The concentration of biotinylated antibody was adjusted to 250 µg/mL by addition of glycerol and stored at -20^{o}C.

3.2.2.4 ahscFv dose optimisation

The 5 different sets of histone coupled microspheres were pooled (20,000 beads per region). 96-well filter plate was blocked with 100 µL Blocking Store Buffer per well for 10 min at room temperature. Buffer was removed by vacuum filtration (Bio-Rad, USA). Pooled microspheres of 25 µL was added in each well. Microspheres solution was removed as before. Biotinylated detection antibody (30 µL) was added as: 0, 0.1, 0.5, 2.5, 12.5, 25 µg/mL. Plate was incubated for 1 h, 650 rpm at room temperature and washed three times with 100 µL Wash Buffer. Streptavidin-PE (2 µg/mL in Block Store Buffer; BioLegend, UK) of 30 µL was added per well and incubated for 30 min in the same condition. Microspheres were washed as before and resuspended in 100 µL Assay Buffer. Before reading, shake plate for 1 min at 900 rpm. Set parameters as before and gate between 7,500 – 15,000.

3.2.2.5 Check the specificity of capture antibodies

Five regions of histone coupled microspheres and biotinylated anti-histone antibody (0, 5, 15, 20 and 25 µg/mL) were used to check the specificity. Please see the protocol in 3.2.2.4 section.

3.2.2.6 Create single-plex of each histone and multiplex in pure system

Five specific antibodies were confirmed in the 3.3.2.5 section and coupled to 5 different regions of microspheres respectively. All the regions were counted and the desired mount of each region was diluted to 400 beads/µL. ahscFv was biotinylated (concentration of stock: 125 µg/mL). After blocking the 96-well filter plate, for the singleplex, 25 µL of beads (1000 beads per well) and 25 µL of recombinant individual histone (three-fold serial dilution: 30 µg/mL to 0.12 µg/mL in Block Store Buffer and blank) were added. Plate was incubated for 2 h, 650 rpm and at room temperature and washed with Wash Buffer 100 µL × 3. Then incubated with 30 µL of ahscFv-biotin (25 µg/mL) for 1 h, 650 rpm and at room temperature. Plate was washed as before and incubated with 30 µL of streptavidin-PE (2 µg/mL) for 30 min, 650 rpm at room temperature. Plate was washed as before and beads were resuspended in 100 µL of Block Store Buffer (plus 0.05% Tween20). Plate was shaken for 1 min at 900 rpm before reading. For the multiplex, 5 regions of beads were pooled, 1000 beads per region per well. Five recombinant histones were mixed and diluted serially. Concentration calculated per histone was as the same as the singleplex. The rest steps were as the same as the singleplex.

3.2.2.7 Standard curve recovery and sample dilution ratio

The effect of different matrix is essential in immunoassay: the standard curve is normally shifted in serum or plasma compared to the buffer pure system. Therefore, we used normal human plasma as a matrix to optimise the standard curve. The ratio between

plasma and buffer is 1:5. We spiked the plasma/buffer with a serial concentration of histones. Because of the proteases in plasma, the cocktail protease inhibitors (Roche, Germany), d-phenylalanyl-l-prolyl-l-arginyl chloromethylketone (PPACK; Merck, Germany) and ethylenediaminetetraacetic acid (EDTA) were added to protect the clotting and protein degradation. The ratio of sample dilution was detected.

3.3 Results

3.3.1 The optimum dose of ahscFv to individual histones

The ahscFv at all different concentration can bind to the individual histones but it appeared that the binding to histone H4 and H3 were higher than H1, H2A and H2B as reflected by mean FI (MFI) values. The binding of biotinylated ahscFv to detect the immobilised histones was concentration dependent with a dose of 25 µg/mL nearly reach plateau for all the histones (Figure 3.2).

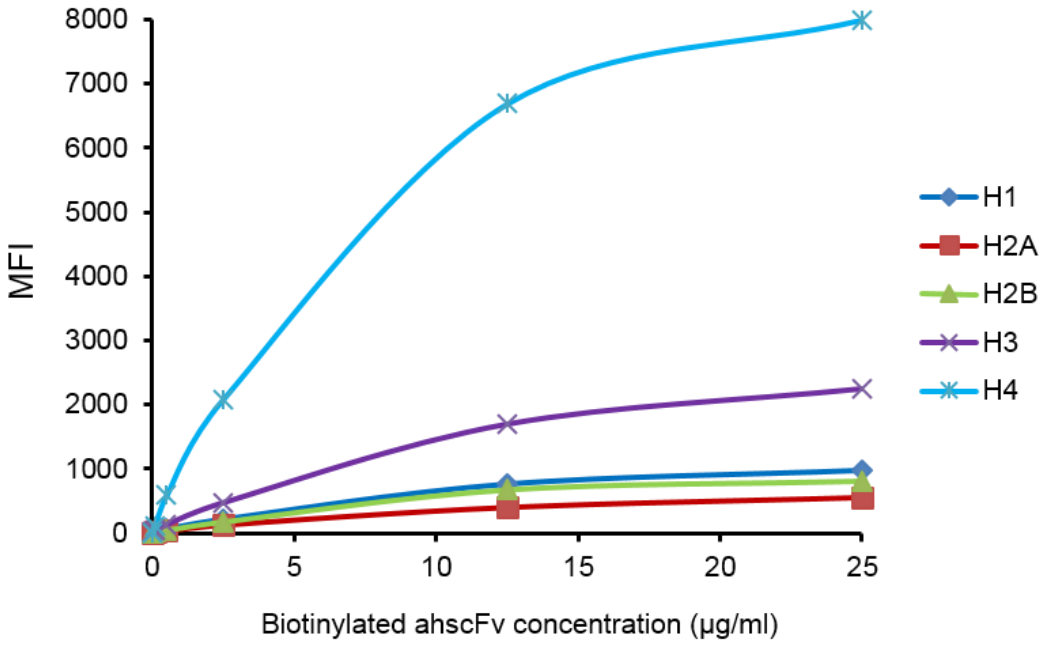

Figure 3.2 The optimum dose of ahscFv to individual histones. Different concentrations of biotinylated ahscFv were used to detect the immobilised histones. ahscFv can bind to all the individual histones but it has higher affinity to histone H4 and H3, while lower affinity to H1, H2A and H2B. The optimal concentration of ahscFv was 25 µg/mL.

3.3.2 All the capture antibodies are specific to the target histones

The specificities of all the capture antibodies were determined by the immobilised histones. Individual histones were coupled to different region of microspheres and the capture antibodies were conjugated with biotin (biotinylated). Each capture antibody was incubated with mixed histone coupled microspheres. Each capture antibody showed dose-dependent binding signal to the target histone, while had minimum cross reaction with other histones (Figure 3.3).

3.3.3 Measuring individual histones in Singleplex and Multiplex

Each capture antibody was coupled to different region of microsphere and the beads counting are shown in Table 3.4. Each histone was detected both in Singleplex and Multiplex (Figure 3.4). The MFI values in both Singleplex and Multiplex of histones H2A, H2B and H3 were constant, implying these 3 antibodies did not have cross-reaction or interference in Multiplex compared to Singleplex. However, MFI values in Multiplex of histones H1 and H4 were higher than that in Singleplex.

Table 3.4 Beads counting of couple histone antibodies

Antibody	Region	Beads count_1	Beads count_2	Average	Beads/µl
H1	33	898	719	808.5	6738
H2A	34	749	712	730.5	6088
H2B	35	791	770	780.5	6504
H3	36	768	743	755.5	6296
H4	37	1044	1059	1051.5	8763

Beads per µL stock = Average × 500/ 30. Dilution factor was 1:500.

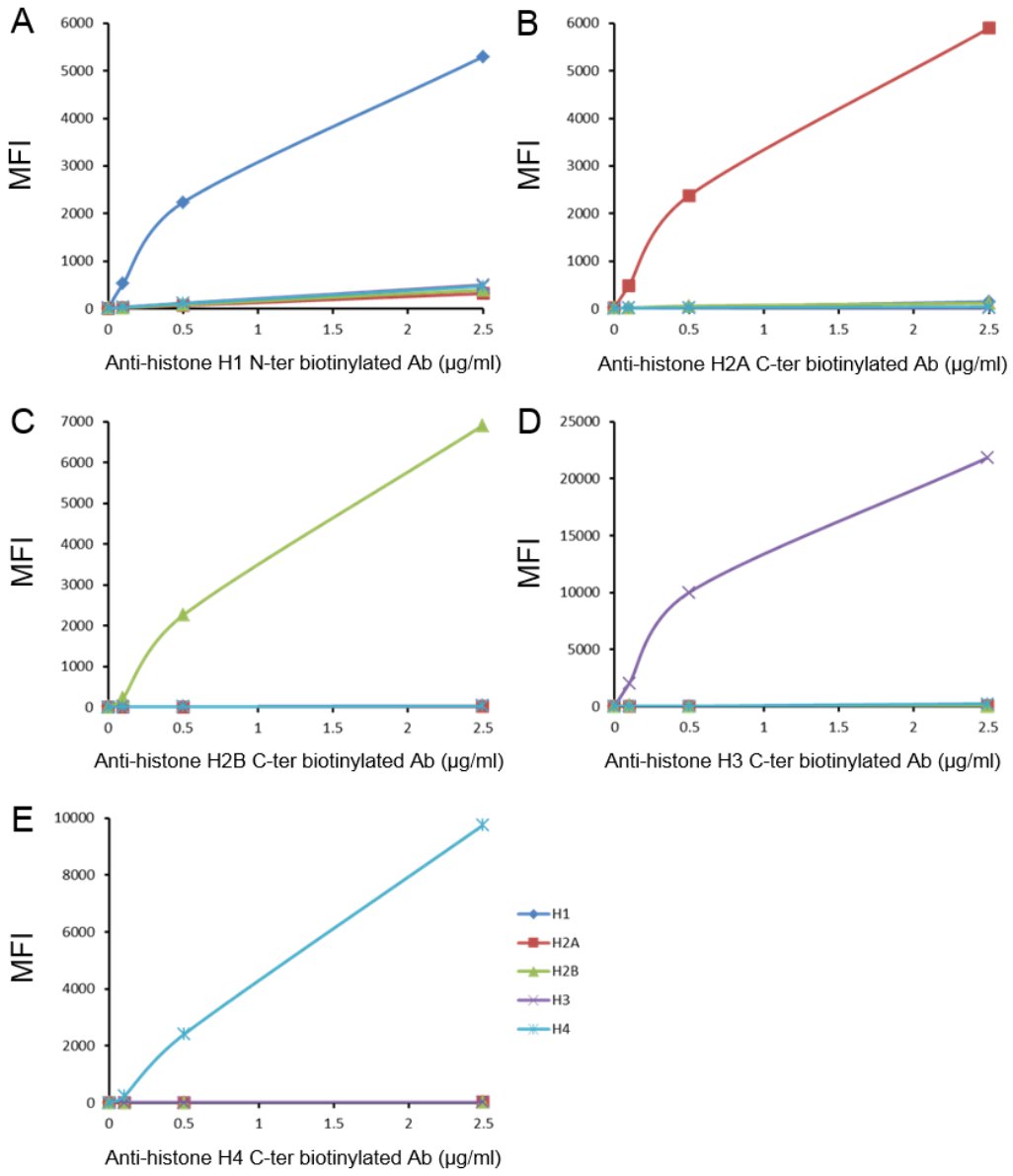

Figure 3.3 Effects of detection antibodies to target histones. Each histone (5 µg) was immobilised to different region of beads. To determine the specificity of each capture antibody, different concentrations of biotinylated antibody (0, 0.1, 0.5 and 2.5 µg/mL) were incubated with the mixture of immobilised histones. Graphs A-E indicate the specificities of the 5 detection antibodies.

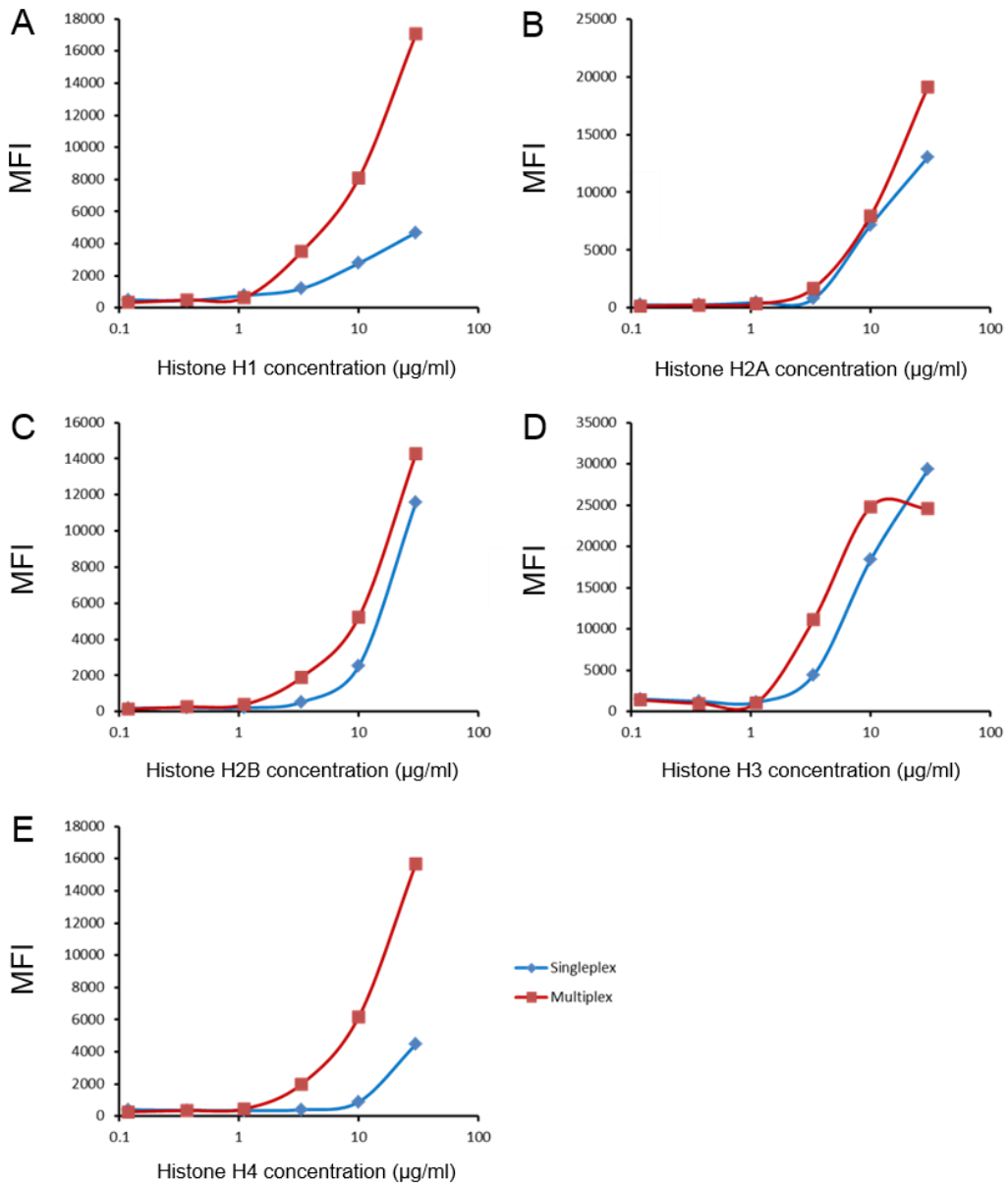

Figure 3.4 Individual histones were measured in Singleplex and Multiplex assays. Graphs A-E depict measured individual histone concentration. Except histones H1 and H4, the MFI values in Singleplex and Multiplex assays were similar in histones H2A, H2B and H3, indicating the specificity of these three capture antibodies. The MFI values of Multiplex were higher than those of Singleplex both in H1 and H4, indicating these two capture antibodies might have cross reaction between histones.

3.3.4 Histone detection is dramatically masked by normal human plasma

Generally, it is better to dilute patient plasma at least 1:5 to avoid the plasma interference to the antibody and the sample clotting. As a result, we tried to optimise the matrix effects by using addition of normal human plasma in PBS (+ 1% BSA) Buffer (1:5 v/v) after creating the standard curves in the Buffer. The MFI values for all histones decreased in the spiked plasma when compared to those in the Buffer (Figure 3.5).

3.3.5 Optimisation of matrix effects according to standard curves

As the depression of plasma to histone detection, we tried to optimise the measurement by adjusting detergent volume, salt concentration, pH value, temperature, incubation time, denature reagents and acid precipitation.

3.3.5.1 Addition of Tween20 maximally increases the detection signal

There are abundant of proteins in normal plasma[214, 261-263], which are prone to hamper the binding between capture antibody and histone. Therefore, different concentrations of Tween20 were added to dissociate the interference between histones and plasma proteins. The addition of Tween20 resulted in increasing histone signals and the background comparing to those without Tween20 in plasma/PBS matrix. However, the concentration of Tween20 was inversely proportional to background within the Tween20 addition groups. Considered the detection signal and background, we decided to use 0.2% Tween20 as the optimal concentration (Figure 3.6).

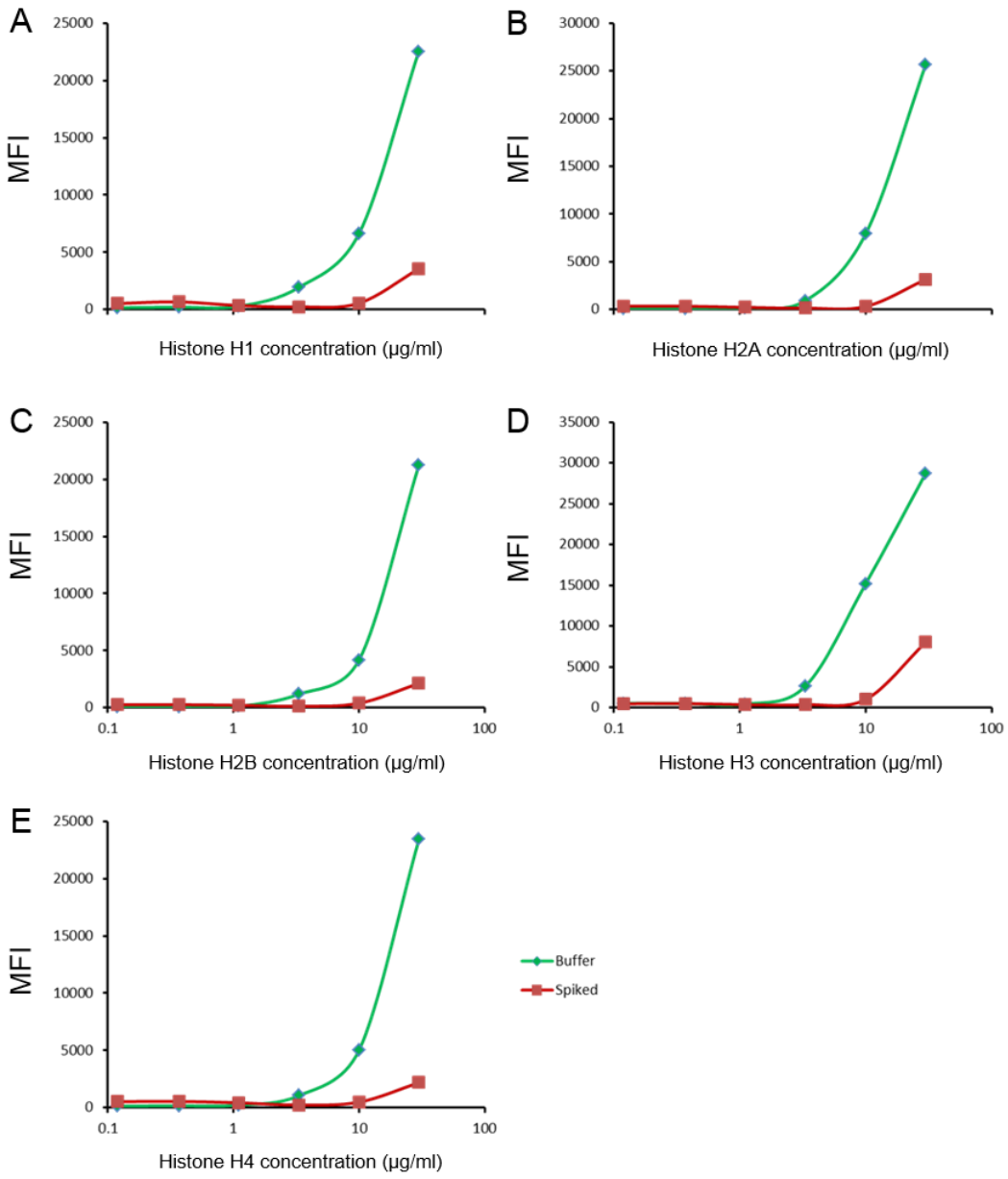

Figure 3.5 Normal human plasma depresses the histone detection in Multiplex assay. Green line is the MFI value detected in PBS (+ 1% BSA) Buffer and the red line is the MFI value of histone spiked normal human plasma/PBS (+ 1% BSA) Buffer (1:5). For all histones (A-E), the MFI values significantly decreased in spiked plasma than those in the Buffer.

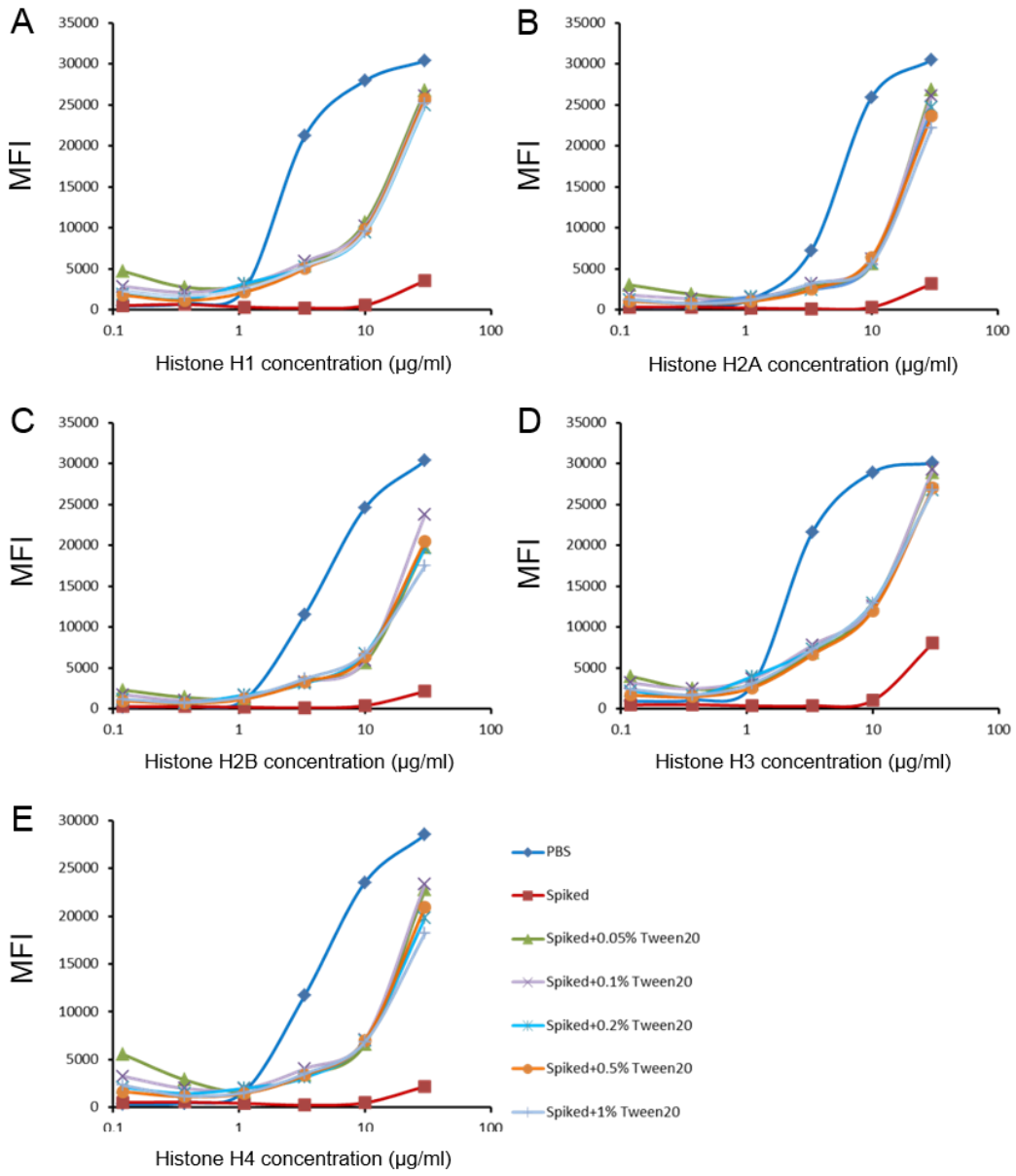

Figure 3.6 Addition of Tween20 maximally increases the detection signal in Multiplex. Graph A-E describe the effects of different concentrations of Tween20 (0, 0.05%, 0.1%, 0.2%, 0.5% and 1%) to dissociate histone-plasma protein interaction. The addition of Tween20 increased the detection signals while the increased background was observed in all the histones detection. However, the higher concentration of Tween20, the lower background of histones. Compare the background and detection signals, 0.2% Tween20 is the optimal concentration.

3.3.5.2 Addition of NaCl increases histone H3 signal

Addition of Tween20 increased the histone detection signals by dissociating histone-plasma protein interaction, but the effect did not make 100% recovery. Salt conditions can also effect the protein-protein interactions. Therefore, different concentrations of NaCl were added in the presence of Tween20. Adding 150 mM of NaCl showed a higher signal with the lowest background in the presence of 0.2% Tween20 (Figure 3.7).

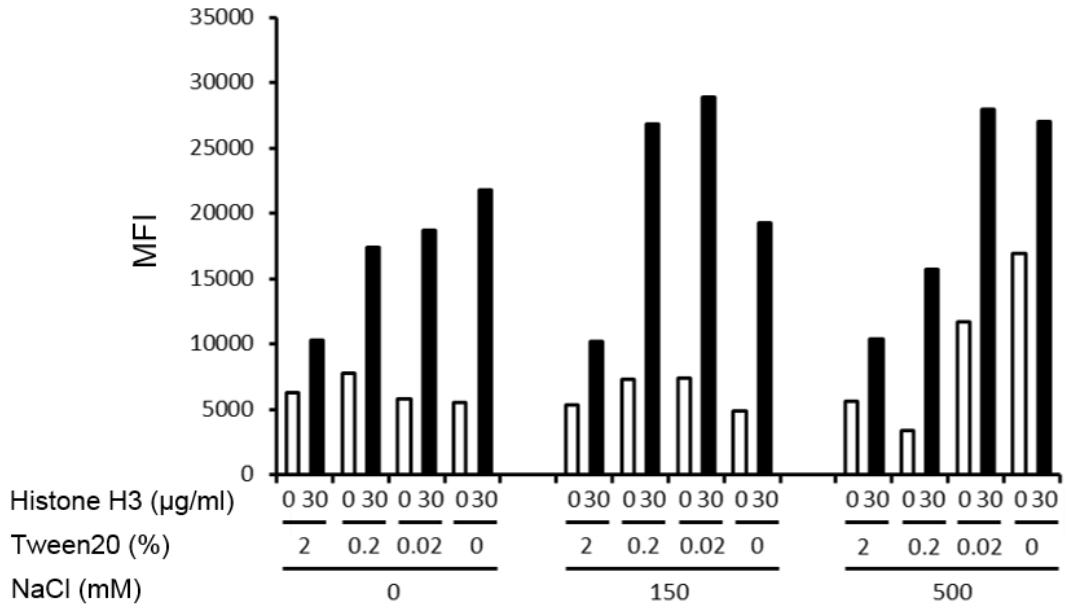

Figure 3.7 Salt condition increases histone H3 detection signal. Different concentrations of NaCl were added to dissociate histone-plasma proteins interaction in the presence of different concentrations of Tween20.

3.3.5.3 Circulating histones in positive patient plasma can't be detected

The positive patient plasma samples with high levels of histones determined by Western blot were measured along with the standards in pure buffer and normal human plasma. In the condition of 0.2% Tween20 and 150 mM NaCl, the 6 patients' plasma samples were undetectable even compared to the spiked normal plasma (Figure 3.8).

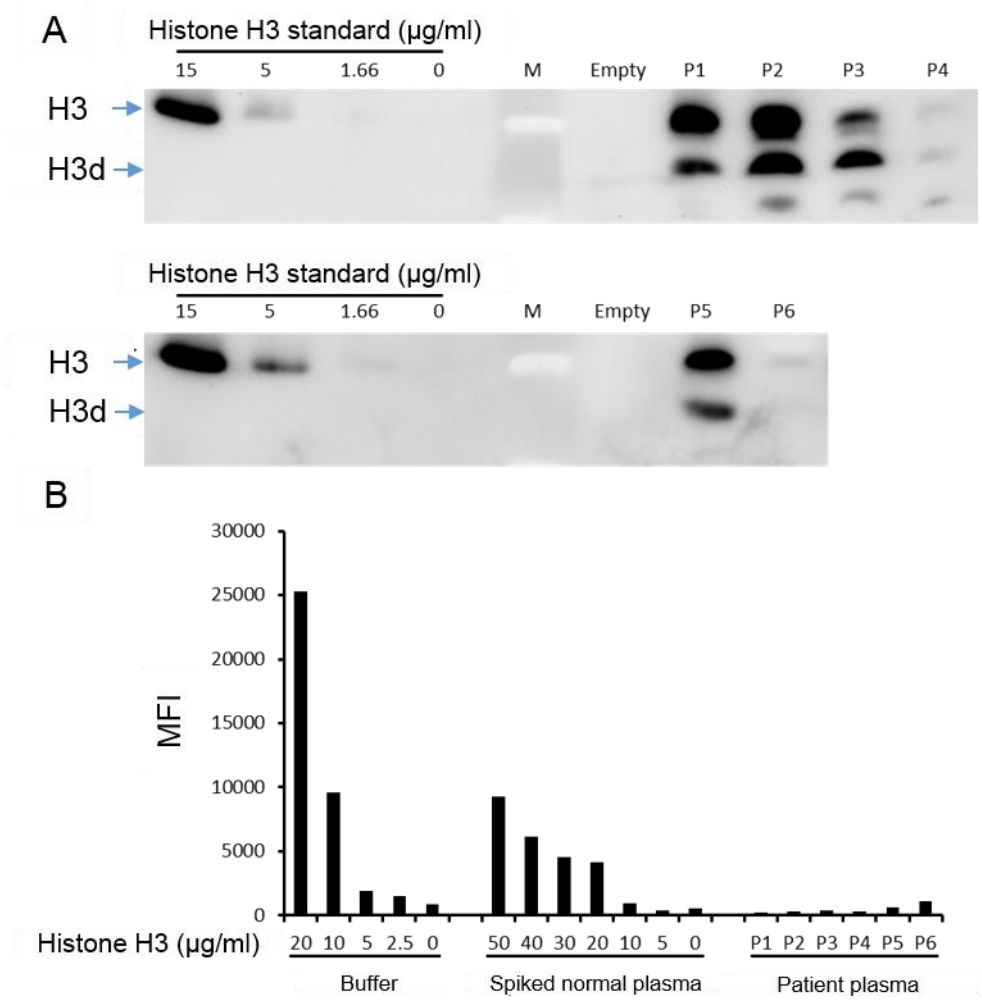

Figure 3.8 Histones in patient plasma are undetectable by the Multiplex assay. (A) Six patients' plasma histone levels were determined using Western blot by measuring histone H3. Presence of different concentrations of circulating histones in human patients. Patient 1 and 2 have the highest level of histone H3 (> 15 µg/mL) while patient 4 and 6 have the lowest levels (< 5 µg/mL). (B) Even with the salt and detergent condition (PBS + 150 mM NaCl + 0.2% Tween20), the Multiplex measurement of patient 1 to 5 were less than 10 µg/mL and patient 6 was more than 10 µg/mL. The results from Western blot and Multiplex assay were not constant, indicating that multiplex assay can't detect positive patient plasma.

3.3.5.4 Tween20 and salt condition can't improve the detection in patient plasma

As the signals in spiked normal plasma have been increased in the Tween20 and salt condition, we tried to optimise the measurement of patient plasma. Three positive patients' plasma were incubated in 150 mM NaCl/PBS buffer with different concentrations of Tween20 (0.02%, 0.05%, 0.1%, 0.2% and 0.5%) to dissociate histone-plasma proteins interference. The signals did not increase in patients' samples (Figure 3.9).

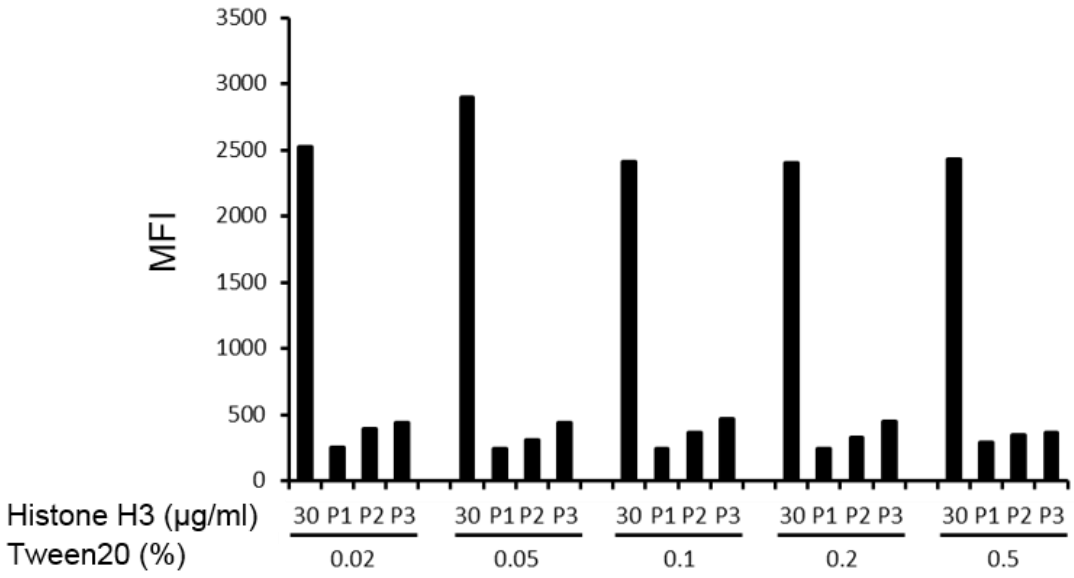

Figure 3.9 Tween20 and salt conditions can't optimise the detection of circulating histones in patient plasma. Different concentrations of Tween20 were added to dissociate histone-plasma proteins interaction in the presence of 150 mM NaCl. There was no significant difference among these 5 groups. Despite Tween20 and salt condition increased signals in spiked normal plasma, no improvement seem in patient plasma.

To confirm this result, we measured 20 more patients and 5 normal healthy donors' plasma in the condition of 0.2% Tween20 and 150 mM NaCl. We found that signals of histones measured by Multiplex assay were not constant with those determined by Western blot. Signals in normal healthy plasma were even higher than some positive patient plasma. Moreover, signals in spiked normal plasma decreased gradually paralleled to histone concentrations until 1.11 or 0.37 µg/mL then increased again in the following lower concentrations. Based on these results, we conclude that circulating histones are strongly bond to plasma proteins and the capture antibodies can bind to some plasma proteins as well.

3.3.5.5 Pre-incubation with acid, urea or Triton-X100 can't increase the signals

As the bind of histone-plasma protein is very difficult to break resulted in masking the epitope of histones, we tried to pre incubate sample with acid, urea and Triton-X100 for 20 min at room temperature respectively. However, signals in patient plasma can't increase either (Figure 3.10).

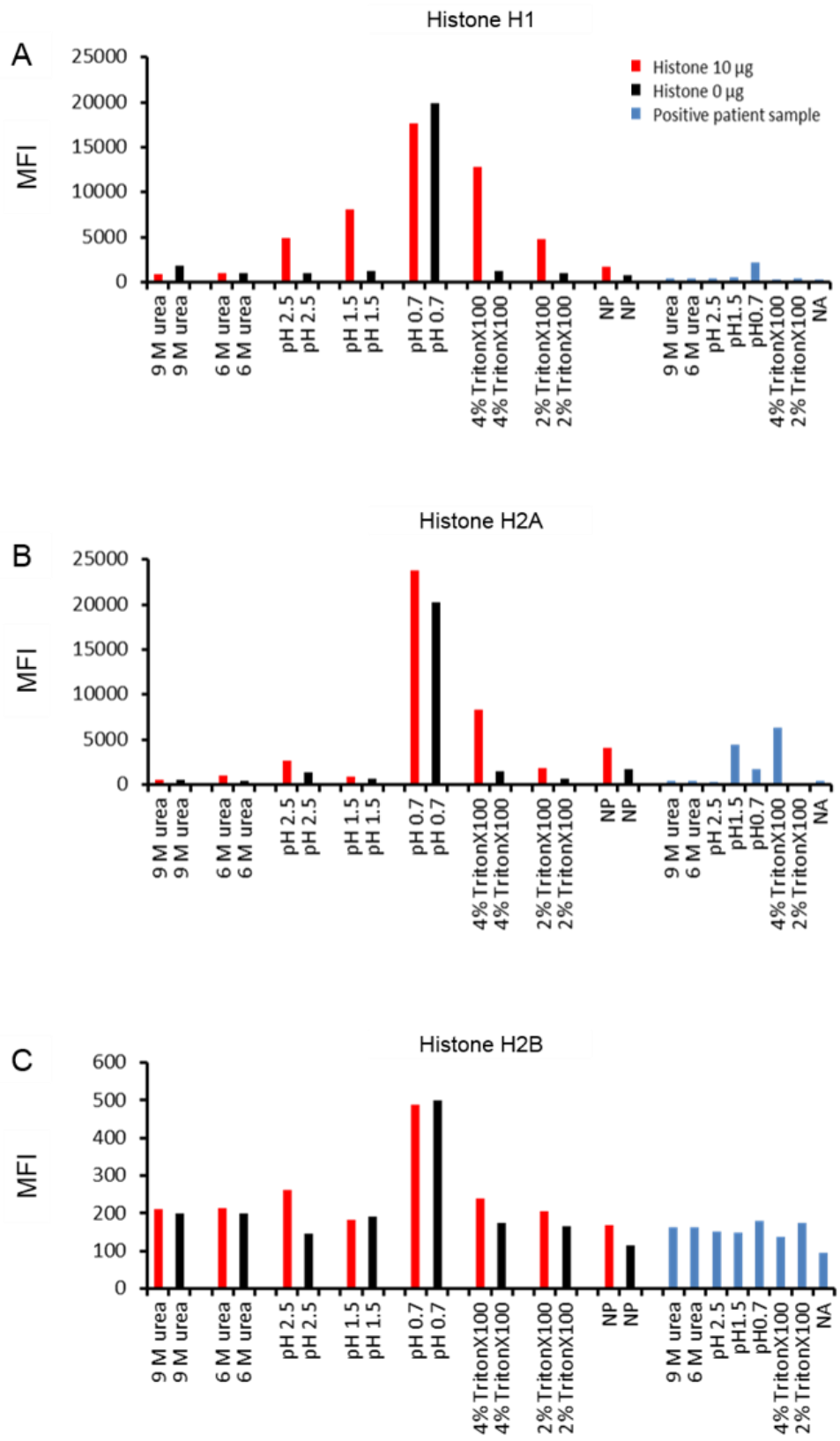
A
Histone H1
MFI
25000
20000
15000
10000
5000
0
Histone 10 µg
Histone 0 µg
Positive patient sample
9 M urea
9 M urea
6 M urea
6 M urea
pH 2.5
pH 2.5
pH 1.5
pH 1.5
pH 0.7
pH 0.7
4% TritonX100
4% TritonX100
2% TritonX100
2% TritonX100
NP
NP
9 M urea
6 M urea
pH 2.5
pH1.5
pH0.7
4% TritonX100
2% TritonX100
NA
B
Histone H2A
MFI
25000
20000
15000
10000
5000
0
9 M urea
9 M urea
6 M urea
6 M urea
pH 2.5
pH 2.5
pH 1.5
pH 1.5
pH 0.7
pH 0.7
4% TritonX100
4% TritonX100
2% TritonX100
2% TritonX100
NP
NP
9 M urea
6 M urea
pH 2.5
pH1.5
pH0.7
4% TritonX100
2% TritonX100
NA
C
Histone H2B
MFI
600
500
400
300
200
100
0
9 M urea
9 M urea
6 M urea
6 M urea
pH 2.5
pH 2.5
pH 1.5
pH 1.5
pH 0.7
pH 0.7
4% TritonX100
4% TritonX100
2% TritonX100
2% TritonX100
NP
NP
9 M urea
6 M urea
pH 2.5
pH1.5
pH0.7
4% TritonX100
2% TritonX100
NA

Figure 3.10 (continued)

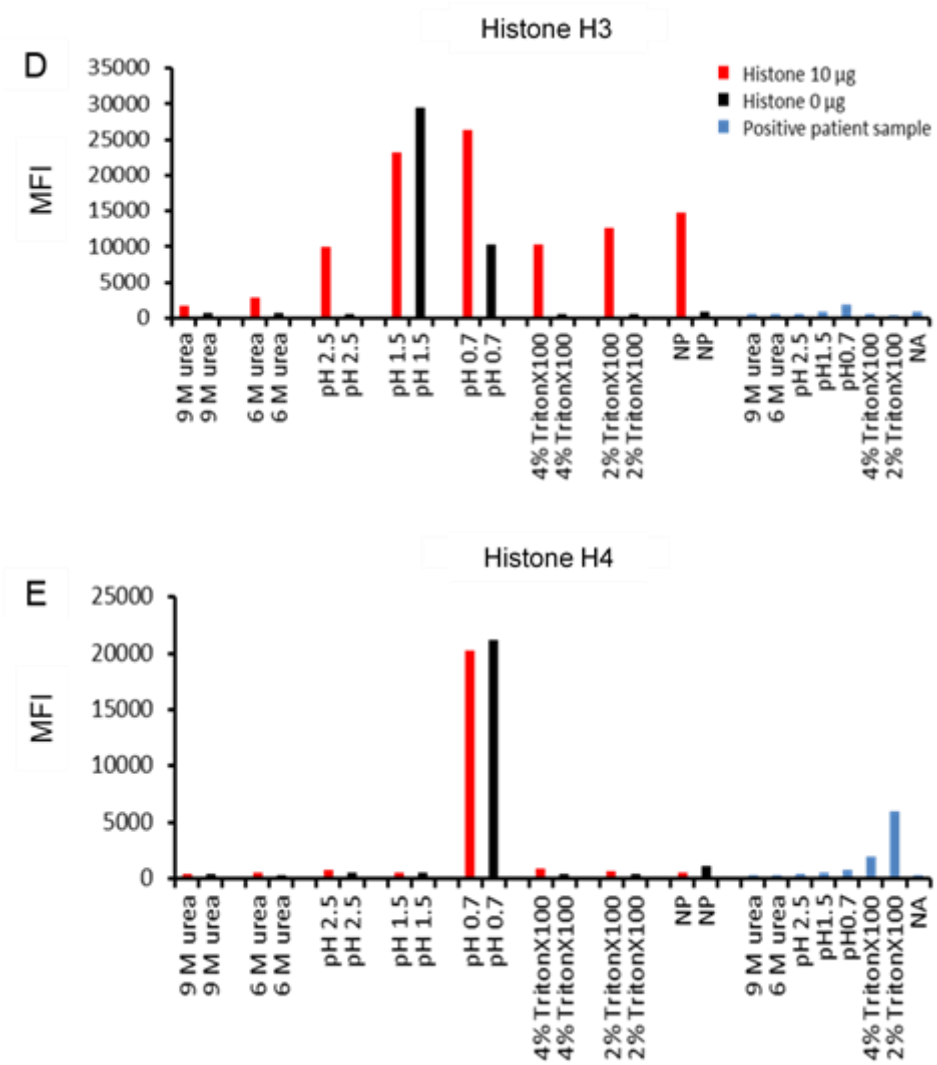

Figure 3.10 Pre-incubation with acid, TritionX100 and urea can't improve the detection of circulating histones in positive patient sample. Individual histone spiked normal plasma (each 10 µg/mL) and one positive patient plasma was pre-incubated with urea (9 and 6 M), HCl (pH 2.5, 1.5 and 0.7), or TritonX100 (4% and 2%) at room temperature for 20 mins before incubation of capture antibodies (A-E). Under the condition of pH 2.5 and 4% TritonX100 pre-incubation, all spiked histones had higher detection signals without significantly increased background. In pH 1.5 histone H3 and in pH 0.7 the rest of histones showed dramatically increased background even higher than the spiked signals without improving the detection of the positive patient plasma.

3.4 Discussion

Histones are released into the circulation after massive cells damage during the critical illness like trauma, sepsis, severe acute pancreatitis, etc[199]. The toxicity of circulating histones has been proved both *in vitro* and *in vivo*. In the Chapter 2, we have shown that not only monomer circulating histones but also truncated histones are toxic to endothelial cells. As monitoring others DAMPs such as circulating nucleosomes[211] have an increasing value in acute critical illness, to determine levels of circulating histones especially at early stage may have great translational value.

The existing method for testing the levels of circulating histones is Western blot, which has the limitation of time consuming (2 days procedure) and only 6 samples can be tested in one membrane. To build up a more robust and comprehensive assay, we adopted a bead based immunofluorescence technology: Luminex xMAP technology. We have created the standard curves for all the five monomers in the pure buffer system. However, all the standard curves were dramatically depressed by the addition of human plasma, which indicates plasma proteins have the capability to interact with circulating histones resulted in the epitope blockage or the cleavage. Then we tried to dissociate histone-plasma protein interaction.

High salt condition can dissociate protein-protein interaction in part. In low pH condition (less than 2.7), histones are still soluble while many of the other plasma proteins might dissociated and precipitated[264]. Detergent, like Tween20, contributes the dissociation somehow. We found that addition of 0.2% Tween20 or 150 mM NaCl increased the signals in spiked standard curves. However, neither detergent nor high salt

condition could increase the signals in patient plasma. The low pH pre incubation did not work either.

More than 30 components in normal plasma have been identified to bind histones by mass spectrometry[14]. Our study also showed C-reactive protein (CRP) elevated after presence of circulating histones in trauma patients and can form CRP-histone complex to reduce the toxicity of histone[265]. Moreover, we found complement C4 was pulled down by immobilised histones in plasma during the acute inflammation phase[265]. All of these results illuminate plasma has the capability to neutralise circulating histones released after cell death, which might be the host protective response. However, when massive cells death occurred, the amount of circulating histones exceed the maximal buffering capability of plasma, resulted in the aggravation of disease.

The key for this assay is to dissociate histones from plasma proteins or generate a more specific antibody.

Chapter 4 – Circulating histone levels reflect disease severity in animal models of acute pancreatitis

4.1 Introduction

Acute pancreatitis is an inflammatory disorder of the pancreas which ranges from mild, self-limiting form to local complication as well as systemic inflammation and multiple dysfunction syndrome (MODS)[266]. Although the understanding and surgical management of acute pancreatitis has improved significantly in the last two decades, there is no licensed specific medicine for this disease. To bridge this gap, better understanding the pathogenesis of acute pancreatitis and its associated local complications and MODS is paramount important[267]. Due to difficulties of accessing human pancreas samples and uncertainty of the admission time of acute pancreatitis patients, research on early cellular events are rarely carried out in human pancreatic acinar cells, not alone currently there is no acceptable methodology to culture primary pancreatic acinar cells.

As a result, animal models of different species have been employed to investigate acute pancreatitis, but in recent years there has been a prevailing trend towards using murine models, especially mice. These mouse models not only provide an opportunity to characterise the role of a specific gene or protein's in the pathogenesis of acute pancreatitis but also enable development of novel therapeutic strategies that target these signalling pathways. Experimental acute pancreatitis models can be generally divided into non-invasive and invasive models. The non-invasive animal models can be induced by simple protocols such as special secretagogue hyperstimulation, diet feeding, amino acid injection, or infection with specific viruses. Invasive models of acute pancreatitis require surgical intervention that is technically demanding and requires more expertise

along with specialised resources. The latter are useful for replicating the obstructive aetiologies of pancreatitis, particularly for investigating gallstone-, vascular- or trauma-induced acute pancreatitis[268].

An ideal animal model should include relevant aetiology, pathobiology, clinical course, histology and outcome, mirroring acute pancreatitis in humans. The current experimental acute pancreatitis models in use have their respective advantages and limitations. The most representative and widely used model are induced by repeated intraperitoneal injections of caerulein and intra-pancreatic ductal infusion of bile acid, respectively. The caerulein-induced acute pancreatitis (CER-AP) model is easy to conduct, highly reproducible, parallels a vast number of *in vitro* studies, making it the most favourable model for acute pancreatitis. It is also compatible with other models, sharing histopathological changes consistent with early phase of human acute pancreatitis[269]. Sodium taurocholate (NaTC) is the most frequently used bile acid to induce biliary acute pancreatitis. The distant organ injury and mortality are in accordance with concentrations of bile acid infused, making it very popular to study biliary acute pancreatitis[270]. Recently, a novel NaTC-induced acute pancreatitis (NaTC-AP) in mice has been developed by Laukkarinen and her colleagues, further facilitates its prevalence.

Similar to that in other critical illnesses, such as severe sepsis[34] and trauma[271], in which cellular breakdown products such as high mobility box 1 (HMGB1)[272], mitochondrial DNA[273] and extracellular histones[213], collectively called damage-associated molecular patterns (DAMPs) may play a significant role in acute pancreatitis[274]. Histones are well-conserved proteins that are essential for DNA packaging and gene regulation[225]. During

tissue damage and cell death, nuclear chromatin is cleaved into nucleosomes, which are released extracellularly[232] and further degraded into individual histones. Recent studies demonstrate their direct toxicity to endothelial cells as well as causing activation of platelets[275] and leukocytes to promote thrombosis[276], disturb the microvascular circulation and stimulate cytokine release[271]. In animal models, elevation of circulating histones is observed in inflammatory diseases such as sepsis[213], acute kidney injury[277], liver injury[278] and peritonitis[279]. Histone infusion causes animal death through MODS, which can be rescued by anti-histone antibodies[271]. The major mechanism for toxicity is due to histones binding phospholipids on cell membranes resulting in calcium influx and cellular injury[271]. In clinical practice, high circulating histone levels have been found in patients with severe blunt trauma and sepsis[271]. These levels are significantly associated with injury severity scores and sequential organ failure assessment (SOFA) scores as well as the incidence of respiratory and circulatory failure[271]. It is known that extensive cell death occurs in severe, particularly necrotising pancreatitis. However, there has been no direct evidence of linking circulating histones with the severity of acute pancreatitis.

In this chapter, we set out for the first time to sequentially measure circulating histone levels in mouse acute pancreatitis models at various time points to explore whether the release of circulating histones correlates with disease severity.

4.2 Materials and methods

4.2.1 Animals and reagents

C57BL/6 male mice of average weight (~22 g) from the SLAC Experimental Animal Centre (Shanghai, China) were housed at 23 ± 2°C under a 12 h light/dark cycle with ad libitum access to standard laboratory chow and water at the Research Centre of Gene Modified Mice, State Education Ministry Laboratory of Developmental Genes & Human Diseases (Southeast University, China). All procedures were performed according to state laws and monitored by local inspectors in compliance with Institutional ethical review processes of Southeast University.

The selection of acute pancreatitis models and the time points of blood collection and euthanization were based on our previous experience and preliminary experiments. All the reagents were at the highest grade from Sigma (Gillingham, UK) unless stated otherwise.

4.2.2 CER-AP

Supraphysiological concentration of caerulein, a cholecystokinin analogue, was dissolved in normal saline at a concentration of 10 μg/mL. Mice received either 4 or 12 repeated intraperitoneal injections of caerulein (50 μg/kg) at 1 h apart to induce oedematous pancreatitis[280] and necrotising pancreatitis[281], respectively. Control mice received same volume of normal saline injections. Blood was taken from tail veins before and various time points after first injection. Mice receiving 4 caerulein injections were sacrificed at 22 h (n = 10). Mice receiving 12 caerulein injections were sacrificed at 22 and 36 h after first injection (n = 10 for each time point). Control mice (n = 10) were sacrificed at 22 h.

4.2.3 NaTC-AP

NaTC-AP was performed by infusion of NaTC into the biliopancreatic duct with a slight modification of previous protocol[282]. Mice were anaesthetized by intraperitoneal injection of 10% chloral hydrate (5 mL/kg) before operation. A midline laparotomy was performed and the first loop of the duodenum together with a portion of pancreas was externalised. After successful cannulation of the biliopancreatic duct, 50 mg/kg NaTC (3.5%, w/v; 1 ml/kg bw) were infused. The success of this infusion is indicated by visualising methylene blue (0.2% w/v mixed with taurocholate) in the head of pancreas under a dissecting microscope. For control, 10 mice were subjected to the same surgical procedure without intraductal perfusion of Na-TC (sham group). Blood was taken before and at various time points after disease induction. Mice in Na-TC infusion group were euthanized at 22 and 36 h (n = 10 for each time point) and mice in the sham group were sacrificed at 22 h (n = 10).

4.2.4 Samples collections

Blood was collected and immediately centrifuged to separate plasma. Plasma was stored at -80^{o}C before use. Pancreas and lungs were extracted and fixed with 4% (w/v) paraformaldehyde for 24 h followed by 70% ethanol until embedded in paraffin.

4.2.5 Detection of circulating histones

The levels of circulating histones were detected using Western blot, as described previously[271]. In brief, plasma was subjected to a sodium dodecyl sulphate polyacrylamide (SDS-PAGE) using recombinant histone H3 protein as standard and detected by Western blot using anti-histone H3 antibody (Abcam, UK). Total histones

were calculated based on the molecular ratios of individual histones within the nucleus, as described previously[265, 271].

4.2.6 Blood biochemistry

Amylase, CK-MB, alanine transaminase (ALT) and creatinine were detected using AU5800 Clinical Chemistry System (Beckman coulter).

4.2.7 Histopathology examination and scoring

Organs were embedded and sections stained with hematoxylin and eosin (H&E). After H&E staining, each slide was graded by two independent observers who were blinded to experimental groups, according to a previously established protocol[283] but with the vacuolisation score was omitted. The severity and extent of pancreatic oedema, inflammatory cell infiltration and necrosis were each given a score of 0-4 and the overall histopathology score was calculated as the sum of the individual scores. For each parameter (e.g. oedema), 10 random fields were chosen and scored and the average score used for data analysis.

4.2.8 Statistical analysis

Results were presented as means ± standard errors of means (SEM) obtained from three or more independent experiments. Analysis of variance (ANOVA) was used to assess differences in parametric primary and secondary outcomes. For non-normally distributed, continuous variables the non-parametric Kruskal-Wallis *H* test was. The association of pathological scores with the levels of circulating histones was analysed using simple linear regression. *P* values of < 0.05 were considered to indicate significant differences.

4.3 Results

4.3.1 Modelling acute pancreatitis

In this study, 5 groups of mice were used, caerulein ×4, caerulein ×12 with 12 injections of saline (saline ×12) as control; NaTC intraductal infusion with a sham group as control in which same surgical procedures were performed but without intraductal infusion. Amylase was analysed in the blood taken at 22 h. All 3 pancreatitis groups showed dramatic increases in amylase (Figure 4.1A), which were significantly higher than that in the saline ×12 and sham groups ($P < 0.01$), indicating that acute pancreatitis was induced. Within the 3 pancreatitis groups, amylase levels were lowest in caerulein ×4 group and highest in NaTC group. Amylase in the sham group was not significantly higher than that in the saline group, which indicates that the surgical procedure alone did not cause pancreatitis.

Injury to heart, kidneys and liver were assessed by measuring CK-MB (Figure 4.1B), creatinine (Figure 4.1C) and ALT (Figure 4.1D), respectively. The mock surgical procedure (sham group) did increase CK-MB and ALT, which was likely due to stress responses. Caerulein ×12 caused significant increases in ALT. NaTC increased all the 3 markers but not when the same dose was administered intravenously (data not shown). These changes are therefore mainly due to pancreatitis.

Pathological examination showed that the caerulein × 4 induced obvious pancreatitis but hardly any necrotic areas were found in sections of the pancreas from all mice in the group. Instead, oedema, neutrophil infiltration and duct enlargement were the dominant pathological changes (Figure 4.1Ea), which are consistent with previous reports[284]. In contrast, caerulein ×12 caused obvious acinar cell death, as reported

previously[285] and substantial areas of necrosis were observed in the pancreas (Figure 4.1Eb). NaTC generated more severe pancreatitis with large areas of necrosis as well as haemorrhage in the pancreas (Figure 4.1Ec) than caerulein ×12. More obvious oedema and neutrophil infiltration were also observed in the caerulein ×12 and NaTC groups than in the caerulein ×4 group. Pathological changes in the lungs consisted mainly of increased thickening of alveolar walls, which were much more obvious in the NaTC group (Figure 4.1Ed-f) to indicate acute lung injury occurring in severe pancreatitis. No obvious pathological changes in liver, heart and kidneys were observed under optical microscopy (data not shown).

4.3.2 Twelve but not four injections of caerulein caused significant increase in circulating histones

Using Western blot, circulating histones were barely detectable in the saline group. Caerulein ×4 only caused slight increases in circulating histones at each time point tested (Figure 4.2A,B). Levels of circulating histones only reached statistical significance at 15 h after the first caerulein injection when compared with that before injection (2.5 ± 1.7 *vs.* 0.7 ± 0.3 μg/mL, $P < 0.05$). In contrast, caerulein ×12 induced dramatic elevation of both full length histone H3 and degraded H3 at 12, 24 and 36 h, as evidenced by strong bands on Western blots (Figure 4.2A,C). Levels of circulating histones reached a peak at 24 h and returned to near normal around 48 h after injection (data not shown). Peak levels of circulating histones were significantly higher than that in the caerulein ×4 group and these concentrations have been reported to be toxic in other experimental models[213].

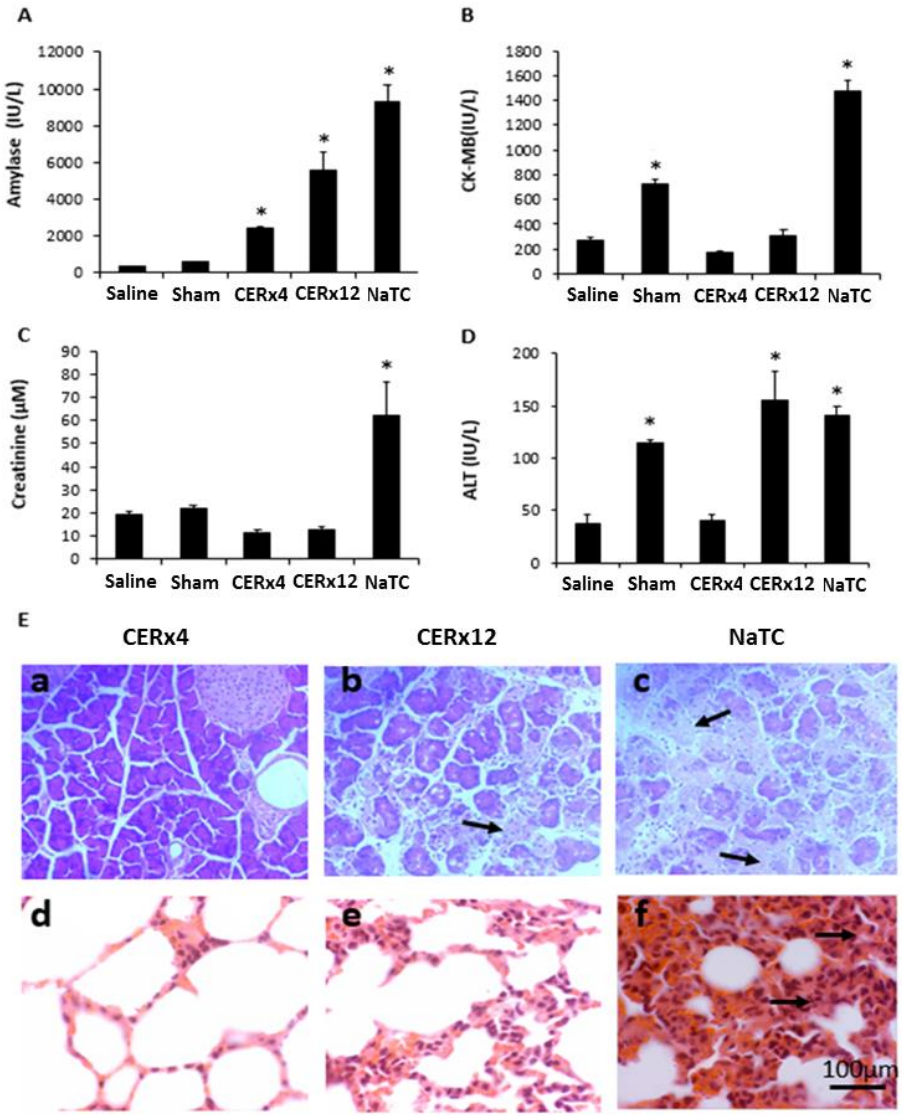

Figure 4.1 Generation of mouse models for oedematous and necrotising pancreatitis. (A-D): Blood amylase for pancreas (A), CK-MB for heart (B), creatinine for kidneys (C) and ALT for liver (D) were measured from 5 groups of mice: control group (UT) with saline i.p. × 12, mock surgical procedures without duct perfusion (Sham), caerulein i.p. × 4 (CER×4) and ×12 (CER×12) and duct perfusion of taurocholate (NaTC). Means ± SEM are presented. *ANOVA test $P < 0.05$ when compared to saline group. (E): Pathological examination of pancreas (upper panels) and lungs (lower panels) of the 3 mouse acute pancreatitis models. Typical images are presented. Black arrows in panels (b) and (c) indicate necrosis of acinar cells. Arrows in (f) indicate increased alveolar wall thickening. Bar = 100 μm.

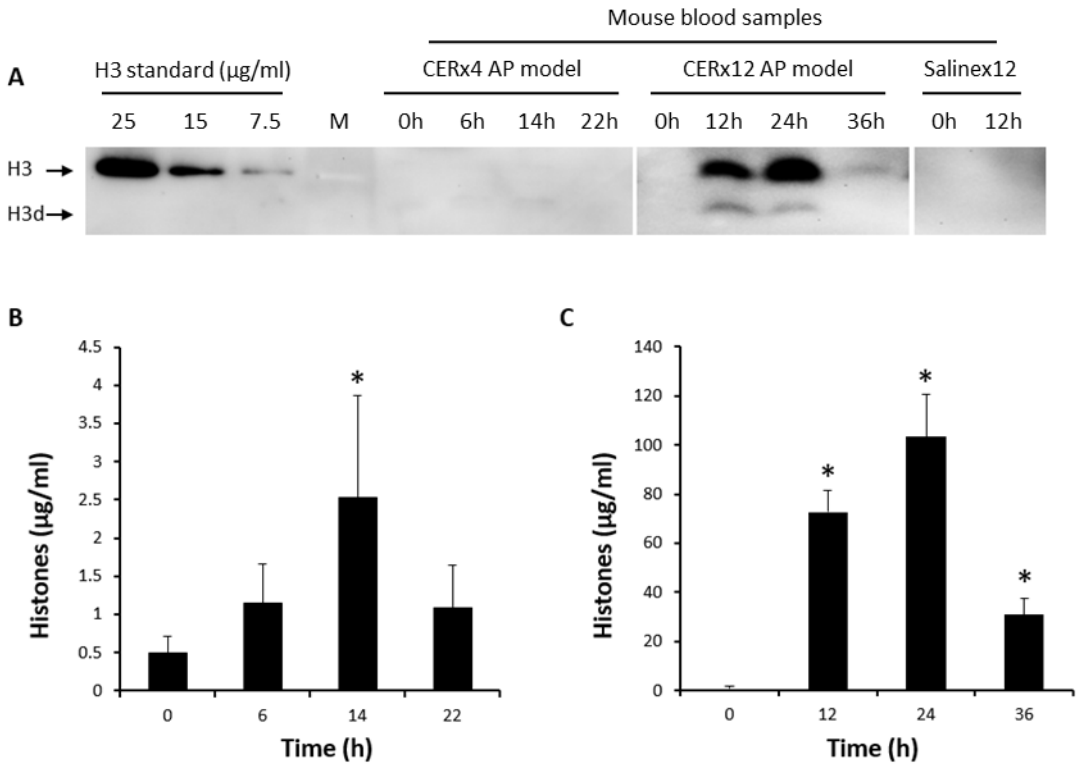

Figure 4.2 Circulating histones in acute pancreatitis models induced by i.p. injection of caerulein. (A) Circulating histone H3 from Caerulein ×4 (CER×4) and ×12 (CER×12) mouse models were detected using Western blot with recombinant H3 protein as standard. (B) Means ± SEM of total histones in CER×4 and (C) CER×12 models. *ANOVA test showed significant increase compared to pre-injection ($P < 0.05$).

4.3.3 Pancreatic duct infusion of NaTC caused the most significant elevation of circulating histones

In the NaTC-AP, circulating histones levels increased significantly from 4 h after NaTC infusion (23.2 ± 9.2 μg/mL; Figure 4.3A, B). There were steady elevations of circulating histone levels that reached a peak around 14 h (149.6 ± 40.6 μg/mL) (Figure 4.3B**).** There were no significant increases of circulating histones in mice in either the sham surgery group or the group receiving intravenous injections of NaTC at all matched time points (data not shown), indicating that the high circulating histone levels were not due to the surgical procedure or systemic toxicity of NaTC but due to NaTC-induced necrotising pancreatitis. Comparing the peak values in three acute pancreatitis models, we found that circulating histones were significantly higher in the NaTC group than in the caerulein ×12 group (149.6 ± 40.6 *vs.* 103.5 ± 17.3 μg/mL, $P = 0.02$) with both being much higher than the caerulein ×4 group (2.5 ± 1.7 μg/mL, $P < 0.05$; Figure 4.3C).

4.3.4 Circulating histone levels correlated with disease severity

Typical pancreatic histopathological changes are presented in Figure 4.1Ea-c and scores for all experimental groups are shown in Figure 4.4. Intraperitoneal saline injections and sham operation did not cause any discernible pancreatic histopathology changes. All 3 acute pancreatitis models showed obvious pancreatic morphological changes which were semi-quantified by histopathological scores, including overall score and its breakdown components – oedema, inflammation and necrosis (Figure 4.4). Caerulein ×12 and NaTC models were significant higher than caerulein ×4 model in all scores. No significant differences in oedema and inflammation scores were seen between caerulein ×12 and NaTC models but the necrosis scores were significantly higher in NaTC model

than in caerulein ×12 model (P = 0.02). By simple linear regression, peak values of circulating histones significantly correlated with necrosis scores (r = 0.63, P = 0.001) but not with inflammation (r = 0.27, P = 0.074) or oedema (r = 0.21, P = 0.132) scores (Table 4.1). These data suggest that damaged pancreatic acinar cells may be a major source of circulating histones.

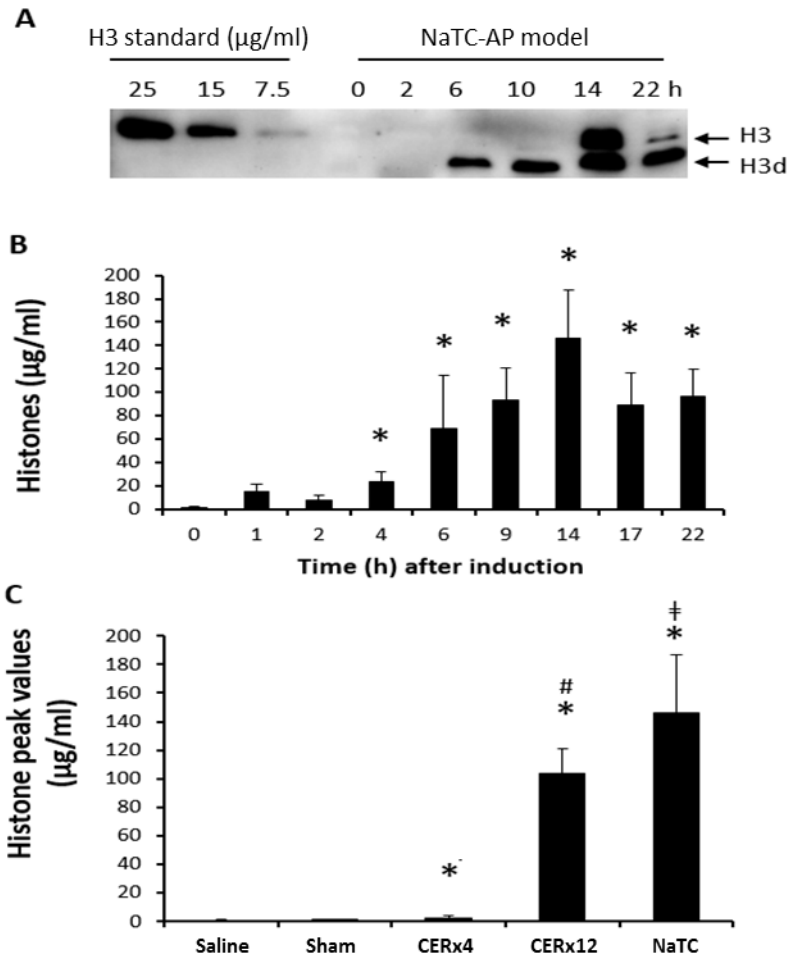

Figure 4.3 Circulating histones in NaTC-AP. (A) A typical Western blot of histone H3 in blood taken from a NaTC-AP at different time points. Top band is full length H3 and the lower band is degraded H3 (H3d). (B) Means ± SEM are presented to show the time course of the elevation in circulating histones.*ANOVA test $P < 0.05$ when compared with that before duct perfusion. (C) Comparison of the means ± SEM in peak values of total histones from 3 AP models and 2 control groups (Saline and Sham). *$P < 0.05$ *vs.* controls; #$P = 0.01$ *vs.* caerulein × 4 (CER×4); ǂ$P = 0.02$ *vs.* caerulein × 12 (CER×12).

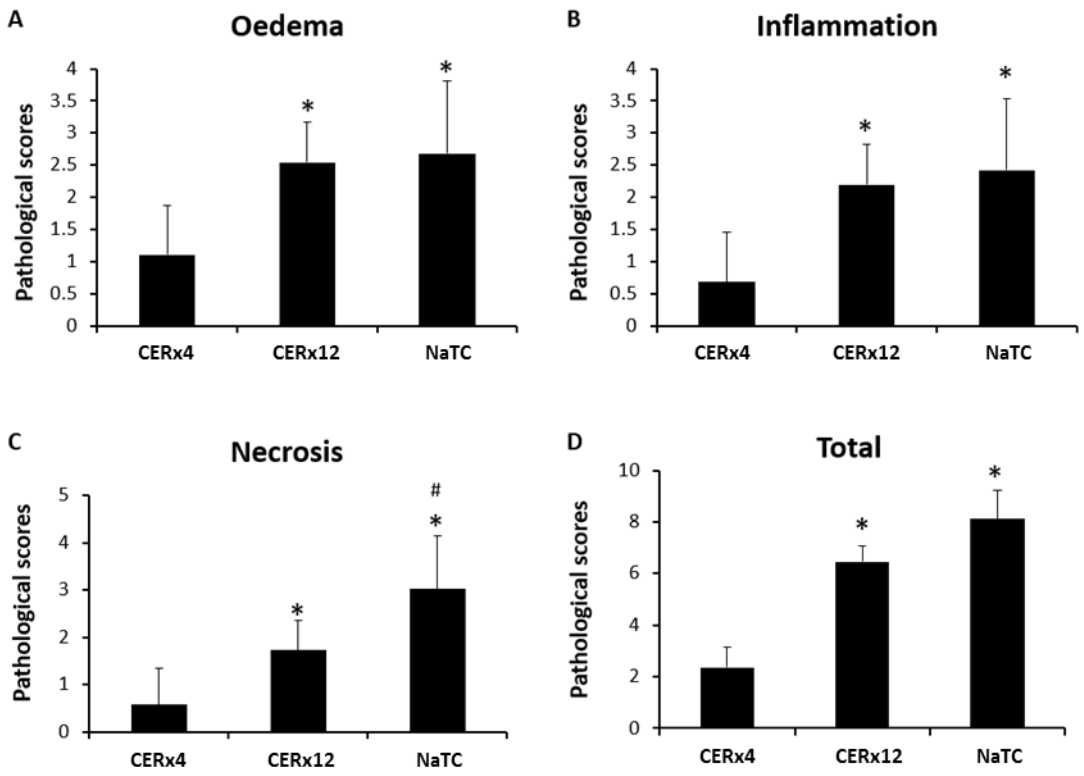

Figure 4.4 Pathological scores of pancreas of mouse acute pancreatitis models. Sections of pancreas collected at 22 h after acute pancreatitis induction were scored as described in Methods. Means ± SEM of the scores for (A) oedema, (B) inflammation and (C) necrosis as well as (D) combined (total = oedema + inflammation + necrosis) are presented. ANOVA test, **P* < 0.05 when compared to caerulein ×4 (CER×4). #*P* < 0.05 when duct perfusion (NaTC) was compared to caerulein ×12 (CER×12).

Table 4.1 Correlation of circulating histones to pancreas pathological scores

Pathological scores	**n**	***r***	***P***
Inflammation	30	0.27	0.074
Oedema	30	0.21	0.132
Necrosis	30	0.63	0.001

4.4 Discussion

This study is the first to demonstrate that there is a significant increase in circulating histones in experimental acute pancreatitis. In our animal models, we show that the significant elevation of circulating histones correlate well with pancreatic necrosis and is accompanied by increased systemic injury such as to the lung, heart, kidneys and liver, which are the most frequently affected distant organs by acute pancreatitis[286, 287].

Many types of acute pancreatitis animal models have been reported and the commonly used models include caerulein-induced models and biliopancreatic duct infusion models[288]. These models are also routinely used in our laboratories. In this study, we have generated acute pancreatitis models with 3 distinguishable levels of severities, with which we have established the association of levels in circulating histones with severity scores, particularly of necrotic scores of pancreas in pathological examination. In human acute pancreatitis, nuclear breakdown products such as HMBG1[289, 290] and DNA[291, 292] have already been shown to be released into the circulation and correlated with disease severity. Treatment with anti-H3 antibody suppresses serum HMGB1 levels and improves survival of L-arginine-induced acute pancreatitis in mice[222]. High levels of circulating histones in critical illnesses have been only reported recently and our study supports a similar principle that the levels of nuclear breakdown products in circulation reflect the severity of tissue damage and the extent of cell death. Histones as the most abundant proteins in nuclei may serve as a much better biomarker for stratification of disease severity.

In general, severe damage of any organ will release large amounts of histones into the circulation. When this exceeds the clearance capacity of the body, histones become

detectable in the circulation. Many diseases, such as severe trauma, burns, organ infarctions and sepsis, will incur simultaneous damage of large number of cells and lead to high levels of circulating histones[271]. In the mouse model of necrotising pancreatitis, a large number of acinar cells may die in a short time period and release large amounts of histones into the circulation where they can be detected. The strong correlation between the levels of circulating histones with pancreatic necrosis scores in mouse models of acute pancreatitis supports the notion that necrosis of acinar cells is a major source of histones. On the other hand, during acute inflammatory responses from a variety of aetiologies, inflammatory cells and neutrophils especially will accumulate and release their nuclear contents that include histones and DNA in the form of extracellular traps or neutrophil extracellular traps (NETs)[34]. Histones in NETs have also been shown to be toxic to the host[36, 37]. Since NET formation and release has not yet been studied in acute pancreatitis, we cannot rule out a significant role of NETs in the severity of acute pancreatitis.

The finding that concentrations of circulating nucleosomes and histones are strongly associated with the severity of trauma and other modes of cellular injury suggests possible usefulness as a new parameter for estimating tissue damage. Circulating histones are likely to be more directly linked to the underlying pathophysiological changes than other indices that are commonly used in clinical practice. In pancreatitis for example, levels of blood amylase are used as a diagnostic parameter although circulating histone levels might prove to be a better index of acinar cell death since amylase in patients with necrotising pancreatitis can be relatively low due to loss of acinar cells[293]. Increases in serum amylase mainly reflect leakage from acinar cells whilst significant increases in circulating histones indicate nuclear and cellular

breakdown. Since circulating histones appear to be directly linked to pathological damage in necrotizing pancreatitis, there is the potential for using circulating histones to stratify the severity of acute pancreatitis, particularly as there are no satisfactory clinical scoring systems, radiological modalities or biochemical makers to fulfill this purpose so far[294, 295].

The pathological roles of high circulating histone levels in severe pancreatitis are still not clear. Since the most lethal complication of severe pancreatitis is MODS, histones may contribute to acute lung injury, as discovered in animal experiments, and lead to respiratory failure which occurs in nearly 50% of patients with severe pancreatitis[296]. In line with previous findings of circulating histones being directly toxic to epithelial cells[297], endothelial cells[213], platelets[275] with secondary tissue injury through microvascular thrombosis[275, 298], these effects might lead to a secondary hit to the pancreas and other organs in increasing disease severity and worsening outcomes. Our findings suggest that release of histones from pancreatic damage may have devastating consequences and neutralising circulating histones may be of therapeutic value. The development of anti-histone therapies to suppress this second hit after the onset of acute pancreatitis might therefore be a rational therapeutic approach in the future.

In conclusion, histones are released into the circulation following the death of pancreatic acinar cells. This promises to be of significant translational potential, both in terms of measuring circulating histones as a biomarker of the severity of pancreatitis and targeting the toxicity of circulating histones to improve the outcome of patients with necrotising pancreatitis.

Chapter 5 – Circulating histone levels predict persistent organ failure and mortality in patients with acute pancreatitis within 24 hours of admission

5.1 Introduction

Acute pancreatitis is one of the leading gastrointestinal disorders that require urgent clinical care with an increasing incidence[299]. The clinical course of acute pancreatitis is variable ranging from mild (80%, uneventful clinical course), through moderate (local complication or transient organ failure) to severe disease (persistent organ failure, POF)[300-302]. Infected pancreatic necrosis[303, 304] and/or sepsis[286] are another major complications contributing to mortality at any stage. However the principal early cause of early death is the presence of POF[286, 305-307]. Early recognition of patients at risk of POF is critical to guide fluid resuscitation and initiate high dependency or intensive care treatment, to reduce morbidity and mortality[301, 308]. Indeed, early stratification of disease severity improves clinical outcomes and significantly reduces length of hospital stay[309].

Improvements in imaging, such as computerised tomographic (CT) scans, have not proven superior to clinical scoring systems in early prediction of acute pancreatitis severity[294, 295]. A recent multicentre study has shown that existing clinical scores such as Systemic Inflammatory Response Syndrome (SIRS), Bedside Index for Severity in Acute Pancreatitis (BISAP), Acute physiology and Chronic Health Examination II (APACHE II), Sequential Organ Failure Assessment (SOFA) either alone or in combination, have reached their maximal efficacy for early prediction of POF in acute pancreatitis patients and are of limited clinical use[295]. This is supported by a latest meta-analysis concluding that there is no adequate predictor for POF within 48 h of hospital admission[310]. A wide spectrum of clinical biomarkers for acute pancreatitis severity has been investigated over the last two decades. These include routine biomarkers[295, 311-314],

pancreas-specific enzymes[313-316], acute phase proteins such as C-reactive protein (CRP)[313, 314, 317], cytokines[313, 314], immunological components[314], transcriptomics[318], proteomics[319] and others[314]. Most of them are of low to moderate predictive value[314] and there is a pressing need for the identification and development of more powerful predictive markers in for these at risk patients.

Recently, damage associated molecular patterns (DAMPs), such as high-mobility group box 1 (HMGB1), cell-free DNA and nucleosomes, have been investigated in human acute pancreatitis and most studies showed their blood levels correlate with severity of the disease[223, 274]. Histones are well-conserved nuclear proteins that are essential for DNA packaging and gene regulation. During tissue damage and cell death, nuclear chromatin is cleaved and released extracellularly where it is degraded into individual histones[232]. Circulating histones, the most abundant nuclear proteins, are rapidly cleared by the liver[218] and are barely detectable in the blood unless there is extensive cell death[211], as in severe sepsis[213, 320, 321] and trauma[271]. Recent studies demonstrate circulating histones act as DAMPs to induce sterile inflammation and contribute to SIRS and organ failure[274]. Extracellular histones are also toxic to endothelial cells[213, 271], platelets[275, 276] and leukocytes[116]. Furthermore, they have been reported to activate coagulation, disturb microvascular circulation and stimulate cytokine release[271, 322, 323]. In mouse models, histone infusion causes animal death through multiple organ failure, which can be rescued by anti-histone antibodies[213, 271, 321]. Clinically, high levels of circulating histones have been found in patients with severe blunt trauma[271] and sepsis[320], with associations to the development of respiratory failure[271], new-onset cardiac complications[320] and thrombocytopenia[324]. We have previously demonstrated that circulating histone levels rise very early in mouse acute pancreatitis models, and are

also strongly associated with disease severity and distant organ injury[325]. Therefore, we hypothesised that plasma levels may predict major clinical outcomes in patients early in acute pancreatitis.

In this chapter, we investigated the ability of circulating histones to predict severe acute pancreatitis within 24 h after onset of abdominal pain in 236 consecutive patients.

5.2 Patients and methods

5.2.1 Study population and ethics

Consecutive acute pancreatitis patient admissions at The Royal Liverpool University Hospital (between June 2010 and March 2014) were enrolled once written informed consent was obtained. Inclusion criteria: (1) first episode of acute pancreatitis as defined by Revised Atlanta Classification (RAC)[300]; (2) blood samples obtained, processed and stored within 24 h of admission. Exclusion criteria: (1) age < 18 or > 85 years; (2) advanced pulmonary, cardiac, renal diseases or malignancy; (3) pregnancy, chronic pancreatitis, pancreatic neoplasm or trauma as aetiologies; (4) time of abdominal pain onset to admission > 24 h.

Peripheral blood samples from acute pancreatitis patients (n = 236) were collected within 24 h of admission (median of 24 h [range 5-48] after onset of abdominal pain) as well as from healthy volunteers (n = 47). White blood cells (WBC) were isolated and viability assessed by 0.1% trypan blue (Life Technologies, Warrington, UK) using a Countess™ automated cell counter (Invitrogen, Glasgow, UK). Serum and plasma were isolated and stored at -80°C in the National Institute for Health Research (NIHR) Liverpool Biomedical Research Unit Acute Pancreatitis Biobank, according to protocols approved by local research ethics committees (REC reference: 10/H1308/31 on 11/02/2010).

5.2.2 Study design

Demographic, laboratory, radiographic, microbiological, surgical and clinical outcome data were prospectively recorded and maintained in an e-database following standard operating procedures (SOPs) according to Good Clinical Laboratory Practice (GCLP)

standards. SIRS, BISAP, APACHE II and SOFA scores were calculated within 24 h of admission[295], according to published definitions. The first and the worst modified CT severity index (MCTSI) were enumerated using contrast-enhanced CT scans.

POF was defined as a truncated SOFA score of ≥ 2 for ≥ 48 h that manifested in failure of at least one of the respiratory, cardiovascular or renal systems[302]. In patients with pre-existing chronic kidney diseases (stage 1-3), a two-point worsening of kidney function, defined by estimated glomerular filtration rate[326], was used to define renal failure regardless of circulating creatinine levels. Local complications were defined as the presence of acute peri-pancreatic fluid collections (or pseudocysts), pancreatic necrosis (acute necrotic collections or walled-off necrosis), splenic or portal vein thromboses, gastric outlet obstruction, or colonic necrosis as per RAC[300]. Major infection was defined as the appearance of either infected pancreatic necrosis, sepsis, or both, which developed at least 3 days after admission.

5.2.3 Clinical biomarker analysis

Plasma histone levels were determined by quantitative Western blot previously established protocols[265, 271, 320, 321, 324]. Interleukin (IL)-6 and IL-8 (R&D, Abingdon, UK) were measured in plasma by enzyme-linked immunosorbent assay (ELISA) as per manufacturers' instructions. All measurements were performed in duplicates or triplicates by experienced laboratory staff, blinded to clinical data. Urea, creatinine, CRP and other routine clinical biomarkers were reported by the Department of Clinical Biochemistry, Royal Liverpool University Hospital, Liverpool, UK.

5.2.4 Statistical analysis

Descriptive data were reported as median with interquartile range (IQR) and number (percentage) for continuous variables and categorical parameters, respectively. Continuous variables were compared by the Mann-Whitney *U* test (2 groups) and Kruskal-Wallis *H* test (3 groups). Categorical data were compared using Chi-square or Fisher's exact tests. The correlation of circulating histones with MCTSI and WBC viability was assessed by Spearman rank correlation. Statistical significance was defined as $P < 0.05$. Receiver operating characteristics (ROC) curves were constructed for circulating histones and other markers in the prediction of POF, major infection and mortality. The area under curve (AUC) with 95% confidence intervals (CI) of circulating histones for each clinical outcome was compared with clinical scores and biomarkers. The optimum cut-offs for sensitivity, specificity, positive predictive value (PPV), negative predictive value (NPV), positive likelihood ratio (PLR) and negative likelihood ratio (NLR) of the assessed parameters were derived from the ROC curves.

5.3 Results

5.3.1 Patient characteristics

A total of 236 consecutive patients (mild: 156 (66.1%); moderate: 57 (24.2%); severe: 23 (9.7%)) fulfilling the inclusion and exclusion criteria were observed in this study. The baseline characteristics and clinical outcomes for each patient group are outlined in Table 5.1. In this cohort 9.7% (23/236) patients developed POF, 25.4% (60/236) developed local complications; with the incidence of acute peri-pancreatic and acute necrotic collection 12.7% (30/236) for both. Major infection occurred in 3.8% (9/236) of the patients. The overall mortality was 3.8% (9/236) and all the patients that died were from the severe acute pancreatitis group.

5.3.2 Circulating histones elevate on admission and indicate disease severity

To assess whether circulating histones are associated with disease severity in acute pancreatitis patients we firstly measured levels among healthy volunteers, mild, moderate and severe acute pancreatitis patients**.** Figure 5.1 shows that circulating histones were barely detectable in healthy volunteers and comparable between both mild and moderate AP patients (median [quartiles] 1.1 [0.6, 2.1] *vs.* 1.3 [0.5, 2.8] μg/ml, $P > 0.05$). Circulating histones were only significantly elevated in patients with severe disease (18.8 [5.9, 33.8] μg/ml, $P < 0.001$), indicating their association with disease severity.

We then compared the relevance of measuring circulating histones to current clinical scores and biomarkers used to assess severity of acute pancreatitis patients (Table 5.2). Like circulating histones, SIRS, BISAP, APACHE II and SOFA scores all increased with disease severity within 24 h of hospital admission and were significantly elevated

in severe acute pancreatitis patients, compared to mild or moderate groups. General biomarkers including circulating urea, creatinine, hematocrit, IL-6 and IL-8 were also significantly higher in patients with severe disease. In contrast, CRP levels showed no significant association with disease severity within 24 h of admission, which only became significantly after 48 h. These data indicate that following acute pancreatitis onset, histones appear within the circulation more rapidly than CRP and synchronously with severe clinical manifestation, which may hold potential benefit for early prediction of disease severity within these patients.

5.3.3 Circulating histones are the earliest indicator of disease severity

POF during the first week of hospitalisation is a marker of fatal outcome in acute pancreatitis patients[306]. In this cohort, 9.7% (23/236) of patients developed POF and along with significantly more clinical complications within the first week of hospital admission (Table 5.1). This was also reflected by significant increased clinical scores on admission, which included; SIRS, BISAP, APACHE II and SOFA (Table 5.2). The AUCs for all the scores were moderate (range 0.68-0.81, Table 5.3) in predicting POF, and both the sensitivity (51-66%) and specificity (74-83%) were poor, most likely due to the transient nature of organ failure in acute pancreatitis patients. Circulating histone levels within 24 h of admission out performed current clinical scores (Table 5.3) and showed a far stronger predictive value (AUC: 0.92; 95%CI: 0.85-0.99) when compared to both CRP (AUC: 0.54; 95%CI: 0.37-0.71) (Figure 5.2A) and urea (AUC: 0.75; 95%CI: 0.63-0.86) (Figure 5.2B). Furthermore, CPR (AUC: 0.89; 95%CI: 0.84-0.94) (Figure 5.2A) and urea (AUC: 0.82; 95%CI: 0.71-0.94) (Figure 2B) only showed relatively strong predictive value of POF at 48 h following admission. Using the optimal circulating histones cut-off value (5.4 μg/ml) for the prediction of POF, they

comparatively surpassed all other parameters measured within this study, with a sensitivity, specificity, PPV, NPV, PLR and NLR were 82.6%, 94.4%, 61.3%, 98.1%, 14.7 and 0.18, respectively (Table 5.4). Furthermore, when combining circulating histones levels with either of the above parameters, the predictive values were not further increased. These data suggest that measuring circulating histones within 24 h after hospital admission accurately and better predicted POF, compared to predictors currently used in routine clinical practice.

5.3.4 Circulating histones have moderate predictive values for major infection

We next assessed the value of measuring circulating histones in predicting major infection, compared to current clinical scores and biomarkers. Circulating histones had a moderate predictive value (AUC 0.78; 95%CI: 0.62-0.94) for major infection. CRP was less effective within 24 h (AUC: 0.72; 95%CI: 0.50-0.94) but became more so at 48 h (AUC: 0.83; 95%CI: 0.75-0.92) (Figure 5.3A). Measuring urea at either 24 (AUC: 0.86; 95%CI: 0.74-0.97) or 48 h (AUC: 0.92; 95%CI: 0.86-0.97) more effectively predicted major infection than circulating histones within 24 h of admission (Figure 5.3B). Similarly, we found that BISAP (AUC: 0.83; 95%CI: 0.72-0.94), APACHE II (AUC: 0.87; 95%CI: 0.75-1.00) and SOFA (AUC: 0.82; 95%CI: 0.64-0.99) scores had stronger predictive value for major infection than measuring circulating histones within 24 h, as did both creatinine (AUC: 0.83; 95%CI: 0.71-0.96) and IL-8 (AUC: 0.80; 95%CI: 0.67-0.94). However, circulating histones exceeded other parameters tested in this study (Table 5.3, Figure 5.3C). At a cut-off of 5.4 μg/ml, the sensitivity, specificity, PPV, NPV, PLR and NLR of circulating histones for the prediction of major infection were 44.4%, 88.8%, 12.9%, 97.6%, 3.7 and 0.63, respectively (Table 5.4).

5.3.5 Circulating histones have high values in predicting mortality

Circulating histones had a higher predictive value for mortality (AUC: 0.96; 95%CI: 0.92-1.00) than any other parameter within 24 hours (Table 5.3), including both CRP (Figure 5.4A) and urea (Figure 5.4B) and was comparable to urea (AUC: 0.97; 95%CI: 0.95-0.99) at 48 h. At an optimal cut-off of 5.4 μg/ml, the sensitivity, specificity, PPV, NPV, PLR and NLR for circulating histones were 88.9%, 89.9%, 25.8%, 99.5%, 8.8 and 0.12, respectively (Table 5.4 and Figure 5.4). Urea at a cut-off of 8 mmol/l had a sensitivity, specificity, PPV, NPV, PLR and NLR of 100%, 93.2%, 37.5%, 100%, 14.8 and 0.00 respectively (Table 5.4 and Figure 5.4B) at 48 h. Both BISAP (≥ 2) within 24 h and CRP (≥ 250 mg/l) at 48 h had reasonable predictive values, but with PLR values (4.6 and 4.4, respectively) much lower than those of both circulating histones within 24 h and urea at 48 h (Table 5.4 and Figure 5.4). Combining circulating histones (≥ 5.4 μg/ml) with either urea (≥ 8 mmol/l, at 48 h) or CRP (≥ 250 mg/l, at 48 h) did not increase specificity compared to the individual parameters alone.

5.3.6 Circulating histones on admission correlate with leucocyte viability but not local complications

We reported that circulating histones significantly correlated with pancreatic necrosis scores in animal models. However, the correlation between histone levels on admission and the first MCTSI (r = 0.17, n = 99, *P* = 0.094), or the worst MCTSI (r = 0.195, n = 99, *P* = 0.054) were not significant. During disease progression, pancreatic necrosis normally occurs 24 h after onset so would therefore not directly affects the histone levels within the first 24 h, but may be contributory after this time. Another source could be the release histones from immune cells following cellular damage or death. We measured the percentage viable WBC in peripheral blood of 62 patients

within this cohort, and found a significant negative association between circulating histone levels and WBC viability within 24 h of admission ($r = -0.515$, $P < 0.01$; Figure 5.5). These data indicate that inflammation-induced immune cell death may be a major source for early elevations in circulating histones.

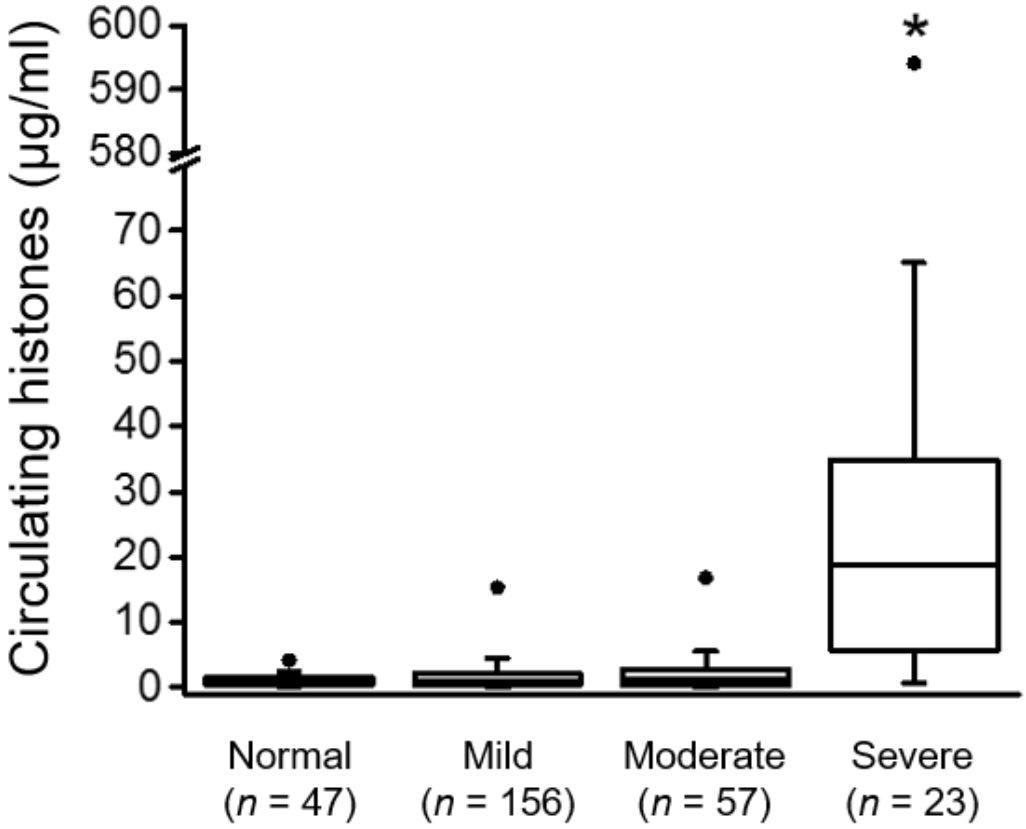

Figure 5.1 Comparison of circulating histone levels in normal and patients with acute pancreatitis on admission. Plasma histones levels (μg/ml) were quantified in health volunteers (normal; n = 47) and in mild (n = 156), moderate (n = 57) and severe (n = 23) acute pancreatitis patients within 24 h of admission. Median ± interquartiles with peak values are presented. *$P < 0.05$ when compared with other groups.

Table 5.1 Demographic and clinical outcomes of the study population

	Total *n* = 236	Mild *n* = 156	Moderate *n* = 57	Severe *n* = 23	*P* value*
Gender, female, *n* (%)	124 (52.5)	91 (58.3)	22 (38.6)	11 (47.8)	0.04†
Age (year), median (IQR)	55.5 (42.3-69)	56 (42-68)	52 (40-67)	62 (52-76.5)	0.064
Updated Charlson score, median (IQR)	0 (0-1)	0 (0-1)	0 (0-1)	0 (0-1)	0.158
Aetiology					
Biliary, *n* (%)	120 (50.8)	83 (53.2)	29 (50.9)	8 (34.8)	0.256
Alcohol, *n* (%)	48 (20.3)	30 (19.2)	13 (22.8)	5 (21.7)	0.835
Others, *n* (%)	68 (28.8)	43 (27.6)	15 (26.3)	10 (43.5)	0.259
Time to admission (h), median (IQR)	8 (4-14)	8 (4-14)	6 (4-12)	11 (6-15)	0.111
Time from admission to sampling (h), median (IQR)	15 (9-20)	14 (8.3-19.8)	17 (9.8-20)	16 (12-20)	0.588
Worst modified CT severity index, median (IQR)	4 (2-7.5)	2 (0-2)	6 (4-8)	6 (6-8)	<0.001†
Acute peri-pancreatic fluid collection, *n* (%)	30 (12.7)	0 (0)	23 (40.4)	7 (30.4)	<0.001†
Pancreatic necrosis, *n* (%)	30 (12.7)	0 (0)	19 (33.3)	11 (47.8)	<0.001†
Infected pancreatic necrosis and/or sepsis, *n* (%)	9 (3.8)	0 (0)	1 (1.8)	8 (34.8)	<0.001‡
Need for antibiotics, *n* (%)	34 (14.4)	9 (5.8)	9 (15.8)	16 (69.6)	<0.001§
Nutritional support, *n* (%)	13 (5.5)	0 (0)	0 (0)	13 (56.5)	<0.001‡
Necrosectomy and/or percutaneous drainage, *n* (%)	11 (4.7)	0 (0)	3 (5.2)	8 (34.8)	<0.001§
Mortality, *n* (%)	9 (3.8)	0 (0)	0 (0)	9 (39.1)	<0.001‡
Length of hospital stay (day), median (IQR)	7 (4-14)	5.5 (3-9)	14 (11-21)	29 (13.5-65.5)	<0.001§

IQR, interquartile range; MCTSI, modified computerised tomography severity index; CT performed: mild (31/156), moderate (49/57), severe (20/23). *P value indicates comparison among three groups. †Mild *vs.* moderate or severe was significant. ‡Severe vs. mild or moderate was significant. §Any two groups comparison was significant.

Table 5.2 Comparison of clinical scores and biomarkers among different severity groups

	Mild *n* = 156	Moderate *n* = 57	Severe *n* = 23	*P* value*
Clinical scores within 24 h of admission				
SIRS	1 (0-1)	1 (1-2)	2 (1-2)	0.002†
BISAP	1 (0-1)	1 (0-1)	2 (1-2)	< 0.001‡
APACHE II	5 (3-7)	7 (5-9)	10 (6-12.5)	< 0.001†
SOFA	0 (0-1)	1 (0-2)	2 (1-4)	< 0.001†
Biomarkers within 24 h of admission				
WBC ($\times 10^9$/l)	12.4 (9.9-15.3)	14.2 (11.5-17.4)	14.4 (11.2-19.3)	0.002‡
Neutrophil/lymphocyte ratio	6.9 (4.1-14.8)	8 (4.3-14.7)	7.7 (5.3-23.6)	0.520
Haematocrit (%)	40.1 (38-42.9)	43.5 (39.3-45.6)	42.8 (37.6-45.4)	0.003‡
Urea (mmol/l)	5 (3.7-6.1)	4.8 (3.7-6.3)	7.3 (5.2-8.9)	0.001§
Creatinine (μmol/l)	71 (61-88)	83 (65-99)	104 (75-157.5)	< 0.001†
CRP (mg/l)	7.5 (5-23.3)	10 (5-33.8)	10 (5-136.5)	0.288
IL-6 (pg/ml)	13.8 (7-57.8)	30.8 (8.6-96.2)	65.1 (21.7-143.4)	0.022//
IL-8 (pg/ml)	9.9 (0.4-19.1)	13.9 (5.4-28.9)	44.5 (18.8-64.2)	< 0.001//
Circulating histones (μg/ml)	1.1 (0.6-2.1)	1.3 (0.5-2.8)	18.8 (5.9-33.8)	< 0.001§
Biomarkers at 48 h admission				
Urea (mmol/l)	3.5 (2.6-4.7)	3.5 (2.7-5.5)	8.7 (5.2-11.7)	< 0.001§
Creatinine (μmol/l)	66 (53.5-79)	65 (54.5-86)	71 (57-172)	0.08§
CRP (mg/l)	38 (11-116)	234 (159-316.5)	327.5 (250-368.3)	0.001†

SIRS, Systemic Inflammatory Response Syndrome; BISAP, Bedside Index for Severity in Acute Pancreatitis; APACHE II, Acute physiology and Chronic Health Examination II; SOFA, Sequential Organ Failure Assessment; WBC, white blood cell; CRP, C-reactive protein; IL, interleukin. *P value indicates comparison among three groups. †Any two groups comparison was significant. ‡Mild *vs.* moderate or severe was significant. §Severe *vs.* mild or moderate was significant. //Mild *vs.* severe was significant.

Table 5.3 AUC of ROC for potential predictors

	POF	*P* value	Major infection	*P* value	Mortality	*P* value
Clinical scores within 24 h of admission						
SIRS	0.68 (0.55-0.81)	0.01	0.67 (0.48-0.87)	0.096	0.72 (0.53-0.91)	0.037
BISAP	0.81 (0.71-0.91)	< 0.001	0.83 (0.72-0.94)	0.002	0.90 (0.80-0.99)	< 0.001
APACHE II	0.74 (0.62-0.87)	< 0.001	0.87 (0.75-1)	< 0.001	0.86 (0.70-1)	0.001
SOFA	0.79 (0.68-0.90)	< 0.001	0.82 (0.64-0.99)	0.001	0.83 (0.66-0.99)	0.001
Biomarkers within 24 h of admission						
WBC ($\times 10^9$/l)	0.62 (0.49-0.74)	0.066	0.67 (0.47-0.86)	0.087	0.67 (0.46-0.87)	0.085
Haematocrit (%)	0.58 (0.43-0.73)	0.253	0.60 (0.35-0.86)	0.316	0.52 (0.3-0.74)	0.848
Urea (mmol/l)	0.75 (0.63-0.86)	< 0.001	0.86 (0.74-0.97)	< 0.001	0.83 (0.69-0.98)	0.001
Creatinine (μmol/l)	0.74 (0.62-0.86)	< 0.001	0.83 (0.71-0.96)	0.001	0.91 (0.81-1)	< 0.001
IL-6 (pg/ml)	0.67 (0.49-0.74)	0.018	0.73 (0.57-0.87)	0.031	0.73 (0.54-0.91)	0.045
IL-8 (pg/ml)	0.76 (0.64-0.89)	0.001	0.80 (0.67-0.94)	0.005	0.89 (0.78-0.99)	0.001
Circulating histones (μg/ml)	0.92 (0.85-0.99)	< 0.001	0.78 (0.62-0.94)	0.005	0.96 (0.92-1)	< 0.001
Biomarkers at 48 h admission						
Urea (mmol/l)	0.82 (0.71-0.94)	< 0.001	0.92 (0.86-0.97)	< 0.001	0.97 (0.95-0.99)	< 0.001
Creatinine (μmol/l)	0.61 (0.44-0.78)	0.129	0.62 (0.36-0.88)	0.253	0.86 (0.65-1)	0.002
CRP (mg/l)	0.89 (0.84-0.94)	< 0.001	0.83 (0.75-0.92)	0.001	0.86 (0.79-0.93)	0.003

POF, persistent organ failure; SIRS, Systemic Inflammatory Response Syndrome; BISAP, Bedside Index for Severity in Acute Pancreatitis; APACHE II, Acute physiology and Chronic Health Examination II; SOFA, Sequential Organ Failure Assessment; WBC, white blood cell; CRP, C-reactive protein; IL, interleukin.

Table 5.4 Comparison of predictive values of the most effective predictors

	Cut-off values	Sensitivity	Specificity	PPV	NPV	PLR	NLR
POF							
BISAP (within 24 h)	≥ 2	68.4	82.8	26.5	96.7	4.0	0.38
Circulating histones (within 24 h)	≥ 5.4 μg/ml	82.6	94.4	61.3	98.1	14.7	0.18
Urea (at 48 h)	≥ 8 mmol/l	60.9	94.7	56.0	95.6	11.5	0.41
CRP (at 48 h)	≥ 250 mg/l	80.0	80.5	29.1	97.6	4.1	0.25
Major infections							
BISAP (within 24 h)	≥ 2	75.0	80.5	12.2	98.9	3.8	0.31
Circulating histones (within 24 h)	≥ 5.4 μg/ml	44.4	88.1	12.9	97.6	3.7	0.63
Urea (at 48 h)	≥ 8 mmol/l	66.7	91.4	24.0	98.5	7.8	0.37
CRP (at 48 h)	≥ 250 mg/l	77.8	77.7	13	98.8	3.5	0.29
Mortality							
BISAP (within 24 h)	≥ 2	87.5	80.9	14.3	99.4	4.6	0.15
Circulating histones (within 24 h)	≥ 5.4 μg/ml	88.9	89.9	25.8	99.5	8.8	0.12
Urea (at 48 h)	≥ 8 mmol/l	100	93.2	37.5	100	14.8	0.00
CRP (at 48 h)	≥ 250 mg/l	100	77.1	10.9	100	4.4	0.00

PPV, positive predictive value; NPV, negative predictive value; PLR, positive likelihood ratio; NLR, negative likelihood ratio; POF, persistent organ failure; BISAP, Bedside Index for Severity in Acute Pancreatitis; CRP, C-reactive protein.

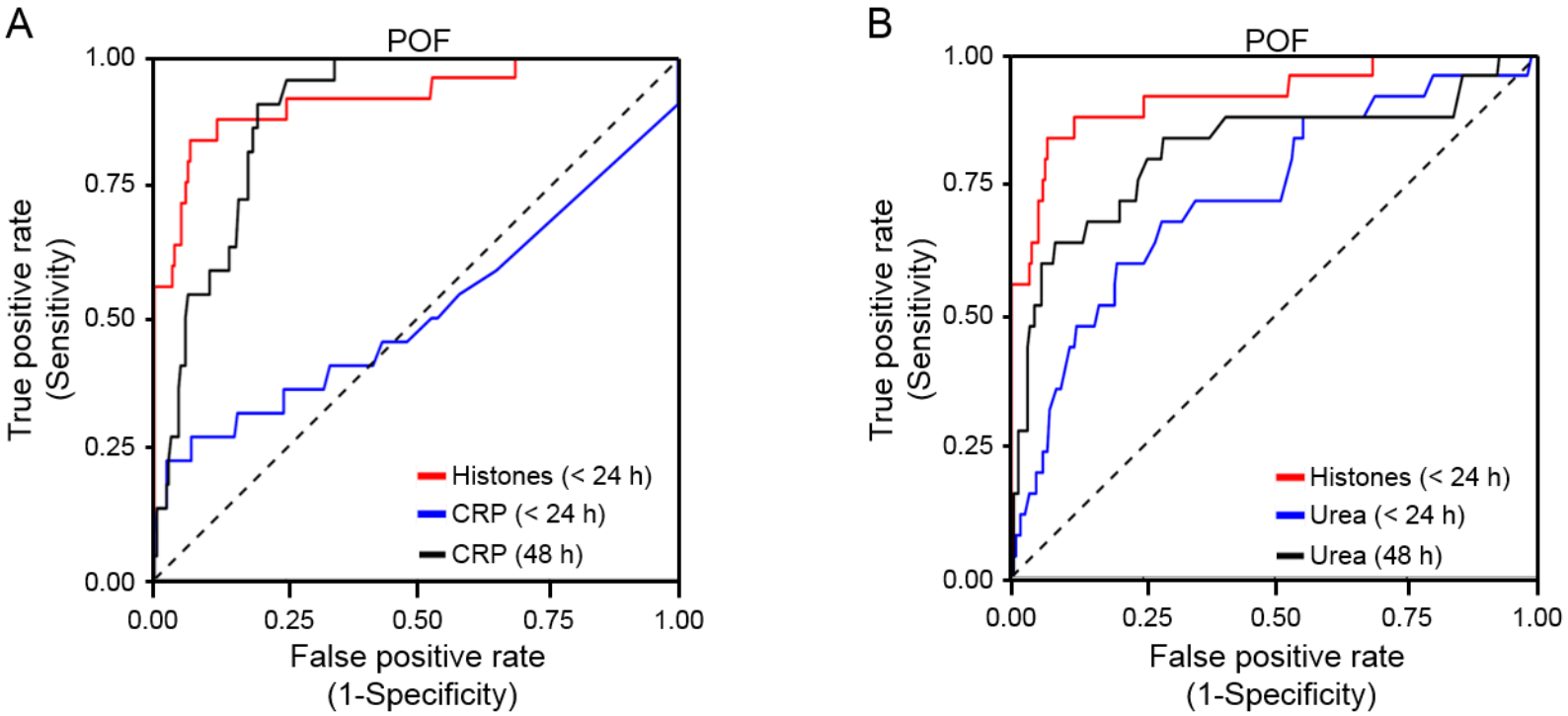

Figure 5.2 Comparison of ROC curves in predicting POF. ROC analysis comparing circulating histone levels within 24 h with either (A) CRP within 24 h and at 48 h or (B) urea within 24 h and at 48 h, in predicting for POF in acute pancreatitis patients (n = 236). Dash line represents ROC reference line.

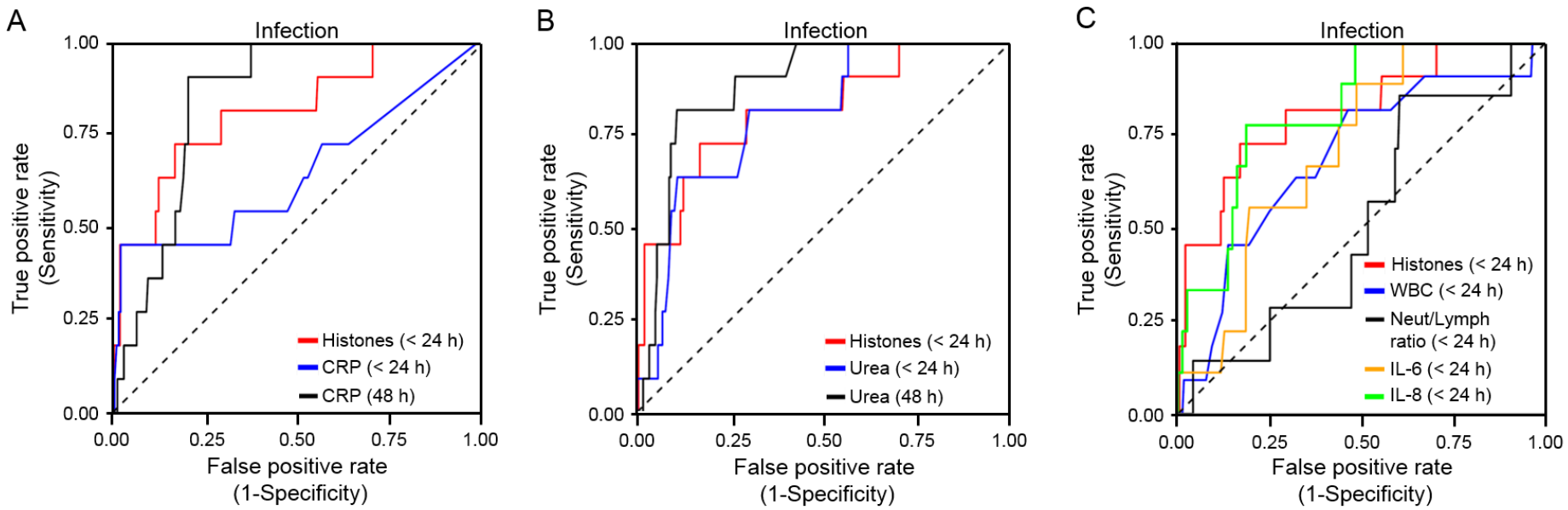

Figure 5.3 Comparison of ROC curves in predicting infection. ROC analysis predicting infection in acute pancreatitis patients (n = 236), comparing circulating histones within 24 h of admission are to (A) CRP within 24 h and at 48 h after admission, (B) urea within 24 h and at 48 h after admission and (C) white blood cell (WBC) counts, neutrophil/lymphocyte ratio, IL-6 and IL-8 within 24 h of admission. Dash line represents ROC reference line.

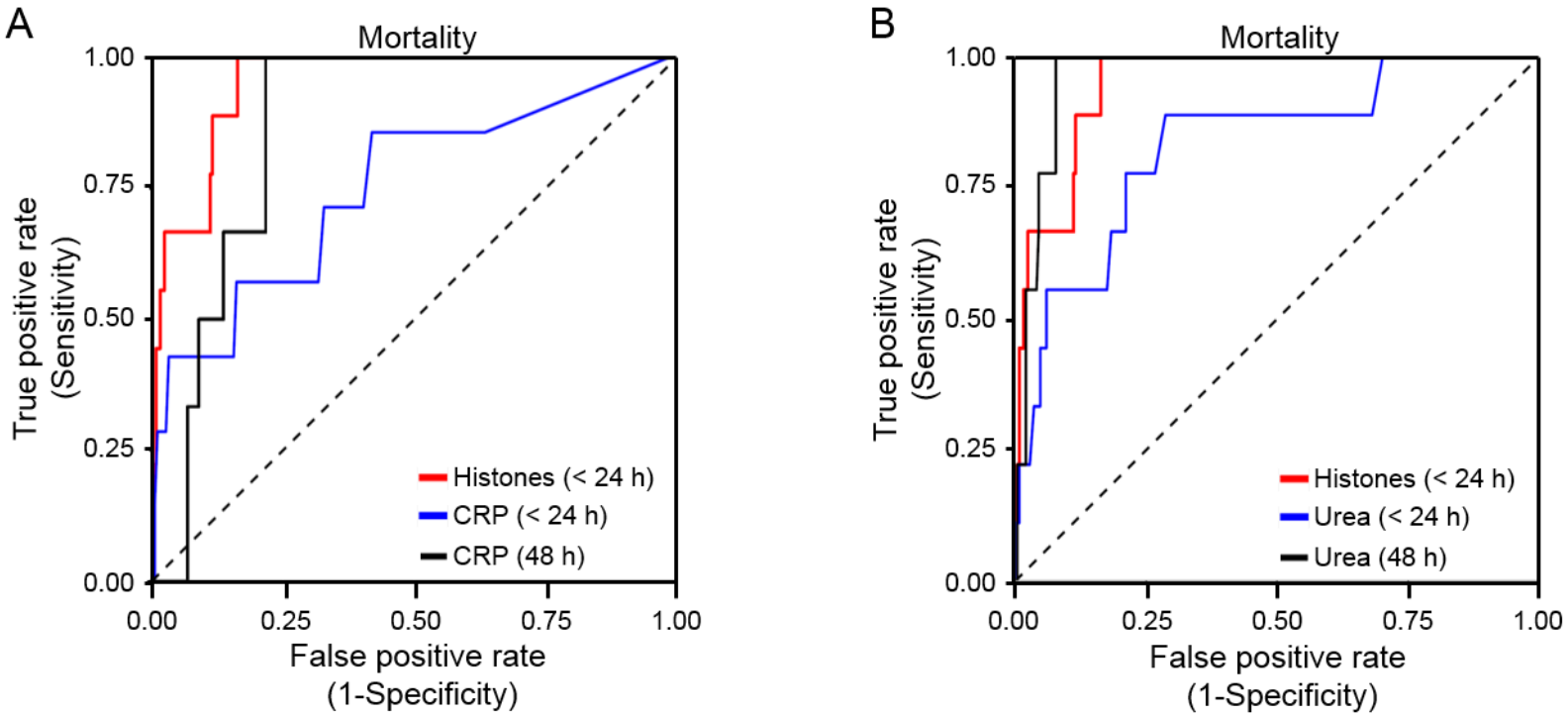

Figure 5.4 Comparison of ROC curves in predicting mortality. ROC analysis comparing circulating histone levels within 24 h with either (A) CRP within 24 h and at 48 h or (B) urea within 24 h and at 48 h, in predicting for mortality in acute pancreatitis patients (n = 236). Dash line represents ROC reference line.

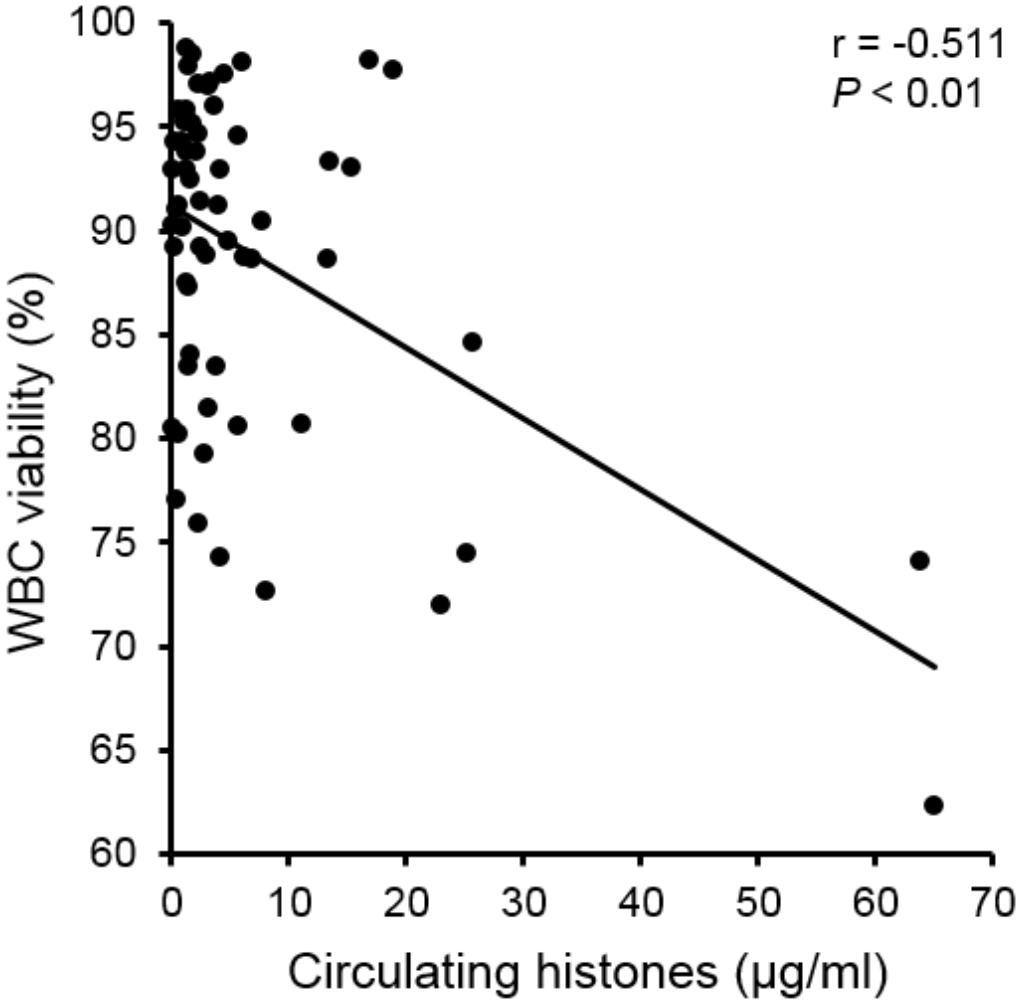

Figure 5.5 Correlation between histone levels and percentage of leucocyte viability on within 24 h of admission. Circulating histone levels (µg/ml) were correlated with percentage of leucocyte viability in acute pancreatitis patients (n = 62) within 24 h of admission.

5.4 Discussion

In this study, we demonstrate for the first time that levels of circulating histones are a robust index of disease severity and capable of predicting POF and mortality, better than indices currently used in the clinical setting within 24 hours of admission. Moreover, we provide supporting evidence that BISAP within 24 hours as well as urea and CRP at 48 hours have good predictive values for POF, major infection and mortality, encouraging their routine clinical use before new markers are developed. The consecutive nature of patient recruitment and short time from onset of pain to sampling, stringently applied, adds strength to these conclusions.

BISAP, which contains blood urea nitrogen (BUN), Glasgow Coma Score, SIRS, age and presence of pleural effusions, is a recently developed and validated clinical score primarily for the prediction of mortality in acute pancreatitis.[294, 295, 327] Our study has shown that BISAP predicted POF and morality reasonably well, inferior only to circulating histones within 24 hours of admission, justifying its clinical use. However, it is a composite of five elements, two of which are scoring systems themselves. Furthermore, the need for an upright X-ray examination may hamper its timely application. On the other hand, we did not observe robust predictive values for SIRS, APACHE II and truncated SOFA, consistent with current literature.[295] As clinical scoring systems generally suffer from their cumbersome nature and are not intrinsically superior to routine biomarkers, clinicians still prefer simple laboratory assays based on novel biomarkers.

BUN is a key component of BISAP and has been validated for predicting mortality.[328] A recent study shows that a rise in BUN within 24 hours of admission is strongly

associated with higher rates of POF and pancreatic necrosis.[312] Findings from our study corroborate those from previous studies and show that urea at 48 hours (≥ 8 mmol/l) had similar predictive values to circulating histones within 24 hours (≥ 5.4 μg/ml); both were very effective for mortality prediction. Urea at 48 hours identified all fatal clinical outcomes with high specificity (93.2%) in our cohort, highlighting its importance for mortality prediction. However, urea was inferior to circulating histones in predicting POF, but better for major infection.

CRP is one of the most widely accepted and used measure in predicting acute pancreatitis severity, but was evaluated primarily based on the 1992 Atlanta Classification.[314, 317] In this study, CRP at 48 hours (≥ 250 mg/l) had relatively strong predictive values for POF (AUC: 0.89; 95%CI: 0.84-0.94), major infection (AUC: 0.83; 95%CI: 0.75-0.92) and mortality (AUC: 0.86; 95%CI: 0.79-0.93). Circulating histones had better predictive values in terms of POF and mortality compared to CRP, but was less effective in the prediction of major infection. CRP only became useful 48 hours after admission and circulating histones outperformed CRP for early prediction. However, CRP values also reflect disease progression, successful intervention and improvement, something as yet untested for circulating histones and so the continued use of CRP should still be strongly recommended. Mechanistically, CRP has recently been shown to rise later than circulating histones in a trauma-induced lung injury and serves as a detoxifying molecule to block the histone binding to cellular membranes.[265] As the emerging role of DAMPs continues to unravel in experimental and human acute pancreatitis, the relationship of CRP to circulating histones, HMGB1, DNA and other DAMPs warrants further investigation.

The value of hematocrit in predicting severity of acute panceatitis has been controversial. We could not confirm predictive values reported by a recent large cohort multicenter study.[312] This discrepancy may be because previous studies looking at hematocrit, urea and BISAP were not as stringent in limiting time from the onset of pain to hospital admission, thus limiting their findings. Our study strictly applied pre-defined inclusion and exclusion criteria and assessed patients early following disease onset, making our findings more reliable. We were unable to observe statistically significant predictive values for neutrophil/lymphocyte ratio or white blood cell count within 24 hours of admission. Other clinical biomarkers such as albumin, total protein, hemoglobin, bicarbonate, prothrombin time, adjusted calcium and magnesium had little predictive value for POF and mortality in out cohort (data not shown). IL-6 and IL-8 had low to moderate predictive value. These findings collectively support the utility of circulating histones in the early prediction of acute pancreatitis severity.

The most studied DAMP in the acute pancreatitis setting is HMGB1. Based on previous reports [329, 330] significant release of HMGB1 also occurs beyond 24 hours in experimental acute pancreatitis thus implying it may not be useful in the early prediction of POF. In contrast, we have previously demonstrated that levels of circulating histones rise within 2 hours in experimental acute pancreatitis[325] and early in human acute pancreatitis as demonstrated here**.** We observed strong correlation between peak histone levels and pancreatic necrosis in animal acute pancreatitis models, [325] however histone levels within 24 hours of admission in this study did not correlate with MCTSI or predict pancreatic necrosis. This discrepancy may be due to the time point of blood collection, or indeed represents a fundamental difference in disease progression, as pancreatic necrosis occurs several days later in humans than in

animal models. Therefore, pancreatic acinar cells are likely to contribute very little to levels of circulating histones in early stage disease. Instead, immune cells such as neutrophils may contribute to the majority of histones detectable in blood released as they may be released during NETosis,[125] as well as primary and secondary necrosis. Our observation that histone levels were strongly associated with the proportion of dead/dying peripheral leukocytes supports this argument. Therefore, histone levels may indeed reflect the intensity of systemic inflammation and auto-amplification of inflammation, thus determining disease severity.

In conclusion, circulating histones predicting major clinical outcomes, particularly POF within 48 hours of disease onset, and are more effective than any available clinical marker. Measuring circulating histones is of great clinical importance and holds immediate translational potential. As such measuring circulating histones may be candidates for integration into current scoring systems to enhance the early, accurate and robust stratification of severe acute pancreatitis and to ensure timely, appropriate care of high-risk patients.

Chapter 6 – Elevated circulating histones are associated with multiple organ dysfunction syndrome in patients with acute pancreatitis

6.1 Introduction

Acute pancreatitis is one of the most common digestive diseases that require emergency admission[301, 331]. The incidence of acute pancreatitis has escalated from 5 to 30 per 10 million people over the last 50 years in the United Kingdom[332]. Approximately 15-20% of acute pancreatitis patients experience a complicated clinical course with manifestations of organ failure, local complications and major infections[304, 333]. These local and systemic determinants formed the basis of the Revised Atlanta Classification (RAC)[300] which stratifies acute pancreatitis severity into mild, moderate and severe. The "severe" category, defined as presence of persistent organ failure (POF), especially multiple organ dysfunction syndrome (MODS)[286, 305, 306, 334, 335], has been well established to be the most critical contributor to mortality, but the underling mechanisms remain to be elucidated.

Studies that have attempted to link pancreatic necrosis to MODS are not conclusive yet. How a single organ lesion triggers the systemic inflammatory response syndrome (SIRS) and the subsequent MODS remains elusive. However, it is generally recognised that immunological factors[336] play important roles. Inflammatory cytokine storm is believed to be the fundamental factor in the pathogenesis of SIRS and MODS in acute pancreatitis[337]. This process is characterised by an initial sterile inflammation that results from injured pancreatic acinar cells, the primary victims of acute pancreatitis[338, 339]. Necrotic or apoptotic acinar cells release their intracellular pro-inflammatory contents, such as histones, high-mobility group box protein 1 (HMGB1), DNA, mitochondrial

components, adenosine triphosphate and heat shock protein 70 into the extracellular space to trigger cytokine release and enhance inflammation[274]. These cellular breakdown products are collectively called damage–associated molecular pattern molecules (DAMPs)[274]. The role of DAMPs has been increasingly identified in critical illness and some of them (e.g. HMGB1 and cell-free DNA) have been shown to correlate positively with disease severity in both experimental models and patients with acute pancreatitis[274].

Intra-nuclear histones are the most abundant nuclear proteins that play essential roles in DNA packaging and gene regulation. However, released histones following extensive cell or organ damage, such as in severe trauma[271], liver injury[322] and severe sepsis[213, 320], are toxic to various mammalian cells causing injury to MODS including the heart, lungs, kidneys and liver[213, 271, 275, 276, 320, 322, 340, 341]. Recent reports showed that in the lungs, neutrophils extracellular traps (NETs) could release histones locally and damage epithelial cells[340, 342]. Cellular toxicity results from direct membrane binding and resultant calcium influx[271, 343]. In addition, circulating histones are directly pro-inflammatory by stimulating leucocytes to secrete cytokines that include tumour necrosis factor-alpha (TNF-α), interleukin (IL)-1, IL-6 and IL-8[322]. This process involves Toll-like receptor (TLR)-2, TLR-4 and TLR-9. The involvement of TLR-4 and IL-6 in the pathogenesis of acute pancreatitis has been extensively described[344, 345]. Recently, histones were reported to activate NLRP3 inflammasomes[278, 279, 342] to enhance the release of IL-1beta (IL-1β) and IL-18, which are also reported to play roles in ACUTE PANCREATITIS[346]. Histones are also pro-thrombotic through endothelial damage, von Willebrand factor-mediated leucocyte recruitment, platelet activation and the protein C anticoagulant pathway[322, 347, 348] and may enhance MODS by impairing

microcirculation. We have reported that extracellular histones can directly trigger neutrophils to release myeloperoxidase and form NETs[271], the later further releases histones. Therefore, a vicious cycle may exist to further damage microcirculation and enhance organ injury[340].

In chapter 4 we showed that circulating histones are significantly elevated in mouse models of necrotising acute pancreatitis and associated with pathological scores of pancreatic necrosis and distal organ injury[349]. In chapter 5, we further demonstrated that on admission elevated circulating histones (≥ 5.4 μg/ml) are accurate predictors for POF and morality in patients with human acute pancreatitis.

In this chapter, we examined (1) whether circulating histone levels are correlated with clinical severity scores, proinflammatory cytokines and individual organ injury markers; (2) whether circulating histones are associated with organ failure status; (3) which factor (e.g. POF, pancreatic necrosis, and infection) is principally associated elevated circulating histones.

6.2 Patients and Methods

6.2.1 Study population and ethics

Consecutive patients primarily admitted to Royal Liverpool University Hospital (RLUH) between 2010 and 2015 were included. A first episode of acute pancreatitis, established by clinical symptoms, laboratory tests and/or imaging as defined by 2012 RAC admitted within 72 h of symptom onset[300]. Exclusion criteria were: (1) age < 18 or > 85 years; (2) trauma, pancreatic neoplasm, pregnancy and chronic pancreatitis as aetiologies; (3) advanced pulmonary, cardiac, renal or malignant diseases. Referral patients with POF admitted to Intensive Care Unit (ICU) fulfilling the above criteria were also included.

For primary admitted patients, peripheral blood samples were obtained within 24 h of admission. For referral patients, blood samples were taken at RLUH ICU admission and daily for up to a week. Blood samples were also collected from heathy volunteers. Serum and plasma were isolated and stored at -80°C in the National Institute for Health Research (NIHR) Liverpool Biomedical Research Unit Control and Acute Pancreatitis Biobanks, according to protocols approved by local research ethics committees (REC references: UoL000933, 11/WNo01/1, 13/NW/0089 and 10/H1308/31). The collection, process and storage of samples stringently followed standard operating procedures (SOPs) according to Good Clinical Laboratory Practice (GCLP) standards.

6.2.2 Clinical data collection

Extensive clinical data were prospectively recorded and maintained in an e-database. SIRS, Acute Physiology and Chronic Health Evaluation II (APACHE II) and SOFA scores (at least one of the respiratory, cardiovascular or renal systems[302]) were calculated

within 24 h of admission for primarily admitted patients or daily for referral patients, respectively, according to published definitions[295].

POF was defined as at least one organ having a SOFA score of ≥ 2 for ≥ 48 h. Local complications (pancreatic necrosis; acute peripancreatic fluid collection, APFC; vein thrombosis) were defined as per RAC[300] according to enhanced computerised tomography (CECT). Pancreatic necrosis was quantified using the modified CT severity index[294]. Infection was defined as positive culture from body fluid, blood and tissue. Major infection was defined as presence of infected pancreatic necrosis and/or sepsis. To study the association of these variables with circulating histones, local complications and infected pancreatic necrosis were calculated by 7 days before or after sampling, while transient organ failure, POF and other infections were calculated by 3 days before or after sampling.

6.2.3 Blood sample analysis

Circulating histone levels were determined by Western blotting as described previously[265, 271, 320, 325, 350, 351]. Cytokines/chemokines, including IL-1β, IL-6, IL-8 and monocyte chemoattractant protein (MCP)-1 were measured using commercial ELISA kits (R&D, Abingdon, UK). Arterial blood gases, serum cardiac troponin T, urea, creatinine, bilirubin, alanine aminotransferase and albumin were reported by the Department of Clinical Biochemistry of the RLUH.

6.2.4 Statistical analysis

Continuous variables and categorical data were described as median with interquartile range (IQR) and number and percentage, respectively. Mann-Whitney *U* test and

Kruskal-Wallis *H* test were used to determine statistical differences between two groups and three or more groups, respectively. Spearman rank correlations were used to analyse the associations between two continuous variables. Univariate analysis was performed for the association of each variable with circulating histones by bivariate logistic regression. Multivariate analysis was further performed included variables with $P < 0.1$ from univariate analysis. These variables were age (≤ 60 or > 60 years), aetiologies (biliary, alcohol and other aetiologies), Charlson score (< 2 or ≥ 2), transient organ failure (presence or absence), POF (presence or absence), pancreatic necrosis (absence, < 30%, 30-50%, ≥ 50%) and major infection (presence or absence). Circulating histones were transformed to dichotomous variables according to cut-off values of 5.4 μg/ml (Chapter 5) and 20 μg/ml[271].

6.3 Results

6.3.1 Patient characteristics and clinical outcomes

A total of 260 consecutive primarily admitted patients and 52 referral patients were included. The patient characteristics and clinical outcomes are shown in Table 6.1. There were 235 primarily admitted patients did not develop POF during hospital stay (176 mild and 59 moderate; Non-POF); 25 developed POF either within 24 h of admission or later (POF < 24 h). All referral patients had POF prior to transfer and the POF persisted at least > 48 h after RLUH ICU admission (POF > 48 h).

For primary patients, the median age was 55 years with 124 (47.7%) males. A hundred thirty-three (51.2%) patients were biliary aetiology, followed by 53 (20.4%) alcohol and others. The median Charlson score was 0. There were 21 (8%) patients needed intensive care, 32 (12.3%) developed APFC and 37 (14.2%) had pancreatic necrosis. Ten (3.8%) patients underwent pancreatic drainage and/or necrosectomy, 14 (5.4%) manifested major infection and 9 (3.5%) patients died, all of them were from the severe group. The median length of hospital stay was 7 days. The median age in the referrals was 61 years with 28 (53.8%) patients were males. Biliary was also the leading cause with 22 (42.3%) patients, followed by 13 (25%) alcoholics and other aetiologies. The median comorbidity score was also 0. Patients were referred at a median of 7.5 days (4-12.8) after primary hospital admission and all patients needed intensive care when transferred. Six (11.5%) patients were detected APFC and 44 (84.6%) had pancreatic necrosis. Twenty-three (44.2%) patients received surgical intervention, 45 (86.5%) patients developed major infection and 11 (21.2%) died. The median hospital stay was more than 10 weeks.

Table 6.1 Patient characteristics and clinical outcomes

Demographics	**Primary** n = 260	**Referral** n = 52
Age, years, median (IQR)	55 (42-69)	61 (43-73)
Gender, males, n (%)	124 (47.7)	28 (53.8)
Aetiology, n (%)		
Biliary	133 (51.2)	22 (42.3)
Alcohol	53 (20.4)	13 (25.0)
ERCP	11 (4.2)	1 (1.9)
Drug-induced	5 (1.9)	0 (0)
Others	58 (22.3)	16 (30.8)
Comorbidity: Charlson score, median (IQR)	0 (0-0)	0 (0-0)
Days to referral, median (IQR)	NA	7.5 (4-12.8)
RAC severity category, n (%)		
Mild	176 (67.7)	0 (0)
Moderate	59 (22.7)	0 (0)
Severe	25 (9.6)	52 (100)
Need for HDU/ICU, n (%)	21 (8.0)	52 (100)
Peripancreatic fluid collection, n (%)	32 (12.3)	6 (11.5)
Pancreatic necrosis, n (%)	37 (14.2)	44 (84.6)
Pancreatic necrosectomy and/or drainage, n (%)	10 (3.8)	23 (44.2)
Infected pancreatic necrosis and/or sepsis, n (%)	14 (5.4)	45 (86.5)
Mortality, n (%)	9 (3.5)	11 (21.2)
Days of hospitalisation, median (IQR)	7 (4-14)	74 (46-128)

IQR, interquartile range; ERCP, endoscopic retrograde cholangiopancreatography; NA, not available; RAC, Revised Atlanta Classification; HDU, high dependence unit; ICU, intensive care unit.

6.3.2 Circulating histones are significantly correlated with clinical severity scores, proinflammatory cytokines and individual organ injury markers

We first analysed the correlation of circulating histones with clinical severity scores, proinflammatory cytokines and individual organ failure markers. Results of Spearman correlation analysis are shown in Table 6.2. It appeared that circulating histones had strong correlation with serum IL-8 levels (r_s = 0.566), followed by SIRS, APACHE II, SOFA, IL-1β and IL-6 (r_s = 0.321-0.425). Circulating histones also signifcnatly correlated with respiratory (PaO_2/FiO_2, r_s = -0.373), cardiac (cardiac troponin T, r_s = 0.321) and renal (urea, r_s = 0.22) injury paramers. However, circulating histones were not signifcnatly correlated with creatine, bilirubin, alanine aminotransferase (all P > 0.05).

6.3.3 Circulating histones are highly associated with organ failure status

As circulating histones were significantly correlated with clinical severity scores, proinflammatory cytokines and individual organ failure markers (assessed at the same time when blood was drawn for histone measurement), we postulated that circulating histones were associated with organ failure status. The circulating histone levels according to different groups are shown in Figure 6.1. There were no significant differences in circulating histone levels among healthy volunteers (median 0.81 μg/ml [IQR: 0.38-1.6]), mild (1.1 μg/ml [0.5-2.1]) and moderate (1.4 μg/ml [0.5-2.8]) patients (all P > 0.05). However, the circulating histones were dramatically elevated in the primary severe group (22.9 μg/ml [5.9-40]) when compared to these three groups (all P < 0.01). Furthermore, the peak circulating histone levels of the referrals (34.1 μg/ml [21.5-80.6]) were even higher than that of the primary severe patients (P < 0.05; Figure 6.1A).

Table 6.2 The correlation of circulating histones to various parameters

Variables	r_s	***P* value**
Clinical severity scores		
SIRS	0.349	< 0.001
APACHE II	0.425	< 0.001
SOFA	0.397	< 0.001
Proinflammatory cytokines		
IL-β (pg/ml)	0.376	< 0.001
IL-6 (pg/ml)	0.367	< 0.001
IL-8 (pg/ml)	0.566	< 0.001
MCP-1 (pg/ml)	0.014	0.285
Individual organ injury markers		
PaO_2/FiO_2 (mmHg)	-0.373	< 0.001
Cardiac troponin T (ng/ml)	0.321	< 0.001
Urea (mmol/l)	0.22	< 0.001
Creatinine (μmol/l)	0.083	0.113
Bilirubin (μmol/l)*	-0.094	0.161
Alanine aminotransferase (U/l)*	-0.008	0.053
Platelets ($\times 10^9$/l)	0.04	0.094

SIRS, Systemic Inflammatory Response Syndrome; APACHE II, Acute physiology and Chronic Health Examination II; SOFA, Sequential Organ Failure Assessment; IL, interleukin; MCP-1, monocyte chemoattractant protein; PaO_2/FiO_2, partial pressure arterial oxygen and fraction of inspired oxygen.

*Biliary aetiology excluded.

We therefore analysed data according to Non-POF (primary mild and moderate), POF < 24 h (primary severe) and POF > 48 h (referrals and severe) categories. The correlation of circulating histones and parameters significantly associated with histones to organ failure status are shown in Table 6.3. All the parameters were significantly different among the three groups in SIRS, APACHE II, SOFA, PaO_2/FiO_2 and circulating histones. There were significant differences for either two groups for all the other parameters assessed. Spearman correlation analyses revealed that the circulating histone levels were most highly associated organ failure status ($r_s = 0.693$), closely followed by SOFA ($r_s = 0.658$), IL-8 ($r_s = 0.625$), APACHE II ($r_s = 0.619$) and PaO_2/FiO_2 ($r_s = -0.565$). While other parameters (SIRS, IL-1β, IL-6, cardiac troponin T and urea) still had significant correlation with organ failure status but the r_s values were less than 0.5.

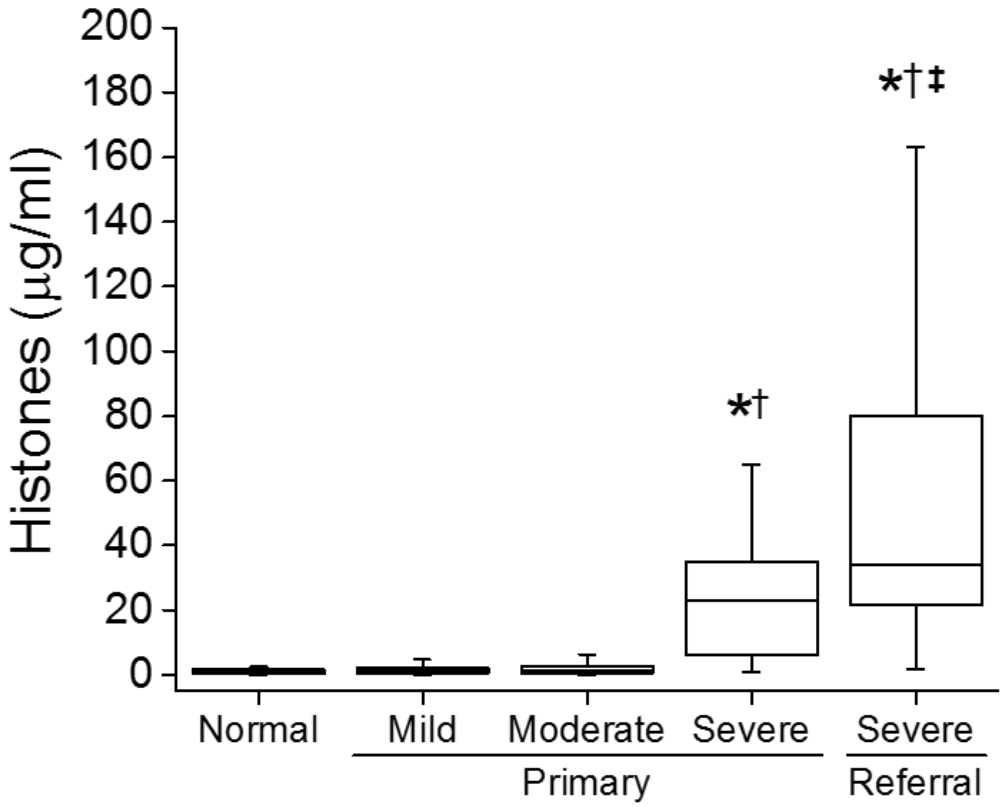

Figure 6.1 Circutlating histones are aossicated with organ failure status. The blood sampling time was within 24 h of admission for primary patients or at RLUH ICU admission and daily for up to a week for referrals. Comparison of circulating histone levels among heathy volunteers (n = 48), primary disease categories (RAC: mild = 176; moderate = 59; severe = 25) and referrals (n = 52). *$P < 0.05$ *vs.* healthy volunteers; †$P < 0.05$ *vs.* mild or moderate primary patients; ‡$P < 0.05$ *vs.* primary severe patients.

Table 6.3 The correlation of circulating histones and other parameters with organ failure status

Parameters	**Group 1 (Non-POF)** n = 235	**Group 2 (POF < 24 h)** n = 25	**Group 3 (POF > 48 h)** n = 52	***P* value***	r_s‖
Clinical scores					
SIRS	1 (0-2)	2 (1-12)	2 (2-3)	< 0.001†	0.475
APACHE II	5 (3-8)	9 (6-12)	16 (12-19)	< 0.001†	0.619
SOFA	1 (0-1)	2 (1-4)	7 (3-9)	< 0.001†	0.658
Inflammatory parameters					
Circulating histones (μg/ml)	1.2 (0.5-2.3)	22.9 (5.9-39.6)	34.1 (21.5-80.6)	< 0.001†	0.693
IL-1β (pg/ml)	0.6 (0-2.6)	2.3 (0-5.7)	2.8 (1.5-4.8)	< 0.001‡	0.369
IL-6 (pg/ml)	24.8 (7.6-62.2)	60.5 (19.7-154.8)	122.5 (30.8-230.8)	< 0.001§	0.408
IL-8 (pg/ml)	11.7 (1.2-25.6)	47.6 (18.4-173.3)	71.1 (41.8-131.5)	< 0.001§	0.625
Individual organ injury markers					
PaO_2/FiO_2 (mmHg)	368 (321-414)	295 (176-358.9)	190.5 (161.6-224.1)	< 0.001†	-0.565
Cardiac troponin T (ng/ml)	5 (3-11)	17.5 (6.8-35.5)	15.7 (4.7-40)	0.001§	0.397
Urea (mmol/l)	4.9 (3.7-6.2)	6.9 (4.8-8.9)	7 (4.1-12.1)	0.003§	0.272

POF, persistent organ failure; SIRS, Systemic Inflammatory Response Syndrome; APACHE II, Acute physiology and Chronic Health Examination II; SOFA, Sequential Organ Failure Assessment; IL, interleukin. PaO_2/FiO_2, partial pressure arterial oxygen and fraction of inspired oxygen.

**P* value indicates comparison among three groups. †Any two groups' comparison was significant. ‡Group 1 *vs.* Group 2 was significant. §Group 1 *vs.* Group 2 or 3 was significant. ‖All $P < 0.001$ in Spearman correlation analyses.

6.3.4 Univariate and multivariate logistic regression analysis

Results of the univariate analysis are shown in Table 6.4. In the univariate analysis, we found that POF, pancreatic necrosis and major infection were significantly associated with elevated circulating histones (≥ 5.4 μg/ml). Whereas age, gender, aetiology, comorbidity, transient organ failure and other local complications were not significantly correlated to elevated circulating histones.

Results of the multivariate analysis are shown in Table 6.5. Fitting the positive parameters (at a cut-off of $P < 0.1$) from univariate analysis into multivariate logistic regression model, we found that only POF had significant association with elevated circulating histones for all primary patients (OR = 57.1, 95% CI: 14.2 to 229.8, $P < 0.001$). Pancreatic necrosis (regardless of necrotic size) and major injection, however, were not found to be statically significant (all $P > 0.05$). When primary and referral patients were combined together, both POF (OR = 121.5, 95%CI: 29.1 to 506.9, $P < 0.001$) and major infection (OR = 4.6, 95%CI: 1.1 to 19.8, $P = 0.041$), but not pancreatic necrosis, were significantly associated with elevated circulating histones. When the circulating histone cut-off value was ≥ 20 μg/ml, a known concentration for direct cytotoxicity[271], POF was even stronger associated with elevated circulating histones in primary patients (OR = 98.1, 95% CI: 14.4 to 669.0, $P < 0.001$). Similar findings were obtained when primary and referral patients were merged (OR = 177.2, 95%CI: 33.4 to 941.2, $P < 0.001$). However, major infection was not further shown to be significantly correlated to the increase of circulating histones in either primary patients or the combined primary and referral patients (both $P < 0.05$). These findings strongly suggest that POF was the dominating factor that associated with raised circulating histones.

Table 6.4 Univariate logistic regression of risk factors for elevated circulating histones

	Primary		**Primary and referral**	
Variables (at histones cut-off ≥ 5.4 μg/ml)	OR (95% CI)	*P* value	OR (95% CI)	*P* value
Age, years	1.06 (0.52-2.17)	0.866	1.32 (0.80-2.20)	0.267
Gender, males	0.90 (0.44-1.82)	0.765	0.90 (0.55-1.49)	0.686
Aetiology				
Biliary	0.73 (0.36-1.49)	0.387	0.70 (0.42-1.16)	0.163
Alcohol	0.75 (0.30-1.92)	0.552	1.10 (0.60-2.02)	0.751
Others*	1.74 (0.84-3.62)	0.139	1.01 (0.58-1.77)	0.974
Comorbidity: Charlson score	1.31 (0.59-2.89)	0.511	1.13 (0.63-2.03)	0.676
Organ failure				
Transient organ failure	0.70 (0.23-2.10)	0.523	0.51 (0.22-1.20)	0.122
Persistent organ failure	73.67 (19.81-273.92)	< 0.001	137.10 (52.31-359.33)	< 0.001
Pancreatic necrosis				
No necrosis†	2.11 (0.83-5.35)	0.116	1.60 (0.77-3.33)	0.207
Necrosis < 30%	2.10 (0.72-6.13)	0.176	2.60 (1.21-5.60)	0.014
Necrosis 30-50%	4.54 (1.22-16.98)	0.024	7.89 (2.95-21.12)	< 0.001
Necrosis > 50%	6.53 (0.89-47.91)	0.065	17.47 (6.40-47.69)	< 0.001
Major infection	11.00 (2.93-41.24)	< 0.001	31.08 (11.60-83.31)	< 0.001

OR, odds ratio; CI, confidence interval.

*Include endoscopic retrograde cholangiopancreatography, drug-induced, idiopathic and unknown aetiologies.

†May include local complications such as acute peripancreatic fluid collection and/or vein thromboses.

Table 6.5 Multivariate logistic regression of independent predictors for elevated circulating histones

	Primary		**Primary and referral**	
Variables (at histones cut-off ≥ 5.4 μg/ml)	OR (95% CI)	*P* value	OR (95% CI)	*P* value
Persistent organ failure	57.2 (14.2-229.8)	< 0.001	121.5 (29.1-506.9)	< 0.001
Necrosis < 30%	NA	NA	0.9 (0.2-4.6)	0.923
Necrosis 30-50%	1.2 (0.1-10.8)	0.853	1.5 (0.2-11.0)	0.713
Necrosis > 50%	1.7 (0.1-40.0)	0.731	0.4 (0.1-2.6)	0.332
Major infection	4.3 (0.7-28.4)	0.126	4.6 (1.1-19.8)	0.041
Variables (at histones cut-off ≥ 20 μg/ml)				
Persistent organ failure	98.1 (14.4-669.0)	< 0.001	177.2 (33.4-941.2	< 0.001
Major infection	4.1 (1.2-11.5)	0.092	4.4 (1.4-14.0)	0.14

OR, odds ratio; CI, confidence interval; NA, not applicable.

6.4 Discussion

This study supports our previous observations in acute pancreatitis mouse models[349] (Chapter 4) and patients (Chapter 5) that circulating histones were elevated in severe disease. The present work found that circulating histones were significantly correlated with clinical severity scores, proinflammatory cytokines and individual organ injury markers. Circulating histones not only significantly elevated early in patients with severe acute pancreatitis but also even more so during disease progressing. We also demonstrate significant associations of distant organ injury and severity of the diseases with the levels of circulating histones. Moreover, multivariate logistic regression analysis reveals that POF, but not pancreatic necrosis or other factors, was most closely associated with elevated circulating histones. These data strongly suggest that histone toxicity may play an important role in the development of distant organ injury and even MODS in acute pancreatitis as reported in other diseases[213, 271, 277, 322].

The role of extracellular histones to be important proinflammatory mediators in sterile inflammation has been increasing recognised[199]. Recently, we[325] and others[125] have shown that circulating histones and NETs (major constitutes are histones) were elevated in experimental and human acute pancreatitis respectively. Furthermore, anti-histone antibody rescued mice from death in experimental acute pancreatitis[222] and neutralising reagents polysialic acid prevented trypsin and signalling activation in isolated pancreatic acinar cells[125]. To elaborate these findings, we have demonstrated most of the primary severe patients had circulating histone levels ≥ 5.4 μg/ml, a concentration that accurately predicted POF and mortality in the Chapter 5. There were 56% (14/25) primary severe and 78.8% (41/52) referral patients had circulating histone levels ≥ 20 μg/ml, a known direct cytotoxicity level in *in vitro* studies[271]. However, the circulating histone levels in mild and moderate patients remained low and were similar to healthy volunteers. In the correlation analysis, we found that circulating histones were strongly correlated to acute

pancreatitis disease severity and stage where patients with fully established POF had highest circulating histone levels. These data demonstrate that elevated circulating histones may be important proinflammatory mediators that contributed to POF in acute pancreatitis.

The toxicity of histones to different organs, such as the lung, heart, kidney and the liver has been demonstrated in different animal models[213, 271, 275, 276, 320, 322, 340, 341, 343, 352]. In our previous study, we found that in mouse acute pancreatitis models, the organ injury markers are associated with histone levels. In this study, we also demonstrate that the biochemical markers of most affected organs in acute pancreatitis, the lung, cardiovascular and renal systems, were significantly correlated to the levels of circulating histones. The PaO_2/FiO_2 ratio is an indicator reflecting whether the patient has hypoxemia or not when the blood is sampled. In the very early stage of acute pancreatitis, hypoxemia is not only affected by respiratory function *per se* but also by other factors such as abdominal pain and fluid therapy. The hypoxemia will be corrected in most of the patients once the pain is controlled and they respond to fluid therapy. This is the case for moderate patients in our study as there were about 1/3 of them had $PaO_2/FiO_2 < 300$ mmHg, a cut-off value for acute respiratory distress syndrome (ARDS) as per Berlin Definition[27], but most of them recovered very soon without any need for intensive care. Circulating histones elevated simultaneously or preceded to ARDS in primary severe acute pancreatitis and much higher levels were observed in the referrals, all of whom had ARDS with 55.5% (29/52) suffered from moderate/severe ARDS. Therefore, elevated circulating histones within 24 h of primary hospital admission may be a better indicator than $PaO_2/FiO_2 < 300$ mmHg for long lasting hypoxemia and impaired respiratory function. Interestingly, in patients with serum cardiac troponin T levels tested, there were 16.8% (20/119), 60% (12/20), 42.3% (22/52) had cardiac troponin T $\geq$ 14 ng/ml for patients with non-POF, POF < 1 d and POF > 3 d, respectively. These findings are indicative that the cardiac injury may be a common phenomenon in acute pancreatitis. In support

of our data, a recently study[6] has shown that brain natriuretic peptide[353] and cardiac troponin I[354] levels (both are indicators for cardiomyopathy) were significantly elevated in severe acute pancreatitis at the first day of admission and positively correlated with SOFA score, serum procalcitonin and C-reactive protein levels. Similar to sepsis[320, 351, 355], these novel findings highlight that in severe acute pancreatitis there was also substantial cell death in myocardium (e.g. caused by histones). Therefore, the previous overlooked cardiac troponin T levels may deserve to be routinely monitored in severe acute pancreatitis. Urea, but not creatinine, also significantly associated with circulating histones, albeit the correlation factor was weaker than those obtained for PaO_2/FiO_2 ratios and cardiac troponin T levels. These observations are suggestive that urea outperformed creatinine to reflect renal function, consistent with previously findings that blood urea nitrogen is a relative good early predictor for severe acute pancreatitis[295] and mortality[328, 356].

Circulating histones have been shown to directly induce liver injury[352] and hepatic failure is an independent predictor for morality of acute pancreatitis[335]. However, the levels of bilirubin or alanine aminotransferase, markers of liver injury, showed no correlation to circulating histones, which was different from the observation in acute pancreatitis animal models[349]. This inconsistence may due to different aetiologies as alcoholics were associated more severe liver injury[335]. This may also due to the overall low incidence of liver injury in our cohorts. Circulating histones have been shown to induce coagulation in diseases such as sepsis[357] and coagulation abnormalities have been linked to severity of acute panreatitis[65]. However, we did not find a significant correlation between platelet counts and circulating histones. In fact, there were only 9 patients distributed in different severity groups with platelets $< 100 \times 10^3/mm^3$. In another study, coagulation failure has not been demonstrated to be an independent predictor for hospital mortality of acute pancreatitis patients[335]. It is worth noting that all the samples were collected

either within 24 h of primary hospital admission or less than 3 weeks of admission, representing a relative acute stage of this disease. Further time-course studies are needed to investigate whether there are correlations of circulating histones to liver injury and coagulation in acute pancreatitis, especially in the disease late stage.

The source of circulating histones is not fully clear. The strong correlations to pancreatic necrosis scores in both animal models[349] and patients indicate that the death of acinar cells could be a major contributor. However, in many patients, the extents of pancreatic necrosis were not closely associated with circulating histone levels, indicating that other sources co-exist. Previous studies suggest that immune cells, such as during NETosis, may release substantial amounts of histones[340], which may occur before acinar cell death and trigger local and systemic inflammation[278, 279, 358] as indicated by the significant increase in proinflammatory cytokines/chemokines, such as IL-1β, IL-6, IL-8 and MCP-1[359]. However, a direct evidence of immune cells contributing to the elevation of circulating histone is still lacking. In our study, multivariate analysis revealed that POF, but not pancreatic necrosis, was significantly and dominantly associated with elevated circulating histones using their relevant cut-offs. These findings suggest that MODS may be companied with large number of cell death which in turn contributes to histone elevation. In addition, histone-enhanced NETs formation[271] may also release histones. Recently, extracellular histones have been shown to induce lymphocyte apoptosis in an experimental sepsis model[360]. As lymphocyte apoptosis has also been associated with severe acute pancreatitis in both animals and patients, it may well be that the circulating histones could be responsible for these results and in turn apoptotic lymphocytes further release more circulating histones. Therefore the actual scenario is complicated and could be a vicious cycle that drives certain acute pancreatitis into a severe form although the pancreatic injury could be severe at the onset. The associations established from this clinical study was in favour of POF-

induced cell death was the major source of circulating histones. However, there is a limitation that the causal-effect relationship between pancreatic necrosis and POF and the real source of circulating histones due to POF cannot be clarified without further investigation.

Circulating histones significantly elevate in patients with severe acute pancreatitis and strongly correlate to disease severity and stage, clinical severity scores, proinflammatory cytokines/chemokines and parameters of MODS. Cell death resulted from POF may be the major sources of circulating histones, which have great potential to serve as prognostic markers and therapeutic targets for the management of severe acute pancreatitis in near future.

Chapter 7 – Overview

In the Chapter 2, we first and systemically tested the cytotoxicity of full length and truncated histone subclasses. In order to synthesise truncated histones (N-terminal or C-terminal), we first generated anti-histone single chain variable fragment (ahscFv) and control IgG chain variable fragment (cscFv). The expression of ahscFv and cscFv was confirmed by Coomassie Brilliant Blue. The binding capacity of ahscFv and cscFv against histone H3 was test by Western blot, shown ahscFv (but not cscFv) bound to the histone. The binding capacity of ahscFv to histone subclasses was further confirmed by gel overlay and biosensor analyses. Therefore, the ahscFv was used in the subsequent studies.

We found that all the fluorescein isothiocyanate-full length and 3 truncated histones (H1.1 C, H2A N, H3.1 N) bound to the cell membrane and induced calcium influx in an endothelial cell line. Other truncated histones did not bind to cell membrane, nor induced calcium influx. These data imply that a portion of histone subclasses still have cytotoxicity effects even when histones are degraded (truncated), highlighting the necessity of measuring all forms of circulating histones (histone-DNA complexes, free or truncated histone subclasses). Having this idea in mind, we endeavoured to develop an assay to measure all forms of circulating histones using xMAP technology in Chapter 3. We successfully generated the stand curves in buffer system, but the recovery ratio in spiked plasma was low and failed to detect the histones in patient plasma which were detectable by Western blot. Our work adds a layer of evidence for the difficulties of developing a rapid, reliable assay to quantify all forms of circulating histones as currently only histone-DNA complexes can be commercially measured by enzyme-linked immunosorbent assay.

In Chapter 4, we tested circulating histones in three experimental acute pancreatitis models in mice with graded severity. Four intraperitoneal injections of caerulein induced only oedematous acute pancreatitis with little systemic inflammation and minimum rise of circulating histones at all time points tested. Early and significant elevation of circulating histones was observed in both 12 caerulein injection model and sodium taurocholate (NaTC) intraductal infusion model. Both of these models developed marked pancreatic necrosis and distant organ injury with the overall severity greater induced by NaTC. The circulating histone levels were significantly associated with pancreatic necrosis and multiple organ injury parameters. We thus postulated that the sources of circulating histones may from both injured pancreas and distant organ injury products.

In Chapter 5 and Chapter 6, we went to testify our hypotheses in human acute pancreatitis admitted to Royal Liverpool University Hospital (RLUH). In Chapter 5, we included a consecutive cohort contained patients admitted within 48 h of disease onset to hospital admission to see whether circulating histones would have a predictive value for major complications of acute pancreatitis. Interestingly, circulating histone levels did not differ from heathy volunteers (n = 47), mild (n = 156) and moderate (n = 57) acute pancreatitis patients (classified by Revised Atlanta Classification[300], RAC). Circulating histones only marked elevated in severe acute pancreatitis (n = 23), a group of patients who had developed persistent organ failure (POF) during the clinical course. At a cut-off value of 5.4 μg/ml, circulating histones accurately predicted POF with sensitivity and specificity of 82.6% and 94.4%, respectively, higher than all clinical scores and biochemical markers tested simultaneously. Circulating histones also had good predictive value for mortality as mortality only occurred in patients with POF which circulating histones can accurately predict. However, circulating histones did not predict or correlate with pancreatic necrosis or any local pancreatic complications, highlighting other sources may exist. In line with this thought, we have observed that circulating histones were strongly associate with leucocyte

viability. This observation opens up the possibility that apoptotic neutrophils or neutrophil extracellular traps (NETs) could be a significant source for circulating histones.

In Chapter 6, we analysed circulating histones and clinical data obtained from two separate cohorts of patients. The first cohort included 260 consecutive patients (mild = 176; moderate = 59; severe = 25) admitted within 72 h of symptom onset and sampled within 24 h of admission. The second cohort included 52 constitutive patients who were referred to the Intensive Care Unit (ICU) of RLUH. All these patients were referral for potential management of local complication and had ongoing POF prior to transfer. Blood samples were obtained when they arrived RLUH ICU and daily for up to 7 days. The peak histone levels from referral patients were used through the study. It was found that circulating histones were significantly associated with clinical severity scores, proinflammatory cytokines and individual organ injury parameters. As circulating histones accurately predicted POF and were associated with disease severity parameters, we reasoned that circulating histones could reflect organ failure status. In another word, circulating histone levels would rise when disease severity has progressed. In agreement with these thoughts, when compared with the primary severe patients sampled on admission, referral patients had much higher elevated circulating histones. As circulating histones did not significant elevate in primary mild and severe patients, we merged these two groups into Group 1 (no POF). Primary severe patients would have POF < 24 h when sampled regardless when the POF occurred, we therefore allocated these patients as Group 2 (POF < 24 h). Referral patients consistently at least had POF > 48 h prior to sampling, these were designated into Group 3 (POF > 48 h). Values of all clinical parameters, proinflammatory cytokines and organ injury parameters tested as well as circulating histones were significantly different among groups. The circulating histones had an even higher correlation than that of Sequential Organ Failure Assessment (SOFA) score to organ failure status, highlighting the close link between circulating histones and

organ failure. To further address the association between circulating histones and organ failure, we carried out univariable and multivariable analyses. The analyses revealed that POF had predominant association with circulating histones. The experimental and human studies in acute pancreatitis suggest:

Elevated circulating histones occur in POF < 24 h and rise to even higher levels during the progression of POF in acute pancreatitis;

POF but not pancreatic necrosis most significantly correlated with elevated histones in acute pancreatitis;

The sources of circulating histones in severe acute pancreatitis warrant more studies;

Histones may have a pathogenic role and might be targeted to treat POF in acute pancreatitis.

The proposed role of circulating histones in acute pancreatitis is shown in Figure 7.1.

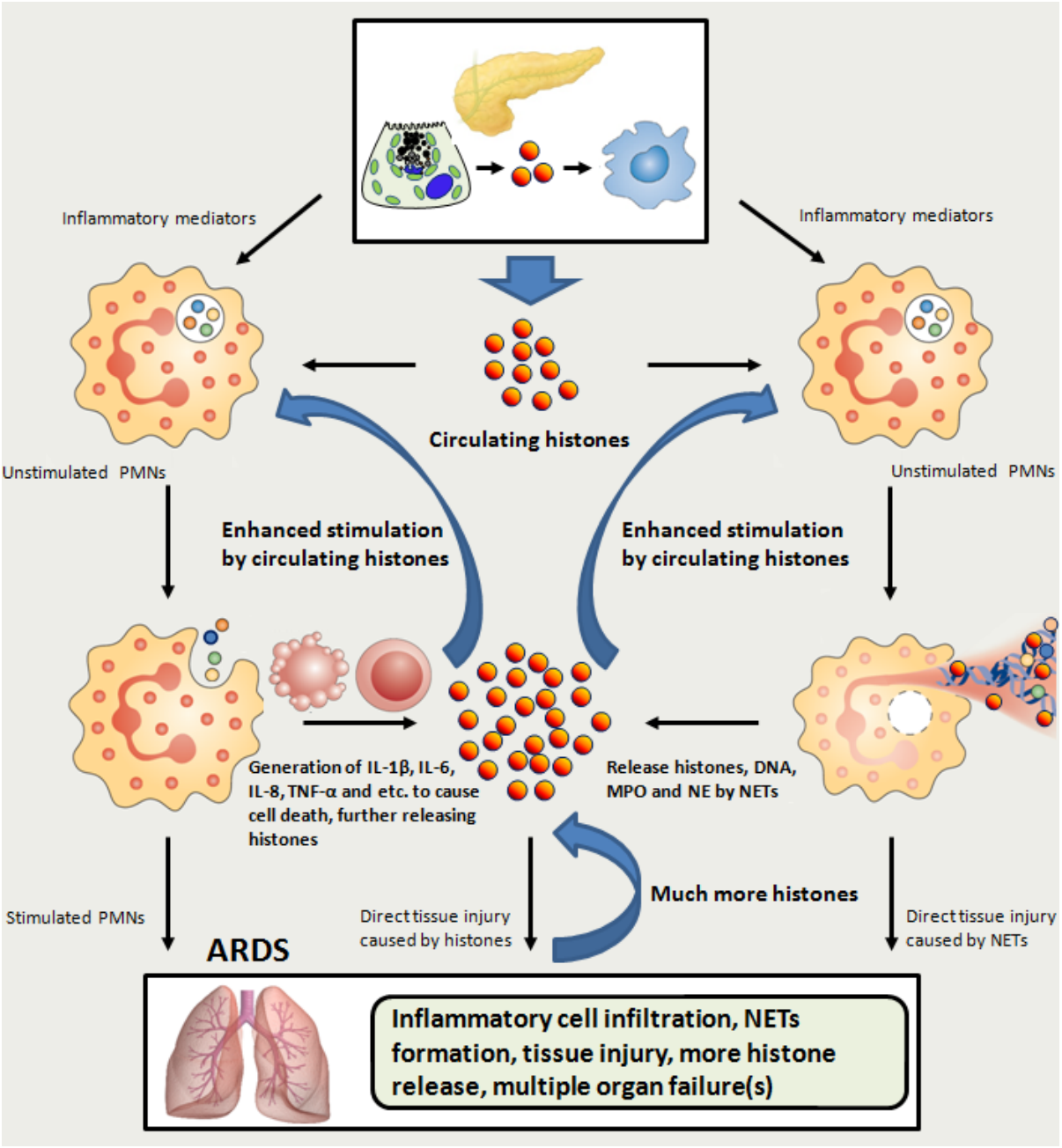

Figure 7.1 Circutlating histones in acute pancreatitis. Pancreatic toxins cause intial injury to the pancreas. Extracellular histones and other inflammatory mediators are relased to stimulate resident immune cells and circulating neutrophils. Apoptotic, necrotic neutrophils and neutrophil extracellular traps (NETs) release more histones and inflammatory mediators to further stimulate more neutrophil infilation and NETs formation. Stimulated neutrophils NETs, histones and other inflammatory cytokines cause multiple organ dysfunction syndrome (MODS) which in turn induce more release of circulating histones, triggering a vicous cycle: uncontroled MODS, coagulation and death.

Supplementary Table 1 Histone precipitated human plasma proteins*

Gene name	Protein
Lipoprotein associated	
APOA1	Apolipoprotein A-I
APOA4	Apolipoprotein A-IV
APOB	Apolipoprotein B-100
APOC3	Apolipoprotein C-III
APOE	Apolipoprotein E
CLU	Clusterin (apolipoprotein J)
GPLD1	Phosphatidylinositol-glycan-specific-phospholipase D
PON1	Serum paraoxonase/arylesterase 1
Proteinase inhibitors	
SERPINA1	α-1-Antitrypsin
A2M	α-2-Macroglobulin
ITIH1	Inter α-trypsin inhibitor heavy chain H1
ITIH2	Inter α-trypsin inhibitor heavy chain H2
ITIH3	Inter α-trypsin inhibitor heavy chain H3
AMBP	Protein AMBP (contains α-1-macroglobulin; bikunin)
Complement associated	
C4BPA	C4b-binding protein α chain
C1R	Complement C1r subcomponent
C1S	Complement C1s subcomponent
C3	Complement C3
C4A	Complement C4-A
Blood coagulation	
FGA	Fibrinogen α-chain
FGB	Fibrinogen β-chain
FGG	Fibrinogen γ-chain
F2	Prothrombin
KNG1	Kininogen-1
Immunoglobulins	
IGHA1	Ig α-1 chain C region
IGHA2	Ig γ-2 chain C region
IGKC	Ig κ-chain C region
IGLC1	Ig λ-chain C region
IGHM	Ig μ-chain C region
Cell adhesion	
FN1	Fibronectin-1
THBS1	Thrombospondin-1
VTN	Vitronectin
Transport	
ALB	Serum albumin
CP	Ceruloplasmin
TF	Serotransferrin
TTR	Transthyretin

*Adapted from Pemberton *et al.* 2010[214]

Supplementary Table 2 Novel identified histone binding molecules

Studies	Histone types*	Binding assay used	Molecules
Friggeri *et al.* 2012[361]	H3	ELISA	Mer receptor, $\alpha_v\beta_5$ integrin
Allam *et al.* 2012[277]	H4	Microscale thermophoresis	TLR2, TLR4/MD2
Lam *et al.* 2013[362]	H4	ELISA Microtiter plates	Human serum albumin, neutralised serum albumin
Abrams *et al.* 2013[265]	Histones	ELISA Gel overlay	C-reactive protein
Nakahara *et al.* 2013[323]	Histones	Quartz crystal microbalance twin sensor	Recombinant thrombomodulin
Wildhagen *et al.* 2014[363]	H3	Western blot and precipitation Surface plasmon resonance	Antithrombin activity depleted heparin
Zhang *et al.* 2014[364]	H4	ELISA	N-acetyl-heparin
Westman *et al.* 2014[365]	H1, H2A, H2B, H3.1, H4	ELISA Surface plasmon resonance	MBP-p33
Daigo *et al.* 2014[366]	Histones, recombinant histones, histone peptides	ELISA Surface plasmon resonance UV-visible spectrum	Pentraxin 3
Chaaban *et al.* 2015[367]	Histones or recombinant histones	ELISA Surface plasmon resonance	High-molecular-weight hyaluronan, inter-α inhibitor protein, heparin
Westman *et al.* 2015[368]	H4	Surface plasmon resonance	TLR4/MD2 on THP-1 cells
Wygrecka *et al.* 2016[369]	H1, H2A, H2B, H3.1, H4, citrullinated histones	ELISA Filter binding assay Microscale thermophoresis	C1 esterase inhibitor, recombinant C1 esterase inhibitor, reactive centre-cleaved C1 esterase inhibitor

ELISA, enzyme-linked immunosorbent assay; TLR, Toll-like receptor.

*All histone subclasses were recombinant.

Supplementary Table 3 Effects of extracellular histones on different cell types

Cell types	General *in vitro and ex vivo* findings	Anti-histone strategies	Relevant receptors
Epithelial cells			
A549 cells[341, 369], BEAS-2B cells[364], LA-4 cells[340], MLE-12 cells[340], mouse alveolar type II cells[369]	CTHs or H4 induced calcium influx, cytokine (IL-1β, IL-6, IL-10, TNF-α) production and cell death (PI or LDH) in multiple cell types; H1 and H4, but not H3, caused significant cell death (LDH) in MLE-12 cells.	Anti-H4, α-histones, APC, heparin, polysialic acid, C1INH	NA
Hepatocyte cell line L02[370]	CTHs dose-dependently induced cell death (Cell Counting Kit-8 and LDH).	Heparin, α-histones	NA
Pancreatic acinar cells[125, 222]	H3 did not cause significant secretion of HMGB1; H2A, H2B, H3 and H4 caused significant increase of trypsin, chymotrypsin activities and cell death (trypan blue); H3 and H4 significantly increased p-STAT3/t-STAT3; CTHs dose-dependently induced cell death (PI).	Polysialic acid	NA
HEK293 cells[322,371], parietal epithelial cells[372], podocytes[372]	CTHs dose-dependently induced TLR2 and TLR4 gene expression in transfected cells, respectively; CTHs induced APC generation in thrombin/TM complex expressing cells.	NA	TLR2, TLR4, TLR2/4
CHO-K1 and CHO-A745 cells[367]	CTHs induced cell death (PI).	NA	NA
Endothelial cells			
HPMECs[271, 369], MLVECs[373]	CTHs induced cell death (PI or LDH).	ahscFv, α-histones, APC, heparin, C1INH,	NA
HCAECs[374]	CTHs or subclasses (H1, H2A, H2B, H3, H4) dose- and time-dependently induced tissue factor mRNA and protein expression, activation of NF-κB and AP-1.	NA	TLR2, TLR4, TLR2/4
EA.hy926 cells[213, 265, 271, 365, 366, 375] and HUVECs[178, 213, 265, 271, 366, 374, 376]	CTHs or subclasses (H1, H2A, H2B, H3.1, H4) induced calcium influx, depletion of IκB and activation of p38-MAPK, NF-κB and AP-1, elevation of tissue factor and sTM, release of large vWF elevation and cell death (PI, FITC-anti-annexin V and/or PI, or LDH); CTHs or H3.3 and H4 (but not H1, H2A, H2B) induced up-regulating of tissue factor and down-regulation of TM[375].	Anti-H4, APC, heparin, polysialic acid, CRP, MBP-p33, PTX3	TLR2, TLR4
Glomerular endothelial cells[372]	CTHs dose-dependently induced TNF-α mRNA expression and cell death (MTT).	α-histones	TLR2/4
Cardiomyocytes			
Murine cardiomyocytes[355], mouse HL-1 cardiomyocytes[351]	CTHs caused cytosolic ROS production, calcium elevation, impaired mitochondria; CTHs dose-dependently caused reduction of contractility and induced calcium influx and cell death (PI); CTHs disturbed both functional and electrical responses of heart.	NA	NA
Immune cells			
Peripheral neutrophils[109, 271], HL-60[367]	CTHs induced IL-6 production and NETs formation; CTHs induced cell death (PI) was acerbated by a hyaluronan inhibitor 4-methylumbelliferone.	ahscFv, IAIP, HMW-HA	TLR2, TLR4, TLR9
Peripheral monocytes[368, 377], MM6[378], U937[370], THP-1[377]	CTHs dose-dependently induced cytokine production (IL-1β, IL-6, IL-8, IL-10, TNF-α) and cell death (PI and LDH); CTHs or H3 and H4 (but not H1, H2A, H2B) dose-dependently increased FXa and tissue factor generation as well as PS expression; H4 induced CXCL10 production in $CD14^{++}CD16^{+}$ monocytes.	Anti-H3, anti-H4, UFH, CRP	TLR4/MD2
Mouse peritoneal macrophages[361], RAW264.7 cells[222, 374], Kupffer cells[322, 358], J774 macrophages[372]	H3 or H4 significantly inhibited phagocytosis of apoptotic neutrophils or thymocytes by macrophages. H3 dose-dependently caused significant secretion of HMGB1; CTHs significant induced elevation of activated caspase-1 expression and TNF-α production; CTHs or subtypes (H1, H2A, H2B, H3, H4) dose- and time-dependently induced tissue factor mRNA and protein expression; lysine-rich CTHs dose-dependent release of vWF antigen, angiopoietin-2 and P-selection; arginine-rich CTHs induced vWF-platelet string formation.	APC	TLR2, TLR4, TLR2/4, TLR9, NLRP3

Human peripheral DCs[279], Human monocyte-derived DCs[379], murine BMDCs[372, 380]	CTHs induce TNF-α production; H2A (10 μg/ml) induced significant loss of ΔψM but not cell death (7-AAD); H4 stimulated significant expression of NLRP3 proteins.	Anti-H1, anti-H4, α-histones, APC, heparin	TLR2, TLR4/MD2, TLR2/4, NLRP3
Human peripheral lymphocytes[360]	CTHs dose- and time-dependently induced early apoptosis that was associated with p38-MAPK phosphorylation, ΔψM decreasing, Bcl2 reduction caspase-3 activation.	NA	NA
Peripheral platelets[265, 275, 276, 323, 362, 365, 367]	CTHs dose-dependently induced calcium influx, platelet aggregation, thrombin generation, PS exposure with elevated expression of P-selection and FV/Va; H3 and H4 significantly induced platelet aggregation.	APC, heparin, CRP, HSA, IAIP, HWM-HA	TLR2, TLR4
Human erythrocytes[365, 381, 382]	Biotin conjugated core histones (each 0.4 μM) bound to but did not penetrate human erythrocytes or erythrocyte ghosts. CTHs and subclasses (H1, H2A, H2B, H3.1, H4) caused significant haemolysis; CTHs dose-dependently induced PS exposure and increased procoagulant parameters on human erythrocytes.	APC, UFH, MBP-p33	NA

CTHs, calf thymus histones; IL, interleukin; TNF-α, tumour necrosis factor-alpha; PI, propidium iodide; LDH, lactate dehydrogenase; APC, activated protein C; C1INH, C1 esterase inhibitor; NA, not available; HMGB1, high-mobility group box 1; p-STAT3, phosphorylated signal transducer and activator of transcription 3; t-STAT3, total STAT3; TLR, Toll-like receptor; TM, thrombomodulin; HPMECs, human pulmonary microvascular endothelial cells; MLVECs, mouse lung vascular endothelial cells; ahscFv, anti-histone single chain variable fragment; HCAECs, human coronary artery endothelial cells; NF-κB, nuclear factor-kappaB; AP-1, activated protein 1; HUVECs, human umbilical vein endothelial cells; MAPK, mitogen-activated protein kinase; sTM, soluble thrombomodulin; vWF, von Willebrand factor; FITC, fluorescein isothiocyanate; CRP, C-reactive protein; PTX, pentraxin 3; MTT, (3-(4,5-dimethylthiazol-2-yl)-2,5-diphenyltetrazolium bromide) tetrazolium; ROS, reactive oxygen species; NETs, neutrophil extracellular traps; IAIP, inter-α inhibitor protein; HMW-HA, high-molecular weight hyaluronan; FXa, Factor Xa; PS, phosphatidylserine; CXCL, C-X-C motif chemokine; UFH, unfractionated heparin; NLRP3, NLR Family Pyrin Domain Containing 3; DCs, dendritic cells; BMDCs, bone marrow derived DCs; ΔψM, mitochondrial membrane potential; 7-AAD, 7-aminoactinomycin D; Bcl-2, B-cell lymphoma 2; HSA, human serum albumin.

Supplementary Table 4 Release of extracellular histones in murine sepsis models

Studies	Murine experimental models*	Histone-based treatment	Potential histone interacting receptors or binding molecules	*In vivo* findings	Treatment effects
Xu *et al.* 2009[213]	LPS (1 or 10 mg/kg, i.v.), CLP, TNF (0.75 mg/kg, i.v.), CTHs (50 or 75 mg/kg, i.v.)	Anti-H4 or anti-H2B (20 mg/kg, i.v.), APC (5 mg/kg, i.v.), PC (2.5 mg/kg, i.v.)	NA	Significant elevation of circulating histones was observed in LPS challenged mice (or baboons); at 50 mg/kg CTHs caused lung neutrophil margination, endothelium vacuolisation, intra-alveolar haemorrhage and thrombosis in mice; at 75 mg/kg CTHs induced rapid death within 1 h.	CTH-induced death was completely prevented by co-administration of APC; anti-H4 partially protected death induced by LPS, CLP and TNF; anti-PC converted a non-lethal dose LPS to cause death, an effect partially prevented by anti-H4, but not anti-H2B.
Li *et al.* 2011[383]	LPS (10, 20 or 35 mg/kg, i.p.)	NA	NA	LPS dose-dependently induced significant death of mice associated with dramatic elevated circulating histones and Cit-H3; serum Cit-H3 levels were most associated with severity of LPS-induced sepsis.	SAHA pre-treatment reduced LPS-induced (20 mg/kg) elevation of circulating histones and Cit-H3 and increased acetylated H3.
Allam *et al.* 2012[277]	LPS (10 mg/kg, i.p.), LPS (1 mg/kg, i.p.) plus CTHs (10 mg/kg, left renal i.a.) 12 h after LPS, renal I/R	Anti-H4 (20 mg/kg, i.p.), CTHs digested by APC (500 nM)	TLR2 or TLR4 KO	CTHs significantly induced renal injury associated with increased mRNA levels of renal cytokines (IL-6, TNF-α, iNOS), TLR2 and TLR4 of mice primed by LPS (1 mg/kg); LPS (10 mg/kg) induced significant tubular cell apoptosis; I/R induced elevation of renal mRNAs of Kim-1, cytokines (IL-6, IL-12, TNF-α), chemokines (CXCL2, CXCL10, CCL5), ICAM and neutrophil infiltration.	APC digested CTHs, anti-H4, or TLR2 or TLR4 KO significantly reduced CHT-induced renal injury in LPS primed mice; anti-H4 significantly reduced renal injury induced by LPS or renal I/R.
Liu *et al.* 2013[360]	CLP, CTHs (60 mg/kg, i.p.)	NA	NA	CLP induced peripheral lymphocyte apoptosis and elevation of circulating histones at 6 h of disease induction; CTHs induced significant lymphocyte apoptosis at 6 h of histone injection.	NA
Wildhagen *et al.* 2014[363]	LPS (20 mg/kg, i.p.), CLP, ConA (30 mg/kg, i.v.)	AADH (570 μg/mouse, i.p.), UFH (114 μg/mouse, i.p.)	NA	All models induced systemic injury and were associated with significant death of mice within 80 h.	AADH, but not UFH, significantly reduced the tail bleeding time; AADH reduced ConA-induced elevation of circulating histones and death; AADH also significantly reduced LPS-induced increase of TNF, lung injury and death; both AADH prophylaxis and treatment significantly decreased CLP-induced death.
Iba *et al.* 2014[384]	LPS (8 mg/kg, i.v.) in rats	NA	AT (125 IU/kg, i.v.), rTM (0.25 mg/kg, i.v.), or AT/rTM	LPS induced significant depletion of WBCs and platelets, reduction of plasma fibrinogen and elevation of circulating histones.	The treatments significantly restored WBCs, platelets and plasma fibrinogen levels, and decreased circulating histones.
Daigo *et al.* 2014[366]	LPS (16 mg/kg, i.p.), CLP, CTHs (50 or 60 mg/kg, i.v.)	PTX3 (N-terminal wild type; 5 or 12 mg/kg, i.p.)	NA	LPS induced dramatic increase of circulating histones with time; LPS, CLP or CTHs (60 mg/kg) induced significant lung injury and death in mice	PTX3 significantly reduced lung injury and death induced by toxins.
Kusano *et al.* 2015[385]	LPS (40 mg/kg, i.p.)	Anti-H1 (4 mg/kg × 2, i.p.)	NA	LPS induced acute lung injury (with histone release) and death with significant elevation of plasma cytokines (IL-1β, IL-6, IL-10, TNF-α) and histones.	Anti-H1 significantly reduced LPS-induced lung injury, systemic inflammation and death.

Kolaczkowska *et al.* 2015[386]	MRSA ($1\text{-}2 \times 10^7$ or $5\text{-}10 \times 10^7$, 200 µl, i.v.)	UFH (400 U/kg × 2, s.c.), PAD4 KO	Anti-vWF (50 µg/mouse, i.v.) or ADAMTS13 (3 µg/mouse, i.v.)	MASA induced accumulation of bacteria in the blood and tested organs (liver, spleen, kidney, lung) with marked liver necrosis, NETs formation (γ-H2AX and NE colocalisation) and increased serum ALT.	Neutrophil depletion (anti-Gr-1 or CD44 KO) abolished liver necrosis and plasma ALT increase; UFH, DNase I, vWF inhibition, PAD4 KO, NE KO or NE inhibitor (sivelestat) significantly reduced γ-H2AX area, liver necrosis and serum ALT.
Kalbitz *et al.* 2015[355]	CLP	α-histone (65 µg per mouse, i.v.)	NLRP3 or caspase, C5aR1 or C5aR2 KO	CLP-induced significant elevation of circulating histones that were associated with abnormalities in systolic and diastolic parameters, reduced left ventricular stroke volume and cardiac output.	Neutrophil depletion, KO of C5aR1, C5aR2, NLRP3, or caspase significantly reduced CLP-induced elevation of circulating histones; anti-histone treatment revered the deranged cardiac dysfunction.
Wang *et al.* 2015[178]	LPS (*Salmonella typhimurium*; 50 mg/kg, i.v.), CLP, CTHs (50 or 75 mg/kg, i.v.)	Heparin (3 or 10 mg/kg, i.v.)	NA	LPS and CLP induced significant lung injury, elevation of plasma histone-DNA complexes and death; CTHs also induced lung injury and at a higher dose caused death within 1 d.	Heparin significantly alleviated lung injury and death induced by LPS, CLP and CTHs. Heparin also reduced LPS- and CLP-induced increase of plasma histone-DNA complexes.
Lee *et al.* 2015[387]	CLP, LPS (*S. aureus*; 2×10^8 cells/mouse, i.p.)	NA	PLD2 KO or inhibitor (4 mg/kg, s.c.)	Both CLP and LPS induced significant multiple organ injury and death; CLP induced lung NETs formation (Cit-H3 and PAD activity).	PLD2 inhibition significantly reduced, while CXCR2 antagonism (SB225002) acerbated multiple organ injury and death; PLD2 inhibition significantly increased lung NETs formation.
Alhamdi *et al.* 2015[320]	LPS (*E coli* K-12, 10^8 colony-forming unit/mouse, i.p.)	ahscFv (10 mg/kg, i.v.)	NA	LPS dramatically increased circulating histones and plasma cardiac troponin levels associated with impaired left ventricular function.	ahscFv significantly reduced cardiac troponin I levels and improved left ventricular function.
Kawai *et al.* 2016[352]	LPS (10 mg/kg, i.p.), I/R model†, CTHs (25-50, 75 or 100 mg/kg, i.v.)	Heparin (10 mg/kg, i.v.), albumin (1 g/kg, i.v.)	NA	Both I/R and LPS significantly increased serum histone-DNA complexes; CTHs dose-dependently increased serum cytokines (IL-1β, IL-6, TNF-α, IL-10), sTM and tissue injury (lung, liver, kidney); CTHs at 75 mg/kg caused significant death within 60 h and at 100 mg/kg caused very rapid death within 2 h.	Heparin, but not albumin, significantly reduced CTH-induced tissue injury and death; boiled CTHs caused significant less death than the natural CTHs.
Biron *et al.* 2016[388]	CLP	Cl-Amidine (50 mg/kg, s.c.)	NA	CLP induced release of circulating histones, NETs formation (Cit-H3) in peritoneal cells, peritoneal fluid and plasma; CLP induced multiple organ injury (elevation of IL-6 in lung, liver, kidney and spleen) and significant death.	Pretreatment of Cl-Amidine reduced NETs formation, systemic injury and death.

LPS, lipopolysaccharides; i.v., intravenous; CLP, cecal ligation puncture; TNF, tumour necrosis factor; CTHs, calf thymus histones; NA, not available; APC, activated protein C; PC, protein C; i.p., intraperitoneal; Cit-H3, citrullinated H3; SAHA, suberoylanilide hydroxamic acid; i.a., intra-artery; I/R, ischaemia-reperfusion; KO, knock out; TLR, Toll-like receptor; IL, interleukin; iNOS, inducible nitric oxide synthase; CXCL, chemokine (C-X-C motif) ligand; CCL, CC chemokine ligands; ICAM, intercellular adhesion molecule; ConA, Concanavalin A; AADH, antithrombin activity depleted heparin; UFH, unfractionated heparin; rTM, recombinant thrombomodulin; AT, antithrombin; WBC, white blood cells; PTX3, pentraxin 3; MRSA, methicillin-resistant Staphylococcus aureus; s.c., subcutaneous; PAD4, protein arginine deiminase 4; vWF, von Willebrand factor; NETs, neutrophil extracellular traps; γ-H2AX, phosphorylated H2AX; NE, neutrophil elastase; ALT, alanine aminotransferase; NLRP3, NLR Family Pyrin

Domain Containing 3; PLD, phospholipase d; CXCR, C-X-C chemokine receptor; ahscFv, anti-histone single chain variable fragment; sTM, soluble thrombomodulin;
*Mice were used if not otherwise stated; †About 30% of blood volume was moved via cardiac puncture, and blood (heparinised) was reperfused into the vein after 1 h of ischaemia.

Supplementary Table 5 Release of extracellular histones in murine acute lung injury models

Studies	Murine experimental models*	Histone-based treatment	Potential histone interacting receptors or binding molecules	*In vivo* findings	Treatment effects
Saffarzadeh *et al.* 2012[341]	LPS (10 µg/mouse, i.t.)	NA	NA	LPS induced NETs formation in the lung tissue (Cit-H3 and MPO colocalisation) and BALF with increased neutrophil infiltration and elastase activity in BALF.	NA
Caudrillier *et al.* 2012[389]	LPS priming (0.1 mg/kg, i.p.) plus anti-MHC-I ($H2K^d$; IgG_{2a}, κ; 0.5-4.5 mg/kg, i.v.)	Anti-H4 (10 mg/kg, i.v.)	NA	LPS plus anti-MHC-I induced acute lung injury was associated with lung NETs formation and increased platelet infiltration, elevated plasma histone-DNA complexes and significant mortality.	Anti-H4, aspirin, tirofiban (an anti-platelet drug), or DNase I significantly reduced lung injury and NETs formation; anti-H4, tirofiban or DNase I completely blocked LPS/anti-MHC-1-induced death.
Abrams *et al.* 2013[271]	Trauma induced by a heavy object falling on each 4 limbs; CTHs (50, 60 or 75 mg/kg, i.v.)	ahscFv (10 mg/kg, i.v.)	NA	Trauma caused multiple organ injury with significant increase of plasma sTM levels and circulating histones; CTHs induced lung NETs formation (Cit-H3), multiple organ failure and elevation of sTM; CTHs at 75 mg/kg caused rapid death.	ahscFv significantly reduced trauma- and CTH-induced lung injury and increase of sTM; ahscFv dose-dependently prevented CTH-induced death.
Bosmann *et al.* 2013[340]	LPS (*E coli* O111:B4; 40 µl, i.t.), IgGIC†, CTHs (50 mg/kg, i.t. or 100 µg/mouse, i.t.)	Anti-H4 (250 µg/mouse, i.v. + 50 µg/mouse, i.t.)	C5a or C5L2 KO	LPS, IgGIC and C5a induced acute lung injury were associated with significant elevation of circulating histones and histone-DNA complexes in BALF; CTHs caused significant lung injury associated with severe disturbances in alveolar-capillary gas exchange, release of alveolar albumin, inflammatory cells, LDH, cytokines (IL-1β, IL-6, IL-9, IL-12, TNF-α, GCSF) and chemokines (eotaxin, CCL2, CCL3, CCL4, CCL5) in BALF.	Anti-H4 significantly reduced severity of C5a-induced lung injury, evidenced by reduction of alveolar albumin and multiple cytokines and chemokines; C5a KO, C5L2 KO, or neutrophil depletion (anti-Ly6G) greatly reduced C5a-induced elevation of circulating histones in BALF.
Zhang *et al.* 2014[364]	HCl (0.01, 0.1, 0.3, 0.5 M, 2 µl/g, i.t.)	Anti-H4 (20 mg/kg, i.v.), heparin or NAH (2.5, 5, 10, 20 mg/kg, i.p.)	NA	HCl dose-dependently increased circulating histones and histone-DNA complexes; HCl at 0.1 M induced significant lung injury evidenced by reduced P_aO_2 and increased lung MPO activity, lung wet/dry ratio and lung histopathology score and plasma APTT levels; HCl at 0.3 M caused significant morality within 24 h of administration.	Both heparin and NAH improved lung injury and coagulation parameters with NAH had better effects; both heparin and NAH dose-dependently reduced HCl-induced death with best effect achieved by highest dose of NAH (20 mg/kg); anti-H4 significantly reduced HCl-induced death;
Zhang *et al.* 2015[390]	HCl (0.1 M, 2 µl/g, i.t.) with or without CTHs (20 mg/kg, i.t.) or H4 (5 mg/kg, i.t.)	Anti-H4 (20 mg/kg, i.v.), heparin (250 IU/kg, s.c.)	NA	HCl induced lung injury associated with elevation of BALF and plasma histones, LDH and MPO activity; administration of CTHs or H4 alone resulted in mild lung injury but significantly acerbated HCl-induced lung injury and mortality.	Anti-H4 and heparin significantly improved HCl-induced lung histopathological score associated with reduction in BALF cytokines (IL-1β, IL-6, , IL-10, TNF-α).
Wygrecka *et al.* 2016[369]	Bleomycin (2.5 U/kg, i.t.), influenza A virus (10^2 PFU, 50µl, inhaled), *S.*	C1 esterase inhibitor (C1INH, or iC1INH; 600 IU/kg, i.v.), α-histone (10 mg/kg, i.p.)	NA	Significant evaluation of circulating histones were observed in all acute lung injury models; bleomycin or CTHs induced typical acute lung injury histopathological changes that were associated with increased lung neutrophil infiltration, wet/dry weight ratio and mRNAs expression of	C1INH significantly reduced bleomycin-induced lung injury and cytokine levels in the BALF; iC1INH significantly reduced CTH-induced lung injury and cytokine levels in the BALF and rescued mice from death.

	penumoniae (5 × 10^6, CFU, transnasally), ventilator, CTHs (50 mg/kg, i.v.)			cytokines/chemokines in the lungs and proteins levels of cytokines/chemokines (IL-1β, TNF-α, CXCL1, CXCL2) in BALF.	

LPS, lipopolysaccharides; i.t., intratracheal; NA, not available; NETs, neutrophil extracellular traps; Cit-H3, citrullinated H3; MPO, myeloperoxidase; BALF, bronchoalveolar lavage fluid; i.p., intraperitoneal; MHC-I, major histocompatibility complex-I; i.v., intravenous; DNase I, deoxyribonuclease I; CTHs, calf thymus histones; ahscFv, anti-histone single chain variable fragment; sTM, soluble thrombomodulin; IgGIC, IgG immune complex; KO, knock out; LDH, lactate dehydrogenase; IL, interleukin; TNF-α, tumour necrosis factor-alpha; GCSF, granulocyte-colony stimulating factor; CCL, CC chemokine ligands; HCl, hydrochloric acid; NAH, N-acetyl-heparin; P_aO_2, partial pressure arterial oxygen; APTT, activated partial thromboplastin time; s.c., subcutaneous; C1INH, C1 esterase inhibitor; iC1INH, reactive centre cleaved- C1INH; CXCL, chemokine (C-X-C motif) ligand.

*Mice were used if not otherwise stated; †IgGIC protocol: anti-BSA IgG (125 µg/mouse, i.t.) followed by BSA (1 mg, i.v.), rmC5a (endotoxin level < 1.0 EU/µg protein, i.t.).

Supplementary Table 6 Release of extracellular histones in murine acute liver and ischaemia-reperfusion injury models

Studies	Murine experimental models*	Histone-based treatment	Potential histone interacting receptors or binding molecules	*In vivo* findings	Treatment effects
Huang *et al.* 2011[358]	Liver I/R, liver I/R plus CTHs (25 mg/kg, i.p.)	Anti-H3 or anti-H4 (20 mg/kg, i.v.)	TLR9 KO or inhibitor (ODN2088; 100 μg/mouse, i.p.) or MyD88 KO	Liver I/R induced significant increase of liver H3 and H4 and circulating histone-DNA complexes over 6 h.	Anti-H3 or anti-H4 significantly alleviated liver necrosis, MAPK proteins, IL-6 and TNF-α as well as serum ALT; receptors inhibition prevented liver necrosis and elevation of serum ALT induced by liver I/R or liver I/R plus CTHs.
Xu *et al.* 2011[322]	ConA (30 mg/kg, i.v.), APAP (500 mg/kg, i.p.)	Anti-H3 or anti-H4 (10 mg/kg, i.v.)	TLR2 or TLR4 KO	ConA and APAP both induced significantly elevation of circulating histones, cytokines (IL-6, TNF-α) and mortality after 2 or 6 h of disease induction.	Anti-H3, TLR2 or TLR4 KO greatly reduced mortality and associated cytokine elevation; anti-H4 also significantly reduced APAP-induced mortality.
Wen *et al.* 2013[391]	GalN (700 mg/kg, i.p.) plus LPS (40 μg/kg, i.p.), GalN (300 mg/kg, i.p.) plus LPS (15 μg/kg, i.p.)	Anti-H4 (20 mg/kg, i.v.)	NA	GalN/LPS induced liver apoptosis and necrosis, increased MPO activity, plasma ALT and TNF-α in circulating histones and histone-DNA complexes; higher doses of GalN/LPS induced significant death within 12 h.	Anti-H4 significantly reduced liver injury, systemic inflammation and death induced by GalN/LPS.
Huang *et al.* 2014[392]	Liver I/R	NA	TLR9 inhibitor (ODN2088; 100 μg/mouse, i.p.), hepatocyte HMGB1 KO	Liver I/R induced significant increase of hepatocellular acetylated histones and γ-H2AX and increased serum histone-DNA complexes.	KO of hepatocyte HMGB1increased nuclear instability led to increased release of histones, liver injury and systemic inflammation induced by liver I/R; TLR9 or PARP-1 (DNA activated receptor) antagonism prevented these effects.
Huang *et al.* 2015[109]	Liver I/R, liver I/R plus CTHs (25 mg/kg, i.p.)	PAD4 inhibitor (YW3-56 or YW4-03; 10 mg/kg, i.p.)	TLR4, TLR9 or MyD88 KO	Liver I/R induced significant increase of mRNA of liver inflammatory cytokines (IL-1β, IL-6, TNF-α, CCL2), liver NETs formation (Cit-H3 and γH2AX) and necrosis, and elevation of serum Cit-H3 and ALT; Liver I/R-induced circulating NETs formation was acerbated by CTHs.	PAD4 inhibitors, DNase I, KO of TLR4, TLR9 or MyD88, or adoptive transfer of TLR4 KO or TLR9 KO neutrophils to neutrophil depleted wild type mice significantly reduced liver injury and systemic inflammation associated with reduced liver and circulation NETs formation.
Wen *et al.* 2016[370]	GalN (500 mg/kg, i.p.) plus LPS (10 μg/kg, i.p.), ConA (20 mg/kg, i.v.), APAP (500 mg/kg, i.p.)	AADH (300 U/kg, s.c.)	NA	GalN/LPS, ConA and APAP induced marked liver necrosis and mortality over 24 h; the liver injury was associated with elevated plasma cytokines (IL-1β, IL-6, IL-8, IL-10, IL-18, TNF-α), ALT and circulating histone-DNA complexes.	AADH significantly prevented liver necrosis, systemic inflammation and mortality induced by liver toxins.
De Meyer *et al.* 2012[393]	Hypoxia, tMCAO and reperfusion† with or without CTHs (10 mg/kg, retro-orbital i.v.)	Anti-H4 (10 mg/kg, i.v.)	NA	Hypoxia induced significant increase of plasma histone-DNA complexes; cerebral I/R caused dramatic increase of plasma cell-free DNA and histone-DNA complexes; addition of CTHs significantly increased I/R-induced infarct volume and worsened neurological function.	Anti-H4 or DNase I significantly reduced I/R-induced infarction volume and alleviated neurology functional scores.
Savchenko *et al.* 2014[347]	Myocardial I/R	PAD4 KO	vWF inhibitor (ADAMTS13;	I/R induced myocardial NETs formation (Cit-H3) and left ventricular infarct that were associated with reduced	PAD KO, DNase I, ADAMTS13, or DNase I plus ADAMTS13 significantly reduced myocardial NETs

			3460 U/kg, retro-orbital i.v.)	ejection fraction and elevated plasma histone-DNA complexes.	formation, left ventricular infarct, circulating histone-DNA complexes thus improved cardiac contractile function.

I/R, ischaemia-reperfusion; CTHs, calf thymus histones; i.p., intraperitoneal; i.v., intravenous; TLR, Toll-like receptor; KO, knock out; MyD88, myeloid differentiation primary response gene 88; MAPK, mitogen-activated protein kinases; IL, interleukin; TNF-α, tumour necrosis factor-alpha; ALT, alanine aminotransferase; ConA, Concanavalin A; APAP, acetaminophen; GalN, D-galactosamine; LPS, lipopolysaccharides; NA, not available; MPO, myeloperoxidase; HMGB1, high motility group box 1; γ-H2AX, phosphorylated H2AX; PARP-1, poly(ADP-ribose) polymerase-1; PAD4, protein arginine deiminase 4; CCL, CC chemokine ligands; Cit-H3, citrullinated H3; NETs, neutrophil extracellular traps; DNase I, deoxyribonuclease I; s.c., subcutaneous; AADH, antithrombin activity depleted heparin; tMCAO, transient middle cerebral artery occlusion; vWF, von Willebrand factor.

*Mice were used if not otherwise stated; †An ischaemia stroke model.

Supplementary Table 7 Release of extracellular histones in murine acute pancreatitis, peritonitis and glomerulonephritis models

Studies	Murine experimental models*	Histone-based treatment	Potential histone interacting receptors or binding molecules	*In vivo* findings	Treatment effects
Kang *et al.* 2014[222]	L-arginine (4 g/kg × 2, i.p.)	Anti-H3 (20 mg/kg, i.p.)	Anti-HMGB1 (20 mg/kg, i.p.), pancreatic HMGB1 KO	L-arginine induced elevation of pancreatic γ-H2AX, H3, H4 and cleaved caspase-3 and was associated with significant death.	Anti-H3 or anti-HMGB1 significantly reduced, but pancreatic HMGB1 KO acerbated severity of acute pancreatitis and mortality.
Merza *et al*. 2014[221]	Taurocholate (5%, i.d.), L-arginine (4 g/kg, i.p.)	Thrombin-derived host defense peptides (GKY20 or GKY25; 0.5 mg/mouse, i.p.)	NA	Taurocholate induced necrotising pancreatitis associated with dramatic release of pancreatic histones, MPO and elevation of serum amylase, IL-6, CXCL2 and lung MPO; L-arginine induced marked pancreatic oedema, neutrophil infiltration and necrosis with increased serum amylase and lung MPO.	Both peptides significantly reduced release of histones, pancreatic injury and systemic injury in both models.
Merza *et al.* 2015[125]	Taurocholate (5%, i.d.), L-arginine (4 g/kg, i.p.)	NA	NA	Taurocholate induced pancreatic NETs formation (EM), release of H3 and H4 and cell-free DNA with elevated plasma DNA and HMGB1, all associated with pancreatic and systemic injury markers assessed at 24 h; L-arginine also induced pancreatic NETs formation and elevation of plasma DNA.	DNase I or anti-Ly6G significantly reduced pancreatic injury, pancreatic NETs formation and histone release; DNase I also reduced systemic injury evidenced by reduction of plasma HMGB1, IL-6, CXCL2, MMP-9 and lung injury.
Ou *et al.* 2015[325]	Caerulein (50 μg/kg/h × 4 or 12, i.p.), taurocholate (3.5%, i.d.)	NA	NA	Taurocholate or 12 injections of caerulein induced necrotising pancreatitis, multiple organ injury and elevation of circulating histones when compared with 4 injections of caerulein or saline controls; circulating histones were significantly associated with pancreatic necrosis score and organ injury parameters.	NA
Allam *et al*. 2013[279]	Acute peritonitis: Necrotic EL4 cells (30 million, 150 μl/mouse, i.p.), H4 (250 μg/mouse, i.p.)	APC (5 mg/kg, i.p.), anti-H4 (20 mg/kg, i.p.)	NLRP3 KO	Necrotic EL4 cells or H4 induced significant neutrophil recruitment into peritoneal cavity.	Necrotic cell-induced peritoneal neutrophil recruitment was nearly abolished by APC, anti-H4, or NLRP3 KO.
Kumar *et al.* 2015[372]	Glomerular necrosis: Anti-GBM serum (100 μl/mouse, i.v.)	Heparin (50 IU/mouse, i.p.), APC (5 mg/kg, i.p.), anti-H4 (20 mg/kg, i.p.), PAD4 inhibitor (Cl-amide; 10 mg/kg, i.p.)	NA	Anti-GBM serum induced severe glomerular necrosis, loss of podocytes and inflammatory cell infiltration, associated with increased urine albumin/creatinine ratio.	Heparin, APC, anti-H4 or PAD4 inhibition had similar effects of reducing anti-GBM-induced glomerular necrosis; delayed histone blockage also significantly improved glomerular necrosis; the combination of anti-histone modalities did not enhance therapeutic effects.

i.p., intraperitoneal; HMGB1, high motility group box 1; KO, knock out; γ-H2AX, phosphorylated H2AX; i.d., intraductal; NA, not available; MPO, myeloperoxidase; IL, interleukin; CXCL, chemokine (C-X-C motif) ligand; NETs, neutrophil extracellular traps; EM, electron microscopy; DNase

I, deoxyribonuclease I; MMP-9, matrix metallopeptidase 9; APC, activated protein C; NLRP3, NLR Family Pyrin Domain Containing 3; GBM, glomerular basement membrane; i.v., intravenous; PAD4, protein arginine deiminase 4.
*Mice were used if not otherwise stated.

Supplementary Table 8 Murine histone-induced coagulopathy models

Studies	**Murine experimental models***	**Histone-based treatment**	**Potential histone interacting receptors or binding molecules**	***In vivo* findings**	**Treatment effects**
Fuchs *et al.* 2011[275]	CTHs (10-50, 60 or 75 mg/kg, i.v.)	UFH (50 mg/kg, i.v.)	β3-integrin KO	CTHs dose-dependently (10-50 mg/kg) depleted platelets from circulation and prolonged tail bleeding time; CTHs at higher doses (60 or 75 mg/kg) caused death within 15 mins of infusion.	UFH and platelet depletion (anti-GP1b) completely or β3-integrin KO partially protected histone-induced death.
Abrams *et al.* 2013[265]	CTHs (75 mg/kg, i.v.)	CRP (1.6, 2.5, or 10 mg/kg, i.v.)	NA	CTHs caused lung oedema, haemorrhage and thrombosis with rapid death in mice.	CRP significantly reduced lung injury and dose-dependently protected mice from CTH-induced death.
Nakahara *et al.* 2013[323]	CTHs (20-95 mg/kg, i.v.)	Recombinant human sTM (40, 80, or 110 mg/kg, i.v. or 110 mg/kg × 2, i.v.)	NA	CTHs dose-dependently induced death of mice, deletion of platelets and white blood cells, deposition of platelets and fibrin(ogen) in the lung, acute right-sided heart failure and ventricular arrest, reduction of plasma fibrinogen and increase of APTT and PPT.	sTM pre-treatment significantly prevented CTH-induced platelets depletion, reduced organ dysfunction (lung and heart) and rescued mice from death.
Kowalska *et al.* 2014[371]	CTHs (20, 50, or 75 mg/kg, i.v.), II a (8 U/kg, i.v.) plus CTHs (0-20 mg/kg, i.v.)	UFH, ODSH (0.5, 5 or 50 mg/kg, i.v.)	NA	CTHs dose-dependently induced plasma APC elevation, the levels of which were significantly higher with low dose II a infusion or in platelet factor KO mice; sublethal, but not low or lethal, dose CTHs caused significant elevation of plasma APC.	Both UFH and oxygen-desulfated UFH abolished sublethal CTH-induced APC rise; only ODSH increased APC generation upon lethal CTH challenge; ODSH, but not UFH, at low to moderate doses did not significantly induce prolonged APTT.
Westman *et al.* 2014[365]	CTHs (0.75 or 1.5 mg/mouse, i.v.)	MBP-p33 (1.5 mg/mouse, i.v.)	NA	CTHs (0.75 mg) infusion caused significant haemolysis and platelets depletion at higher dose (1.5 mg) caused rapid death in mice.	MBP-p33 (an endothelial surface protein) significantly reduced CTH-induced haemolysis, platelets depletion and death.
Chaaban *et al.* 2015[367]	CTHs (50 mg/kg, i.v.)	IAIP (50 mg/kg, retro-orbital i.v.), HMW-HA (90 mg/kg, retro-orbital i.v.)	NA	CTH-induced thrombocytopenia associated with prolonged bleeding time, elevation of cytokines (IL-1β, IL-6, IL-10, TNF-α,), chemokines (CXCL1, CCL2) and lung injury.	CTH-induced thrombocytopenia and tissue toxicity was significantly prevented by pre-treatment of IAIP or HMW-HA.
Iba *et al.* 2015[394]	H3 (25, 50 or 100 mg/kg, i.v.) in rats	UFH (350 or 700 U/kg, i.v.) or LMWH (2 or 4 mg/kg, i.v.)	NA	H3 at all doses cause significant death; H3 also significantly reduced WBCs and platelets as well as increased plasma fibrin/fibrinogen degradation products, ALT and BUN levels.	Both UHF and LMWH significantly reduced rats from histone-induced death, and improved coagulation parameters and systemic injury inflammation parameters.
Alhamdi *et al.* 2016[351]	CTHs (20-75 mg/kg, i.v.)	ahscFv (10 mg/kg, i.v.)	NA	CTHs induced cardiomyopathy and pulmonary microvascular obstruction; CTHs dose-dependently induced NETs formation (Cit-H3) and fibrin deposition in the lung tissue.	Anti-histone pretreatment significantly restored cardiac function.
Lam *et al.* 2016[376]	CTHs (75 mg/kg, i.v.)	NA	NA	CTHs induced significant elevation of plasma vWF and thrombin-anti-thrombin levels as well as decrease of platelets.	NA

Michels *et al.* 2016[395]	CTHs (10-40 mg/kg, retro-orbital i.v.)	NA	NA	All CTHs increased vWF and angiopoietin-2 expression and depleted platelets.	NA

CTHs, calf thymus histones; i.v., intravenous; KO, knock out; UFH, unfractionated heparin; CRP, C-reactive protein; NA, not available; sTM, soluble thrombomodulin; APTT, activated partial thromboplastin time; PPT, partial thromboplastin time; ODSH, partially desulfated 2-O, 3-O desulfated heparin; APC, activated protein C; IAIP, inter-α inhibitor protein; HMW-HA, high-molecular weight hyaluronan; IL, interleukin; TNF-α, tumour necrosis factor-alpha; CXCL, C-X-C motif chemokine; CCL, CC chemokine ligands; LMWH, low-molecular weight heparin; WBCs, white blood cells; ALT, alanine aminotransferase; BUN, blood urea nitrogen; ahscFv, anti-histone single chain variable fragment; NETs, neutrophil extracellular traps; Cit-H3, citrullinated H3; vWF, von Willebrand factor.
*Mice were used if not otherwise state

Statement of originality

The work presented in the thesis was conducted when I was a PhD candidate studying in the Institute of Infection and Global Health at the University of Liverpool between May 2011 and April 2015. I have done all the work and written up the thesis, except for the specific contributions listed as follows:

In Chapter 2, Dr Simon T. Abrams performed experiments on FITC-histone membrane binding and histone-induced calcium influx and cell death in endothelial cells. In Chapter 3, Dr Dunhao Su assisted me for the generation of anti-histone single chain variable fragment. In Chapter 4, all the samples from *in vivo* experiments were provided by Mr Zhengxing Cheng from Southeast University of China. In Chapters 5 and 6, Dr Wei Huang and Mr Peter Szatmary assisted me with data collection and analyses.

Publications and presentations arising from this thesis

Publications (#indicates co-first authors):

1. Abrams ST, Zhang N, Manson J, **Liu T,** Dart C, Baluwa F, Wang SS, Brohi K, Kipar A, Yu W, Wang G, Toh CH. Circulating histones are mediators of trauma-associated lung injury. Am J Respir Crit Care Med 2013; 187(2): 160-169. (IF 13.1)
2. Ou X#, Cheng Z#, **Liu T#,** Tang Z, Huang W, Szatmary P, Zheng S, Sutton R, Toh CH*, Zhang N, Wang G. Circulating Histone Levels Reflect Disease Severity in Animal Models of Acute Pancreatitis. Pancreas. 2015;44(7):1089-95. (IF 3.0)
3. Alhamdi Y, Zi M, Abrams ST, **Liu T,** Su D, Welters I, Dutt T, Cartwright EJ, Wang G, Toh CH. Circulating Histone Concentrations Differentially Affect the Predominance of Left or Right Ventricular Dysfunction in Critical Illness. Crit Care Med. 2016;44(5):e278-88. (IF 7.4)
4. **Liu T#**, Huang W#, Szatmary P, Abrams ST, Alhamdi Y, Lin Z, Greenhalf W, Wang G, Sutton R, Toh CH*. Accuracy of circulating histones to predict persistent organ failure and mortality in patients with acute pancreatitis. Brit J Surg 2017 ID: BJS10538 in press. (IF 5.5)

Presentations:

1. **Liu T,** Wang G, Abrams ST, Toh CH. Monitoring circulating histone levels as an indication clinically of activated coagulation and endothelial damage. British Society for Haematology 53rd Annual Scientific Meeting 2013. Liverpool, Merseyside, UK. 2013.04.15-04.17. (Oral presentation)
2. **Liu T,** Cheng ZX, Su DH, Szatmary P, Huang W, Abrams S, Greenhalf W, Welters I, Wang G, Sutton R, Toh CH. Elevation of circulating histones represents disease severity in human and murine acute pancreatitis. The 45th Annual Meeting of American Pancreatic Association. Big Island, Hawaii, USA. 2014.11.05-11.08. (Poster presentation)
3. **Liu T,** Huang W, Szatmary P, Abrams ST, Greenhalf W, Welters I, Wang G, Sutton R, Toh CH. Early Prediction of Major Clinical Outcomes of Patients with Acute Pancreatitis by Circulating Histones. The 47th Annual Meeting of the European Pancreatic Club. Toledo, Spain. 2015.06.24-06.26. (Poster presentation and travel grant award)
4. **Liu T,** Huang W, Abrams S, Wang L, Szatmary P, Alhamdi Y, Lin ZQ, Welters I, Wang G, Toh CH, Sutton R. Elevated circulating histones associate with multiple organ dysfunction syndrome in acute pancreatitis. The 47th Annual Meeting of American Pancreatic Association. Boston, MA, USA. 2016.10.26-10.29. (Oral presentation)

Bibliography

1. Adhikari NK, Fowler RA, Bhagwanjee S, et al. Critical care and the global burden of critical illness in adults. Lancet 2010;376:1339-46.
2. Dowdy DW, Eid MP, Sedrakyan A, et al. Quality of life in adult survivors of critical illness: a systematic review of the literature. Intensive Care Med 2005;31:611-20.
3. Myhren H, Ekeberg O, Stokland O. Health-related quality of life and return to work after critical illness in general intensive care unit patients: a 1-year follow-up study. Crit Care Med 2010;38:1554-61.
4. Cerro G, Checkley W. Global analysis of critical care burden. Lancet Respir Med 2014;2:343-4.
5. Coopersmith CM, Wunsch H, Fink MP, et al. A comparison of critical care research funding and the financial burden of critical illness in the United States. Crit Care Med 2012;40:1072-9.
6. Zhao B, Ni TT, Zhou W, et al. Prognostic value of brain natriuretic peptide and cardiac troponin I for severe acute pancreatitis. Critical Care Medicine 2016;44:p221.
7. Edbrooke D, Hibbert C, Corcoran M. Review for the NHS Executive of Adult Critical Care Services: An International Perspective. 1999.
8. Moritz ML, Ayus JC. Maintenance Intravenous Fluids in Acutely Ill Patients. N Engl J Med 2015;373:1350-60.
9. Sadaka F, Juarez M, Naydenov S, et al. Fluid resuscitation in septic shock: the effect of increasing fluid balance on mortality. J Intensive Care Med 2014;29:213-7.
10. Dellinger RP, Levy MM, Rhodes A, et al. Surviving sepsis campaign: international guidelines for management of severe sepsis and septic shock: 2012. Crit Care Med 2013;41:580-637.
11. Barr J, Fraser GL, Puntillo K, et al. Clinical practice guidelines for the management of pain, agitation, and delirium in adult patients in the intensive care unit. Crit Care Med 2013;41:263-306.
12. Casaer MP, Van den Berghe G. Nutrition in the acute phase of critical illness. N Engl J Med 2014;370:1227-36.
13. Yasumoto M, Okamoto K, Sato T, et al. Prognosis of critically ill patients with multiple organ failure. J Anesth 1994;8:269-73.
14. Marshall JC. The multiple organ dysfunction syndrome. Surgical Treatment: Evidence-Based and Problem-Oriented 2001.
15. Vincent JL, Marshall JC, Namendys-Silva SA, et al. Assessment of the worldwide burden of critical illness: the intensive care over nations (ICON) audit. Lancet Respir Med 2014;2:380-6.
16. Singer M, Deutschman CS, Seymour CW, et al. The Third International Consensus Definitions for Sepsis and Septic Shock (Sepsis-3). JAMA 2016;315:801-10.
17. Wilmer A. ICU management of severe acute pancreatitis. Eur J Intern Med 2004;15:274-280.
18. Nathens AB, Curtis JR, Beale RJ, et al. Management of the critically ill patient with severe acute pancreatitis. Crit Care Med 2004;32:2524-36.
19. Werner J, Feuerbach S, Uhl W, et al. Management of acute pancreatitis: from surgery to interventional intensive care. Gut 2005;54:426-36.

20. Patton H, Misel M, Gish RG. Acute liver failure in adults: an evidence-based management protocol for clinicians. Gastroenterol Hepatol (N Y) 2012;8:161-212.
21. Willars C. Update in intensive care medicine: acute liver failure. Initial management, supportive treatment and who to transplant. Curr Opin Crit Care 2014;20:202-9.
22. Sweeney RM, McAuley DF. Acute respiratory distress syndrome. Lancet 2016.
23. Ashbaugh DG, Bigelow DB, Petty TL, et al. Acute respiratory distress in adults. Lancet 1967;2:319-23.
24. Murray JF, Matthay MA, Luce JM, et al. An expanded definition of the adult respiratory distress syndrome. Am Rev Respir Dis 1988;138:720-3.
25. Bernard GR, Artigas A, Brigham KL, et al. The American-European Consensus Conference on ARDS. Definitions, mechanisms, relevant outcomes, and clinical trial coordination. Am J Respir Crit Care Med 1994;149:818-24.
26. Ferguson ND, Davis AM, Slutsky AS, et al. Development of a clinical definition for acute respiratory distress syndrome using the Delphi technique. J Crit Care 2005;20:147-54.
27. Force ADT, Ranieri VM, Rubenfeld GD, et al. Acute respiratory distress syndrome: the Berlin Definition. JAMA 2012;307:2526-33.
28. Zhao X, Huang W, Li J, et al. Noninvasive Positive-Pressure Ventilation in Acute Respiratory Distress Syndrome in Patients With Acute Pancreatitis: A Retrospective Cohort Study. Pancreas 2016;45:58-63.
29. Bellani G, Laffey JG, Pham T, et al. Epidemiology, Patterns of Care, and Mortality for Patients With Acute Respiratory Distress Syndrome in Intensive Care Units in 50 Countries. JAMA 2016;315:788-800.
30. Frat JP, Thille AW, Mercat A, et al. High-flow oxygen through nasal cannula in acute hypoxemic respiratory failure. N Engl J Med 2015;372:2185-96.
31. Coggins AR, Cummins EN, Burns B. Management of critical illness with non-invasive ventilation by an Australian HEMS. Emerg Med J 2016.
32. Vincent JL, De Backer D. Circulatory shock. N Engl J Med 2013;369:1726-34.
33. Sakr Y, Reinhart K, Vincent JL, et al. Does dopamine administration in shock influence outcome? Results of the Sepsis Occurrence in Acutely Ill Patients (SOAP) Study. Crit Care Med 2006;34:589-97.
34. Angus DC, van der Poll T. Severe sepsis and septic shock. N Engl J Med 2013;369:840-51.
35. Peacock WFt, De Marco T, Fonarow GC, et al. Cardiac troponin and outcome in acute heart failure. N Engl J Med 2008;358:2117-26.
36. Vasile VC, Chai HS, Abdeldayem D, et al. Elevated cardiac troponin T levels in critically ill patients with sepsis. Am J Med 2013;126:1114-21.
37. Altmann DR, Korte W, Maeder MT, et al. Elevated cardiac troponin I in sepsis and septic shock: no evidence for thrombus associated myocardial necrosis. PLoS One 2010;5:e9017.
38. Pro CI, Yealy DM, Kellum JA, et al. A randomized trial of protocol-based care for early septic shock. N Engl J Med 2014;370:1683-93.
39. Investigators A, Group ACT, Peake SL, et al. Goal-directed resuscitation for patients with early septic shock. N Engl J Med 2014;371:1496-506.
40. Mouncey PR, Osborn TM, Power GS, et al. Trial of early, goal-directed resuscitation for septic shock. N Engl J Med 2015;372:1301-11.
41. Haydock MD, Mittal A, Wilms HR, et al. Fluid therapy in acute pancreatitis: anybody's guess. Ann Surg 2013;257:182-8.

42. De Backer D, Biston P, Devriendt J, et al. Comparison of dopamine and norepinephrine in the treatment of shock. N Engl J Med 2010;362:779-89.
43. Levy B, Perez P, Perny J, et al. Comparison of norepinephrine-dobutamine to epinephrine for hemodynamics, lactate metabolism, and organ function variables in cardiogenic shock. A prospective, randomized pilot study. Crit Care Med 2011;39:450-5.
44. Gamper G, Havel C, Arrich J, et al. Vasopressors for hypotensive shock. Cochrane Database Syst Rev 2016;2:CD003709.
45. Singri N, Ahya SN, Levin ML. Acute renal failure. JAMA 2003;289:747-51.
46. Bellomo R, Kellum JA, Ronco C. Acute kidney injury. Lancet 2012;380:756-66.
47. Schrier RW, Wang W. Acute renal failure and sepsis. N Engl J Med 2004;351:159-69.
48. Uchino S, Kellum JA, Bellomo R, et al. Acute renal failure in critically ill patients: a multinational, multicenter study. JAMA 2005;294:813-8.
49. Mehta RL, Burdmann EA, Cerda J, et al. Recognition and management of acute kidney injury in the International Society of Nephrology 0by25 Global Snapshot: a multinational cross-sectional study. Lancet 2016;387:2017-25.
50. Chawla LS, Eggers PW, Star RA, et al. Acute kidney injury and chronic kidney disease as interconnected syndromes. N Engl J Med 2014;371:58-66.
51. Lameire N, Van Biesen W, Vanholder R. Acute renal failure. Lancet 2005;365:417-30.
52. Network VNARFT, Palevsky PM, Zhang JH, et al. Intensity of renal support in critically ill patients with acute kidney injury. N Engl J Med 2008;359:7-20.
53. Pannu N, Klarenbach S, Wiebe N, et al. Renal replacement therapy in patients with acute renal failure: a systematic review. JAMA 2008;299:793-805.
54. Gaudry S, Hajage D, Schortgen F, et al. Initiation Strategies for Renal-Replacement Therapy in the Intensive Care Unit. N Engl J Med 2016;375:122-33.
55. Lee WM. Acute liver failure. N Engl J Med 1993;329:1862-72.
56. Caraceni P, Van Thiel DH. Acute liver failure. Lancet 1995;345:163-9.
57. Bernal W, Jalan R, Quaglia A, et al. Acute-on-chronic liver failure. Lancet 2015;386:1576-87.
58. Bernal W, Auzinger G, Dhawan A, et al. Acute liver failure. Lancet 2010;376:190-201.
59. Bernal W, Wendon J. Acute liver failure. N Engl J Med 2013;369:2525-34.
60. Levi M, Opal SM. Coagulation abnormalities in critically ill patients. Crit Care 2006;10:222.
61. Hunt BJ. Bleeding and coagulopathies in critical care. N Engl J Med 2014;370:847-59.
62. Levi M, Ten Cate H. Disseminated intravascular coagulation. N Engl J Med 1999;341:586-92.
63. Toh CH, Alhamdi Y. Current consideration and management of disseminated intravascular coagulation. Hematology Am Soc Hematol Educ Program 2013;2013:286-91.
64. Gando S, Levi M, Toh CH. Disseminated intravascular coagulation. Nat Rev Dis Primers 2016;2:16037.
65. Kakafika A, Papadopoulos V, Mimidis K, et al. Coagulation, platelets, and acute pancreatitis. Pancreas 2007;34:15-20.

66. Maeda K, Hirota M, Ichihara A, et al. Applicability of disseminated intravascular coagulation parameters in the assessment of the severity of acute pancreatitis. Pancreas 2006;32:87-92.
67. Radenkovic DV, Bajec DD, Karamarkovic AR. Discussion on applicability of disseminated intravascular coagulation parameters in the assessment of the severity of acute pancreatitis. Pancreas 2006;33:106-7; author reply 107-8.
68. Wilde JT, Thomas WE, Lane DA, et al. Acquired dysfibrinogenaemia masquerading as disseminated intravascular coagulation in acute pancreatitis. J Clin Pathol 1988;41:615-8.
69. Ahmed Z, Mohyuddin Z. Complete gastric outlet obstruction following acid ingestion complicated by acute pancreatitis and disseminated intravascular coagulation. Postgrad Med J 1997;73:421-3.
70. Saif MW. DIC secondary to acute pancreatitis. Clin Lab Haematol 2005;27:278-82.
71. Tsokos M, Braun C. Acute pancreatitis presenting as sudden, unexpected death: an autopsy-based study of 27 cases. Am J Forensic Med Pathol 2007;28:267-70.
72. Toh CH, Alhamdi Y, Abrams ST. Current Pathological and Laboratory Considerations in the Diagnosis of Disseminated Intravascular Coagulation. Ann Lab Med 2016;36:505-12.
73. Kobayashi N, Maekawa T, Takada M, et al. Criteria for diagnosis of DIC based on the analysis of clinical and laboratory findings in 345 DIC patients collected by the Research Committee on DIC in Japan. Bibl Haematol 1983:265-75.
74. Gando S, Iba T, Eguchi Y, et al. A multicenter, prospective validation of disseminated intravascular coagulation diagnostic criteria for critically ill patients: comparing current criteria. Crit Care Med 2006;34:625-31.
75. Taylor FB, Jr., Toh CH, Hoots WK, et al. Towards definition, clinical and laboratory criteria, and a scoring system for disseminated intravascular coagulation. Thromb Haemost 2001;86:1327-30.
76. Bakhtiari K, Meijers JC, de Jonge E, et al. Prospective validation of the International Society of Thrombosis and Haemostasis scoring system for disseminated intravascular coagulation. Crit Care Med 2004;32:2416-21.
77. Gando S, Saitoh D, Ogura H, et al. Natural history of disseminated intravascular coagulation diagnosed based on the newly established diagnostic criteria for critically ill patients: results of a multicenter, prospective survey. Crit Care Med 2008;36:145-50.
78. Levi M, Toh CH, Thachil J, et al. Guidelines for the diagnosis and management of disseminated intravascular coagulation. British Committee for Standards in Haematology. Br J Haematol 2009;145:24-33.
79. Thachil J, Falanga A, Levi M, et al. Management of cancer-associated disseminated intravascular coagulation: guidance from the SSC of the ISTH. J Thromb Haemost 2015;13:671-5.
80. Wijdicks EF, Kokmen E, O'Brien PC. Measurement of impaired consciousness in the neurological intensive care unit: a new test. J Neurol Neurosurg Psychiatry 1998;64:117-9.
81. Teasdale G, Jennett B. Assessment of coma and impaired consciousness. A practical scale. Lancet 1974;2:81-4.
82. Teasdale G, Maas A, Lecky F, et al. The Glasgow Coma Scale at 40 years: standing the test of time. Lancet Neurol 2014;13:844-54.
83. Gill MR, Reiley DG, Green SM. Interrater reliability of Glasgow Coma Scale scores in the emergency department. Ann Emerg Med 2004;43:215-23.

84. Bruno MA, Ledoux D, Lambermont B, et al. Comparison of the Full Outline of UnResponsiveness and Glasgow Liege Scale/Glasgow Coma Scale in an intensive care unit population. Neurocrit Care 2011;15:447-53.
85. Laureys S, Bodart O, Gosseries O. The Glasgow Coma Scale: time for critical reappraisal? Lancet Neurol 2014;13:755-7.
86. Pironi L, Arends J, Baxter J, et al. ESPEN endorsed recommendations. Definition and classification of intestinal failure in adults. Clin Nutr 2015;34:171-80.
87. Kirkpatrick AW, Roberts DJ, De Waele J, et al. Intra-abdominal hypertension and the abdominal compartment syndrome: updated consensus definitions and clinical practice guidelines from the World Society of the Abdominal Compartment Syndrome. Intensive Care Med 2013;39:1190-206.
88. Abdominal compartment syndrome. BMJ Best Practise 2015.
89. van Brunschot S, Schut AJ, Bouwense SA, et al. Abdominal compartment syndrome in acute pancreatitis: a systematic review. Pancreas 2014;43:665-74.
90. Marshall JC, Cook DJ, Christou NV, et al. Multiple organ dysfunction score: a reliable descriptor of a complex clinical outcome. Crit Care Med 1995;23:1638-52.
91. Le Gall JR, Klar J, Lemeshow S, et al. The Logistic Organ Dysfunction system. A new way to assess organ dysfunction in the intensive care unit. ICU Scoring Group. JAMA 1996;276:802-10.
92. Vincent JL, Moreno R, Takala J, et al. The SOFA (Sepsis-related Organ Failure Assessment) score to describe organ dysfunction/failure. On behalf of the Working Group on Sepsis-Related Problems of the European Society of Intensive Care Medicine. Intensive Care Med 1996;22:707-10.
93. Vincent JL, de Mendonca A, Cantraine F, et al. Use of the SOFA score to assess the incidence of organ dysfunction/failure in intensive care units: results of a multicenter, prospective study. Working group on "sepsis-related problems" of the European Society of Intensive Care Medicine. Crit Care Med 1998;26:1793-800.
94. Ferreira FL, Bota DP, Bross A, et al. Serial evaluation of the SOFA score to predict outcome in critically ill patients. JAMA 2001;286:1754-8.
95. Jones AE, Trzeciak S, Kline JA. The Sequential Organ Failure Assessment score for predicting outcome in patients with severe sepsis and evidence of hypoperfusion at the time of emergency department presentation. Crit Care Med 2009;37:1649-54.
96. Vincent JL, Moreno R. Clinical review: scoring systems in the critically ill. Crit Care 2010;14:207.
97. Brown KA, Brain SD, Pearson JD, et al. Neutrophils in development of multiple organ failure in sepsis. Lancet 2006;368:157-69.
98. Yang ZW, Meng XX, Xu P. Central role of neutrophil in the pathogenesis of severe acute pancreatitis. J Cell Mol Med 2015;19:2513-20.
99. Taylor NJ, Nishtala A, Manakkat Vijay GK, et al. Circulating neutrophil dysfunction in acute liver failure. Hepatology 2013;57:1142-52.
100. Heinzelmann M, Mercer-Jones MA, Passmore JC. Neutrophils and renal failure. Am J Kidney Dis 1999;34:384-99.
101. Nathan C. Neutrophils and immunity: challenges and opportunities. Nat Rev Immunol 2006;6:173-82.

102. Mantovani A, Cassatella MA, Costantini C, et al. Neutrophils in the activation and regulation of innate and adaptive immunity. Nat Rev Immunol 2011;11:519-31.
103. Kolaczkowska E, Kubes P. Neutrophil recruitment and function in health and inflammation. Nat Rev Immunol 2013;13:159-75.
104. Remijsen Q, Kuijpers TW, Wirawan E, et al. Dying for a cause: NETosis, mechanisms behind an antimicrobial cell death modality. Cell Death Differ 2011;18:581-8.
105. Mayadas TN, Cullere X, Lowell CA. The multifaceted functions of neutrophils. Annu Rev Pathol 2014;9:181-218.
106. Brinkmann V, Reichard U, Goosmann C, et al. Neutrophil extracellular traps kill bacteria. Science 2004;303:1532-5.
107. Steinberg BE, Grinstein S. Unconventional roles of the NADPH oxidase: signaling, ion homeostasis, and cell death. Sci STKE 2007;2007:pe11.
108. Brinkmann V, Zychlinsky A. Beneficial suicide: why neutrophils die to make NETs. Nat Rev Microbiol 2007;5:577-82.
109. Huang H, Tohme S, Al-Khafaji AB, et al. Damage-associated molecular pattern-activated neutrophil extracellular trap exacerbates sterile inflammatory liver injury. Hepatology 2015;62:600-14.
110. Seong SY, Matzinger P. Hydrophobicity: an ancient damage-associated molecular pattern that initiates innate immune responses. Nat Rev Immunol 2004;4:469-78.
111. van den Berg JM, van Koppen E, Ahlin A, et al. Chronic granulomatous disease: the European experience. PLoS One 2009;4:e5234.
112. Fuchs TA, Abed U, Goosmann C, et al. Novel cell death program leads to neutrophil extracellular traps. J Cell Biol 2007;176:231-41.
113. Remijsen Q, Vanden Berghe T, Wirawan E, et al. Neutrophil extracellular trap cell death requires both autophagy and superoxide generation. Cell Res 2011;21:290-304.
114. Kaplan MJ, Radic M. Neutrophil extracellular traps: double-edged swords of innate immunity. J Immunol 2012;189:2689-95.
115. Hamaguchi S, Hirose T, Akeda Y, et al. Identification of neutrophil extracellular traps in the blood of patients with systemic inflammatory response syndrome. J Int Med Res 2013;41:162-8.
116. Fuchs TA, Brill A, Duerschmied D, et al. Extracellular DNA traps promote thrombosis. Proc Natl Acad Sci U S A 2010;107:15880-5.
117. Brill A, Fuchs TA, Savchenko AS, et al. Neutrophil extracellular traps promote deep vein thrombosis in mice. J Thromb Haemost 2012;10:136-44.
118. Martinod K, Demers M, Fuchs TA, et al. Neutrophil histone modification by peptidylarginine deiminase 4 is critical for deep vein thrombosis in mice. Proc Natl Acad Sci U S A 2013;110:8674-9.
119. Martinod K, Wagner DD. Thrombosis: tangled up in NETs. Blood 2014;123:2768-76.
120. Carestia A, Rivadeneyra L, Romaniuk MA, et al. Functional responses and molecular mechanisms involved in histone-mediated platelet activation. Thromb Haemost 2013;110:1035-45.
121. Yu Y, Su K. Neutrophil Extracellular Traps and Systemic Lupus Erythematosus. J Clin Cell Immunol 2013;4.

122. Lood C, Blanco LP, Purmalek MM, et al. Neutrophil extracellular traps enriched in oxidized mitochondrial DNA are interferogenic and contribute to lupus-like disease. Nat Med 2016;22:146-53.
123. Marcos V, Zhou Z, Yildirim AO, et al. CXCR2 mediates NADPH oxidase-independent neutrophil extracellular trap formation in cystic fibrosis airway inflammation. Nat Med 2010;16:1018-23.
124. Cheng OZ, Palaniyar N. NET balancing: a problem in inflammatory lung diseases. Front Immunol 2013;4:1.
125. Merza M, Hartman H, Rahman M, et al. Neutrophil Extracellular Traps Induce Trypsin Activation, Inflammation, and Tissue Damage in Mice With Severe Acute Pancreatitis. Gastroenterology 2015;149:1920-1931 e8.
126. Korhonen JT, Dudeja V, Dawra R, et al. Neutrophil Extracellular Traps Provide a Grip on the Enigmatic Pathogenesis of Acute Pancreatitis. Gastroenterology 2015;149:1682-5.
127. Leppkes M, Maueroder C, Hirth S, et al. Externalized decondensed neutrophil chromatin occludes pancreatic ducts and drives pancreatitis. Nat Commun 2016;7:10973.
128. Wong SL, Demers M, Martinod K, et al. Diabetes primes neutrophils to undergo NETosis, which impairs wound healing. Nat Med 2015;21:815-9.
129. Schauer C, Janko C, Munoz LE, et al. Aggregated neutrophil extracellular traps limit inflammation by degrading cytokines and chemokines. Nat Med 2014;20:511-7.
130. Dinarello CA. Historical insights into cytokines. Eur J Immunol 2007;37 Suppl 1:S34-45.
131. Wajant H, Pfizenmaier K, Scheurich P. Tumor necrosis factor signaling. Cell Death Differ 2003;10:45-65.
132. Brenner D, Blaser H, Mak TW. Regulation of tumour necrosis factor signalling: live or let die. Nat Rev Immunol 2015;15:362-74.
133. Sedger LM, McDermott MF. TNF and TNF-receptors: From mediators of cell death and inflammation to therapeutic giants - past, present and future. Cytokine Growth Factor Rev 2014;25:453-72.
134. Kalliolias GD, Ivashkiv LB. TNF biology, pathogenic mechanisms and emerging therapeutic strategies. Nat Rev Rheumatol 2016;12:49-62.
135. Dinarello CA. Immunological and inflammatory functions of the interleukin-1 family. Annu Rev Immunol 2009;27:519-50.
136. Van Snick J. Interleukin-6: an overview. Annu Rev Immunol 1990;8:253-78.
137. Rath T, Billmeier U, Waldner MJ, et al. From physiology to disease and targeted therapy: interleukin-6 in inflammation and inflammation-associated carcinogenesis. Arch Toxicol 2015;89:541-54.
138. Hunter CA, Jones SA. IL-6 as a keystone cytokine in health and disease. Nat Immunol 2015;16:448-57.
139. Luster AD. Chemokines--chemotactic cytokines that mediate inflammation. N Engl J Med 1998;338:436-45.
140. Schulte W, Bernhagen J, Bucala R. Cytokines in sepsis: potent immunoregulators and potential therapeutic targets--an updated view. Mediators Inflamm 2013;2013:165974.
141. Blackwell TS, Christman JW. Sepsis and cytokines: current status. Br J Anaesth 1996;77:110-7.
142. Makhija R, Kingsnorth AN. Cytokine storm in acute pancreatitis. J Hepatobiliary Pancreat Surg 2002;9:401-10.

143. Kim B, Lee Y, Kim E, et al. The Interleukin-1alpha Precursor is Biologically Active and is Likely a Key Alarmin in the IL-1 Family of Cytokines. Front Immunol 2013;4:391.
144. Dinarello CA, Simon A, van der Meer JW. Treating inflammation by blocking interleukin-1 in a broad spectrum of diseases. Nat Rev Drug Discov 2012;11:633-52.
145. Schett G, Dayer JM, Manger B. Interleukin-1 function and role in rheumatic disease. Nat Rev Rheumatol 2016;12:14-24.
146. Zlotnik A, Yoshie O. Chemokines: a new classification system and their role in immunity. Immunity 2000;12:121-7.
147. Moser B, Willimann K. Chemokines: role in inflammation and immune surveillance. Ann Rheum Dis 2004;63 Suppl 2:ii84-ii89.
148. Charo IF, Ransohoff RM. The many roles of chemokines and chemokine receptors in inflammation. N Engl J Med 2006;354:610-21.
149. Turner MD, Nedjai B, Hurst T, et al. Cytokines and chemokines: At the crossroads of cell signalling and inflammatory disease. Biochim Biophys Acta 2014;1843:2563-2582.
150. Baggiolini M, Clark-Lewis I. Interleukin-8, a chemotactic and inflammatory cytokine. FEBS Lett 1992;307:97-101.
151. Harada A, Sekido N, Akahoshi T, et al. Essential involvement of interleukin-8 (IL-8) in acute inflammation. J Leukoc Biol 1994;56:559-64.
152. Gerszten RE, Garcia-Zepeda EA, Lim YC, et al. MCP-1 and IL-8 trigger firm adhesion of monocytes to vascular endothelium under flow conditions. Nature 1999;398:718-23.
153. Deshmane SL, Kremlev S, Amini S, et al. Monocyte chemoattractant protein-1 (MCP-1): an overview. J Interferon Cytokine Res 2009;29:313-26.
154. Shi C, Pamer EG. Monocyte recruitment during infection and inflammation. Nat Rev Immunol 2011;11:762-74.
155. Nauseef WM, Borregaard N. Neutrophils at work. Nat Immunol 2014;15:602-11.
156. de Oliveira S, Rosowski EE, Huttenlocher A. Neutrophil migration in infection and wound repair: going forward in reverse. Nat Rev Immunol 2016;16:378-91.
157. Reis e Sousa C. Dendritic cells in a mature age. Nat Rev Immunol 2006;6:476-83.
158. Swiecki M, Colonna M. The multifaceted biology of plasmacytoid dendritic cells. Nat Rev Immunol 2015;15:471-85.
159. Gordon S, Taylor PR. Monocyte and macrophage heterogeneity. Nat Rev Immunol 2005;5:953-64.
160. Mosser DM, Edwards JP. Exploring the full spectrum of macrophage activation. Nat Rev Immunol 2008;8:958-69.
161. Murray PJ, Wynn TA. Protective and pathogenic functions of macrophage subsets. Nat Rev Immunol 2011;11:723-37.
162. Ginhoux F, Jung S. Monocytes and macrophages: developmental pathways and tissue homeostasis. Nat Rev Immunol 2014;14:392-404.
163. Marshall JS. Mast-cell responses to pathogens. Nat Rev Immunol 2004;4:787-99.
164. Abraham SN, St John AL. Mast cell-orchestrated immunity to pathogens. Nat Rev Immunol 2010;10:440-52.
165. Chen GY, Nunez G. Sterile inflammation: sensing and reacting to damage. Nat Rev Immunol 2010;10:826-37.

166. Kroemer G, El-Deiry WS, Golstein P, et al. Classification of cell death: recommendations of the Nomenclature Committee on Cell Death. Cell Death Differ 2005;12 Suppl 2:1463-7.
167. Galluzzi L, Bravo-San Pedro JM, Vitale I, et al. Essential versus accessory aspects of cell death: recommendations of the NCCD 2015. Cell Death Differ 2015;22:58-73.
168. Hengartner MO. The biochemistry of apoptosis. Nature 2000;407:770-6.
169. Riedl SJ, Shi Y. Molecular mechanisms of caspase regulation during apoptosis. Nat Rev Mol Cell Biol 2004;5:897-907.
170. Taylor RC, Cullen SP, Martin SJ. Apoptosis: controlled demolition at the cellular level. Nat Rev Mol Cell Biol 2008;9:231-41.
171. Hotchkiss RS, Strasser A, McDunn JE, et al. Cell death. N Engl J Med 2009;361:1570-83.
172. Czabotar PE, Lessene G, Strasser A, et al. Control of apoptosis by the BCL-2 protein family: implications for physiology and therapy. Nat Rev Mol Cell Biol 2014;15:49-63.
173. Klionsky DJ. Autophagy: from phenomenology to molecular understanding in less than a decade. Nat Rev Mol Cell Biol 2007;8:931-7.
174. Kroemer G, Levine B. Autophagic cell death: the story of a misnomer. Nat Rev Mol Cell Biol 2008;9:1004-10.
175. Youle RJ, Narendra DP. Mechanisms of mitophagy. Nat Rev Mol Cell Biol 2011;12:9-14.
176. Choi AM, Ryter SW, Levine B. Autophagy in human health and disease. N Engl J Med 2013;368:651-62.
177. Marino G, Niso-Santano M, Baehrecke EH, et al. Self-consumption: the interplay of autophagy and apoptosis. Nat Rev Mol Cell Biol 2014;15:81-94.
178. Wang F, Zhang N, Li B, et al. Heparin defends against the toxicity of circulating histones in sepsis. Front Biosci (Landmark Ed) 2015;20:1259-70.
179. Declercq W, Vanden Berghe T, Vandenabeele P. RIP kinases at the crossroads of cell death and survival. Cell 2009;138:229-32.
180. Wrighton KH. Cell death: A killer puts a stop on necroptosis. Nat Rev Mol Cell Biol 2011;12:279.
181. Vanlangenakker N, Vanden Berghe T, Vandenabeele P. Many stimuli pull the necrotic trigger, an overview. Cell Death Differ 2012;19:75-86.
182. Ofengeim D, Yuan J. Regulation of RIP1 kinase signalling at the crossroads of inflammation and cell death. Nat Rev Mol Cell Biol 2013;14:727-36.
183. Linkermann A, Green DR. Necroptosis. N Engl J Med 2014;370:455-65.
184. Chan FK, Luz NF, Moriwaki K. Programmed necrosis in the cross talk of cell death and inflammation. Annu Rev Immunol 2015;33:79-106.
185. Conrad M, Angeli JP, Vandenabeele P, et al. Regulated necrosis: disease relevance and therapeutic opportunities. Nat Rev Drug Discov 2016;15:348-66.
186. Lemasters JJ, Nieminen AL, Qian T, et al. The mitochondrial permeability transition in cell death: a common mechanism in necrosis, apoptosis and autophagy. Biochim Biophys Acta 1998;1366:177-96.
187. Crompton M. The mitochondrial permeability transition pore and its role in cell death. Biochem J 1999;341 (Pt 2):233-49.
188. Brenner C, Moulin M. Physiological roles of the permeability transition pore. Circ Res 2012;111:1237-47.
189. Brenner C, Grimm S. The permeability transition pore complex in cancer cell death. Oncogene 2006;25:4744-56.

190. Bergsbaken T, Fink SL, Cookson BT. Pyroptosis: host cell death and inflammation. Nat Rev Microbiol 2009;7:99-109.
191. Fatokun AA, Dawson VL, Dawson TM. Parthanatos: mitochondrial-linked mechanisms and therapeutic opportunities. Br J Pharmacol 2014;171:2000-16.
192. Dixon SJ, Lemberg KM, Lamprecht MR, et al. Ferroptosis: an iron-dependent form of nonapoptotic cell death. Cell 2012;149:1060-72.
193. Dixon SJ, Stockwell BR. The role of iron and reactive oxygen species in cell death. Nat Chem Biol 2014;10:9-17.
194. Xie Y, Hou W, Song X, et al. Ferroptosis: process and function. Cell Death Differ 2016;23:369-79.
195. Matzinger P. Tolerance, danger, and the extended family. Annu Rev Immunol 1994;12:991-1045.
196. Takeuchi O, Akira S. Pattern recognition receptors and inflammation. Cell 2010;140:805-20.
197. Angus DC, van der Poll T. Severe sepsis and septic shock. N Engl J Med 2013;369:2063.
198. Wang H, Ma S. The cytokine storm and factors determining the sequence and severity of organ dysfunction in multiple organ dysfunction syndrome. Am J Emerg Med 2008;26:711-5.
199. Chen R, Kang R, Fan XG, et al. Release and activity of histone in diseases. Cell Death Dis 2014;5:e1370.
200. Lotze MT, Tracey KJ. High-mobility group box 1 protein (HMGB1): nuclear weapon in the immune arsenal. Nat Rev Immunol 2005;5:331-42.
201. Galluzzi L, Kepp O, Kroemer G. Mitochondria: master regulators of danger signalling. Nat Rev Mol Cell Biol 2012;13:780-8.
202. Silva MT. Secondary necrosis: the natural outcome of the complete apoptotic program. FEBS Lett 2010;584:4491-9.
203. Kono H, Rock KL. How dying cells alert the immune system to danger. Nat Rev Immunol 2008;8:279-89.
204. Nimah M, Brilli RJ. Coagulation dysfunction in sepsis and multiple organ system failure. Crit Care Clin 2003;19:441-58.
205. Bersten A, Sibbald WJ. Circulatory disturbances in multiple systems organ failure. Crit Care Clin 1989;5:233-54.
206. Swank GM, Deitch EA. Role of the gut in multiple organ failure: bacterial translocation and permeability changes. World J Surg 1996;20:411-7.
207. Magnotti LJ, Upperman JS, Xu DZ, et al. Gut-derived mesenteric lymph but not portal blood increases endothelial cell permeability and promotes lung injury after hemorrhagic shock. Ann Surg 1998;228:518-27.
208. Deitch EA. Role of the gut lymphatic system in multiple organ failure. Curr Opin Crit Care 2001;7:92-8.
209. Deitch EA. Multiple organ failure. Pathophysiology and potential future therapy. Ann Surg 1992;216:117-34.
210. Linkermann A, Stockwell BR, Krautwald S, et al. Regulated cell death and inflammation: an auto-amplification loop causes organ failure. Nat Rev Immunol 2014;14:759-67.
211. Holdenrieder S, Stieber P. Clinical use of circulating nucleosomes. Crit Rev Clin Lab Sci 2009;46:1-24.
212. Chen Q, Ye L, Jin Y, et al. Circulating nucleosomes as a predictor of sepsis and organ dysfunction in critically ill patients. Int J Infect Dis 2012;16:e558-64.

213. Xu J, Zhang X, Pelayo R, et al. Extracellular histones are major mediators of death in sepsis. Nat Med 2009;15:1318-21.
214. Pemberton AD, Brown JK, Inglis NF. Proteomic identification of interactions between histones and plasma proteins: implications for cytoprotection. Proteomics 2010;10:1484-93.
215. Freeman CG, Parish CR, Knox KJ, et al. The accumulation of circulating histones on heparan sulphate in the capillary glycocalyx of the lungs. Biomaterials 2013;34:5670-6.
216. Isobe T, Kofuji K, Okada K, et al. Adsorption of histones on natural polysaccharides: The potential as agent for multiple organ failure in sepsis. Int J Biol Macromol 2016;84:54-7.
217. Fattahi F, Grailer JJ, Jajou L, et al. Organ distribution of histones after intravenous infusion of FITC histones or after sepsis. Immunol Res 2015;61:177-86.
218. Gauthier VJ, Tyler LN, Mannik M. Blood clearance kinetics and liver uptake of mononucleosomes in mice. J Immunol 1996;156:1151-6.
219. Burlingame RW, Volzer MA, Harris J, et al. The effect of acute phase proteins on clearance of chromatin from the circulation of normal mice. J Immunol 1996;156:4783-8.
220. Marsman G, Zeerleder S, Luken BM. Extracellular histones, cell-free DNA, or nucleosomes: differences in immunostimulation. Cell Death Dis 2016;7:e2518.
221. Merza M, Rahman M, Zhang S, et al. Human thrombin-derived host defense peptides inhibit neutrophil recruitment and tissue injury in severe acute pancreatitis. Am J Physiol Gastrointest Liver Physiol 2014;307:G914-21.
222. Kang R, Zhang Q, Hou W, et al. Intracellular Hmgb1 inhibits inflammatory nucleosome release and limits acute pancreatitis in mice. Gastroenterology 2014;146:1097-107.
223. Penttila AK, Rouhiainen A, Kylanpaa L, et al. Circulating nucleosomes as predictive markers of severe acute pancreatitis. J Intensive Care 2016;4:14.
224. Kornberg RD. Chromatin structure: a repeating unit of histones and DNA. Science 1974;184:868-71.
225. Luger K, Mader AW, Richmond RK, et al. Crystal structure of the nucleosome core particle at 2.8 A resolution. Nature 1997;389:251-60.
226. Kulaeva OI, Hsieh FK, Studitsky VM. RNA polymerase complexes cooperate to relieve the nucleosomal barrier and evict histones. Proc Natl Acad Sci U S A 2010;107:11325-30.
227. Vignali M, Workman JL. Location and function of linker histones. Nat Struct Biol 1998;5:1025-8.
228. Zhou YB, Gerchman SE, Ramakrishnan V, et al. Position and orientation of the globular domain of linker histone H5 on the nucleosome. Nature 1998;395:402-5.
229. Fan L, Roberts VA. Complex of linker histone H5 with the nucleosome and its implications for chromatin packing. Proc Natl Acad Sci U S A 2006;103:8384-9.
230. McBryant SJ, Lu X, Hansen JC. Multifunctionality of the linker histones: an emerging role for protein-protein interactions. Cell Res 2010;20:519-28.
231. Zhou BR, Jiang J, Feng H, et al. Structural Mechanisms of Nucleosome Recognition by Linker Histones. Mol Cell 2015;59:628-38.
232. Holdenrieder S, Stieber P, Bodenmuller H, et al. Nucleosomes in serum as a marker for cell death. Clin Chem Lab Med 2001;39:596-605.

233. Happel N, Doenecke D. Histone H1 and its isoforms: contribution to chromatin structure and function. Gene 2009;431:1-12.
234. Maze I, Noh KM, Soshnev AA, et al. Every amino acid matters: essential contributions of histone variants to mammalian development and disease. Nat Rev Genet 2014;15:259-71.
235. Tanaka Y, Tawaramoto-Sasanuma M, Kawaguchi S, et al. Expression and purification of recombinant human histones. Methods 2004;33:3-11.
236. Grynkiewicz G, Poenie M, Tsien RY. A new generation of Ca2+ indicators with greatly improved fluorescence properties. J Biol Chem 1985;260:3440-50.
237. Venkatesh S, Workman JL. Histone exchange, chromatin structure and the regulation of transcription. Nat Rev Mol Cell Biol 2015;16:178-89.
238. Hong S, Leroueil PR, Janus EK, et al. Interaction of polycationic polymers with supported lipid bilayers and cells: nanoscale hole formation and enhanced membrane permeability. Bioconjug Chem 2006;17:728-34.
239. Tan-No K, Esashi A, Nakagawasai O, et al. Nociceptive behavior induced by poly-L-lysine and other basic compounds involves the spinal NMDA receptors. Brain Res 2004;1008:49-53.
240. Strand BL, Ryan TL, In't Veld P, et al. Poly-L-Lysine induces fibrosis on alginate microcapsules via the induction of cytokines. Cell Transplant 2001;10:263-75.
241. Gamberucci A, Fulceri R, Marcolongo P, et al. Histones and basic polypeptides activate Ca2+/cation influx in various cell types. Biochem J 1998;331 (Pt 2):623-30.
242. Ferreira L, Pereira L, Faria R. Fluorescent dyes as a reliable tool in P2X7 receptor-associated pore studies. J Bioenerg Biomembr 2015;47:283-307.
243. Elssner A, Duncan M, Gavrilin M, et al. A novel P2X7 receptor activator, the human cathelicidin-derived peptide LL37, induces IL-1 beta processing and release. J Immunol 2004;172:4987-94.
244. Sainz B, Jr., Alcala S, Garcia E, et al. Microenvironmental hCAP-18/LL-37 promotes pancreatic ductal adenocarcinoma by activating its cancer stem cell compartment. Gut 2015;64:1921-35.
245. Chen Q, Jin Y, Zhang K, et al. Alarmin HNP-1 promotes pyroptosis and IL-1beta release through different roles of NLRP3 inflammasome via P2X7 in LPS-primed macrophages. Innate Immun 2014;20:290-300.
246. Lee DY, Huang CM, Nakatsuji T, et al. Histone H4 is a major component of the antimicrobial action of human sebocytes. J Invest Dermatol 2009;129:2489-96.
247. Nangami G, Koumangoye R, Shawn Goodwin J, et al. Fetuin-A associates with histones intracellularly and shuttles them to exosomes to promote focal adhesion assembly resulting in rapid adhesion and spreading in breast carcinoma cells. Exp Cell Res 2014;328:388-400.
248. Fernandes JM, Kemp GD, Molle MG, et al. Anti-microbial properties of histone H2A from skin secretions of rainbow trout, Oncorhynchus mykiss. Biochem J 2002;368:611-20.
249. Ferrari D, Pizzirani C, Gulinelli S, et al. Modulation of P2X7 receptor functions by polymyxin B: crucial role of the hydrophobic tail of the antibiotic molecule. Br J Pharmacol 2007;150:445-54.
250. Lundy PM, Nelson P, Mi L, et al. Pharmacological differentiation of the P2X7 receptor and the maitotoxin-activated cationic channel. Eur J Pharmacol 2004;487:17-28.

251. Schilling WP, Wasylyna T, Dubyak GR, et al. Maitotoxin and P2Z/P2X(7) purinergic receptor stimulation activate a common cytolytic pore. Am J Physiol 1999;277:C766-76.
252. Schilling WP, Sinkins WG, Estacion M. Maitotoxin activates a nonselective cation channel and a P2Z/P2X(7)-like cytolytic pore in human skin fibroblasts. Am J Physiol 1999;277:C755-65.
253. Ojcius DM, Muller S, Hasselkus-Light CS, et al. Plasma membrane-associated proteins with the ability to partially inhibit perforin-mediated lysis. Immunol Lett 1991;28:101-8.
254. Schoenauer R, Atanassoff AP, Wolfmeier H, et al. P2X7 receptors mediate resistance to toxin-induced cell lysis. Biochim Biophys Acta 2014;1843:915-22.
255. Papathanassoglou ED, Moynihan JA, Ackerman MH. Does programmed cell death (apoptosis) play a role in the development of multiple organ dysfunction in critically ill patients? a review and a theoretical framework. Crit Care Med 2000;28:537-49.
256. Yasuhara S, Asai A, Sahani ND, et al. Mitochondria, endoplasmic reticulum, and alternative pathways of cell death in critical illness. Crit Care Med 2007;35:S488-95.
257. Horan PK, Wheeless LL, Jr. Quantitative single cell analysis and sorting. Science 1977;198:149-57.
258. Fulton RJ, McDade RL, Smith PL, et al. Advanced multiplexed analysis with the FlowMetrix system. Clin Chem 1997;43:1749-56.
259. Vignali DA. Multiplexed particle-based flow cytometric assays. J Immunol Methods 2000;243:243-55.
260. Wang LS, Leung YY, Chang SK, et al. Comparison of xMAP and ELISA assays for detecting cerebrospinal fluid biomarkers of Alzheimer's disease. J Alzheimers Dis 2012;31:439-45.
261. Anderson NL, Anderson NG. The human plasma proteome: history, character, and diagnostic prospects. Mol Cell Proteomics 2002;1:845-67.
262. Anderson NL. The roles of multiple proteomic platforms in a pipeline for new diagnostics. Mol Cell Proteomics 2005;4:1441-4.
263. Anderson NL. The clinical plasma proteome: a survey of clinical assays for proteins in plasma and serum. Clin Chem 2010;56:177-85.
264. Shechter D, Dormann HL, Allis CD, et al. Extraction, purification and analysis of histones. Nat Protoc 2007;2:1445-57.
265. Abrams ST, Zhang N, Dart C, et al. Human CRP defends against the toxicity of circulating histones. J Immunol 2013;191:2495-502.
266. Pandol SJ, Saluja AK, Imrie CW, et al. Acute pancreatitis: bench to the bedside. Gastroenterology 2007;133:1056 e1-1056 e25.
267. El-Serag HB, Rudolph KL. Hepatocellular carcinoma: epidemiology and molecular carcinogenesis. Gastroenterology 2007;132:2557-76.
268. Modlin IM, Bilchik AJ, Zucker KA, et al. Cholecystokinin augmentation of 'surgical' pancreatitis. Benefits of receptor blockade. Arch Surg 1989;124:574-8.
269. Rifai Y, Elder AS, Carati CJ, et al. The tripeptide analog feG ameliorates severity of acute pancreatitis in a caerulein mouse model. Am J Physiol Gastrointest Liver Physiol 2008;294:G1094-9.
270. Wan MH, Huang W, Latawiec D, et al. Review of experimental animal models of biliary acute pancreatitis and recent advances in basic research. HPB (Oxford) 2012;14:73-81.

271. Abrams ST, Zhang N, Manson J, et al. Circulating histones are mediators of trauma-associated lung injury. Am J Respir Crit Care Med 2013;187:160-9.
272. Wang H, Liao H, Ochani M, et al. Cholinergic agonists inhibit HMGB1 release and improve survival in experimental sepsis. Nat Med 2004;10:1216-21.
273. Zhang Q, Raoof M, Chen Y, et al. Circulating mitochondrial DAMPs cause inflammatory responses to injury. Nature 2010;464:104-7.
274. Kang R, Lotze MT, Zeh HJ, et al. Cell death and DAMPs in acute pancreatitis. Mol Med 2014;20:466-77.
275. Fuchs TA, Bhandari AA, Wagner DD. Histones induce rapid and profound thrombocytopenia in mice. Blood 2011;118:3708-14.
276. Semeraro F, Ammollo CT, Morrissey JH, et al. Extracellular histones promote thrombin generation through platelet-dependent mechanisms: involvement of platelet TLR2 and TLR4. Blood 2011;118:1952-61.
277. Allam R, Scherbaum CR, Darisipudi MN, et al. Histones from dying renal cells aggravate kidney injury via TLR2 and TLR4. J Am Soc Nephrol 2012;23:1375-88.
278. Huang H, Chen HW, Evankovich J, et al. Histones activate the NLRP3 inflammasome in Kupffer cells during sterile inflammatory liver injury. J Immunol 2013;191:2665-79.
279. Allam R, Darisipudi MN, Tschopp J, et al. Histones trigger sterile inflammation by activating the NLRP3 inflammasome. Eur J Immunol 2013;43:3336-42.
280. Kim MS, Hong JH, Li Q, et al. Deletion of TRPC3 in mice reduces store-operated Ca2+ influx and the severity of acute pancreatitis. Gastroenterology 2009;137:1509-17.
281. Singh VP, Bren GD, Algeciras-Schimnich A, et al. Nelfinavir/ritonavir reduces acinar injury but not inflammation during mouse caerulein pancreatitis. Am J Physiol Gastrointest Liver Physiol 2009;296:G1040-6.
282. Laukkarinen JM, Van Acker GJ, Weiss ER, et al. A mouse model of acute biliary pancreatitis induced by retrograde pancreatic duct infusion of Na-taurocholate. Gut 2007;56:1590-8.
283. Zhou X, Xue C. Ghrelin inhibits the development of acute pancreatitis and nuclear factor kappaB activation in pancreas and liver. Pancreas 2009;38:752-7.
284. Wildi S, Kleeff J, Mayerle J, et al. Suppression of transforming growth factor beta signalling aborts caerulein induced pancreatitis and eliminates restricted stimulation at high caerulein concentrations. Gut 2007;56:685-92.
285. Kim H. Cerulein pancreatitis: oxidative stress, inflammation, and apoptosis. Gut Liver 2008;2:74-80.
286. Guo Q, Li A, Xia Q, et al. The role of organ failure and infection in necrotizing pancreatitis: a prospective study. Ann Surg 2014;259:1201-7.
287. Toouli J, Brooke-Smith M, Bassi C, et al. Guidelines for the management of acute pancreatitis. J Gastroenterol Hepatol 2002;17 Suppl:S15-39.
288. Su KH, Cuthbertson C, Christophi C. Review of experimental animal models of acute pancreatitis. HPB (Oxford) 2006;8:264-86.
289. Kocsis AK, Szabolcs A, Hofner P, et al. Plasma concentrations of high-mobility group box protein 1, soluble receptor for advanced glycation end-products and circulating DNA in patients with acute pancreatitis. Pancreatology 2009;9:383-91.
290. Yasuda T, Ueda T, Takeyama Y, et al. Significant increase of serum high-mobility group box chromosomal protein 1 levels in patients with severe acute pancreatitis. Pancreas 2006;33:359-63.

291. Gornik I, Wagner J, Gasparovic V, et al. Free serum DNA is an early predictor of severity in acute pancreatitis. Clin Biochem 2009;42:38-43.
292. Gornik O, Gornik I, Wagner J, et al. Evaluation of cell-free DNA in plasma and serum as early predictors of severity in acute pancreatitis. Pancreas 2011;40:787-8.
293. Otsuki M, Takeda K, Matsuno S, et al. Criteria for the diagnosis and severity stratification of acute pancreatitis. World J Gastroenterol 2013;19:5798-805.
294. Bollen TL, Singh VK, Maurer R, et al. A comparative evaluation of radiologic and clinical scoring systems in the early prediction of severity in acute pancreatitis. Am J Gastroenterol 2012;107:612-9.
295. Mounzer R, Langmead CJ, Wu BU, et al. Comparison of existing clinical scoring systems to predict persistent organ failure in patients with acute pancreatitis. Gastroenterology 2012;142:1476-82; quiz e15-6.
296. Shields CJ, Winter DC, Redmond HP. Lung injury in acute pancreatitis: mechanisms, prevention, and therapy. Curr Opin Crit Care 2002;8:158-63.
297. Kleine TJ, Gladfelter A, Lewis PN, et al. Histone-induced damage of a mammalian epithelium: the conductive effect. Am J Physiol 1995;268:C1114-25.
298. Esmon CT. Molecular circuits in thrombosis and inflammation. Thromb Haemost 2013;109:416-20.
299. Peery AF, Crockett SD, Barritt AS, et al. Burden of Gastrointestinal, Liver, and Pancreatic Diseases in the United States. Gastroenterology 2015;149:1731-1741 e3.
300. Banks PA, Bollen TL, Dervenis C, et al. Classification of acute pancreatitis--2012: revision of the Atlanta classification and definitions by international consensus. Gut 2013;62:102-11.
301. Tenner S, Baillie J, DeWitt J, et al. American College of Gastroenterology guideline: management of acute pancreatitis. Am J Gastroenterol 2013;108:1400-15; 1416.
302. Dellinger EP, Forsmark CE, Layer P, et al. Determinant-based classification of acute pancreatitis severity: an international multidisciplinary consultation. Ann Surg 2012;256:875-80.
303. Besselink MG, van Santvoort HC, Boermeester MA, et al. Timing and impact of infections in acute pancreatitis. Br J Surg 2009;96:267-73.
304. Petrov MS, Shanbhag S, Chakraborty M, et al. Organ failure and infection of pancreatic necrosis as determinants of mortality in patients with acute pancreatitis. Gastroenterology 2010;139:813-20.
305. Buter A, Imrie CW, Carter CR, et al. Dynamic nature of early organ dysfunction determines outcome in acute pancreatitis. Br J Surg 2002;89:298-302.
306. Johnson CD, Abu-Hilal M. Persistent organ failure during the first week as a marker of fatal outcome in acute pancreatitis. Gut 2004;53:1340-4.
307. Sharma M, Banerjee D, Garg PK. Characterization of newer subgroups of fulminant and subfulminant pancreatitis associated with a high early mortality. Am J Gastroenterol 2007;102:2688-95.
308. Wu BU, Banks PA. Clinical management of patients with acute pancreatitis. Gastroenterology 2013;144:1272-81.
309. Dimagno MJ, Wamsteker EJ, Rizk RS, et al. A combined paging alert and web-based instrument alters clinician behavior and shortens hospital length of stay in acute pancreatitis. Am J Gastroenterol 2014;109:306-15.

310. Yang CJ, Chen J, Phillips AR, et al. Predictors of severe and critical acute pancreatitis: a systematic review. Dig Liver Dis 2014;46:446-51.
311. Singh VK, Wu BU, Bollen TL, et al. A prospective evaluation of the bedside index for severity in acute pancreatitis score in assessing mortality and intermediate markers of severity in acute pancreatitis. Am J Gastroenterol 2009;104:966-71.
312. Koutroumpakis E, Wu BU, Bakker OJ, et al. Admission Hematocrit and Rise in Blood Urea Nitrogen at 24 h Outperform other Laboratory Markers in Predicting Persistent Organ Failure and Pancreatic Necrosis in Acute Pancreatitis: A Post Hoc Analysis of Three Large Prospective Databases. Am J Gastroenterol 2015;110:1707-16.
313. Al-Bahrani AZ, Ammori BJ. Clinical laboratory assessment of acute pancreatitis. Clin Chim Acta 2005;362:26-48.
314. Meher S, Mishra TS, Sasmal PK, et al. Role of Biomarkers in Diagnosis and Prognostic Evaluation of Acute Pancreatitis. J Biomark 2015;2015:519534.
315. Huang W, Altaf K, Jin T, et al. Prediction of the severity of acute pancreatitis on admission by urinary trypsinogen activation peptide: a meta-analysis. World J Gastroenterol 2013;19:4607-15.
316. Deng L, Wang L, Yong F, et al. Prediction of the severity of acute pancreatitis on admission by carboxypeptidase-B activation peptide: A systematic review and meta-analysis. Clin Biochem 2015;48:740-6.
317. Neoptolemos JP, Kemppainen EA, Mayer JM, et al. Early prediction of severity in acute pancreatitis by urinary trypsinogen activation peptide: a multicentre study. Lancet 2000;355:1955-60.
318. Blenkiron C, Askelund KJ, Shanbhag ST, et al. MicroRNAs in mesenteric lymph and plasma during acute pancreatitis. Ann Surg 2014;260:341-7.
319. Sandstrom A, Andersson R, Segersvard R, et al. Serum proteome profiling of pancreatitis using recombinant antibody microarrays reveals disease-associated biomarker signatures. Proteomics Clin Appl 2012;6:486-96.
320. Alhamdi Y, Abrams ST, Cheng Z, et al. Circulating Histones Are Major Mediators of Cardiac Injury in Patients With Sepsis. Crit Care Med 2015;43:2094-103.
321. Alhamdi Y, Zi M, Abrams ST, et al. Circulating Histone Concentrations Differentially Affect the Predominance of Left or Right Ventricular Dysfunction in Critical Illness. Crit Care Med 2015.
322. Xu J, Zhang X, Monestier M, et al. Extracellular histones are mediators of death through TLR2 and TLR4 in mouse fatal liver injury. J Immunol 2011;187:2626-31.
323. Nakahara M, Ito T, Kawahara K, et al. Recombinant thrombomodulin protects mice against histone-induced lethal thromboembolism. PLoS One 2013;8:e75961.
324. Alhamdi Y, Abrams ST, Lane S, et al. Histone-associated thrombocytopenia in patients who are critically ill. JAMA 2016 in-press.
325. Ou X, Cheng Z, Liu T, et al. Circulating Histone Levels Reflect Disease Severity in Animal Models of Acute Pancreatitis. Pancreas 2015;44:1089-95.
326. Stevens PE, Levin A, Kidney Disease: Improving Global Outcomes Chronic Kidney Disease Guideline Development Work Group M. Evaluation and management of chronic kidney disease: synopsis of the kidney disease: improving global outcomes 2012 clinical practice guideline. Ann Intern Med 2013;158:825-30.

327. Papachristou GI, Muddana V, Yadav D, et al. Comparison of BISAP, Ranson's, APACHE-II, and CTSI scores in predicting organ failure, complications, and mortality in acute pancreatitis. Am J Gastroenterol 2010;105:435-41; quiz 442.
328. Wu BU, Bakker OJ, Papachristou GI, et al. Blood urea nitrogen in the early assessment of acute pancreatitis: an international validation study. Arch Intern Med 2011;171:669-76.
329. Yasuda T, Ueda T, Shinzeki M, et al. Increase of high-mobility group box chromosomal protein 1 in blood and injured organs in experimental severe acute pancreatitis. Pancreas 2007;34:487-8.
330. Shen X, Li WQ. High-mobility group box 1 protein and its role in severe acute pancreatitis. World J Gastroenterol 2015;21:1424-35.
331. Lankisch PG, Apte M, Banks PA. Acute pancreatitis. Lancet 2015.
332. Roberts SE, Akbari A, Thorne K, et al. The incidence of acute pancreatitis: impact of social deprivation, alcohol consumption, seasonal and demographic factors. Aliment Pharmacol Ther 2013;38:539-48.
333. Vege SS, Gardner TB, Chari ST, et al. Low mortality and high morbidity in severe acute pancreatitis without organ failure: a case for revising the Atlanta classification to include "moderately severe acute pancreatitis". Am J Gastroenterol 2009;104:710-5.
334. Kadiyala V, Suleiman SL, McNabb-Baltar J, et al. The Atlanta Classification, Revised Atlanta Classification, and Determinant-Based Classification of Acute Pancreatitis: Which Is Best at Stratifying Outcomes? Pancreas 2016;45:510-5.
335. Halonen KI, Pettila V, Leppaniemi AK, et al. Multiple organ dysfunction associated with severe acute pancreatitis. Crit Care Med 2002;30:1274-9.
336. Zheng L, Xue J, Jaffee EM, et al. Role of immune cells and immune-based therapies in pancreatitis and pancreatic ductal adenocarcinoma. Gastroenterology 2013;144:1230-40.
337. Gunjaca I, Zunic J, Gunjaca M, et al. Circulating cytokine levels in acute pancreatitis-model of SIRS/CARS can help in the clinical assessment of disease severity. Inflammation 2012;35:758-63.
338. Hoque R, Malik AF, Gorelick F, et al. Sterile inflammatory response in acute pancreatitis. Pancreas 2012;41:353-7.
339. Hoque R, Sohail M, Malik A, et al. TLR9 and the NLRP3 inflammasome link acinar cell death with inflammation in acute pancreatitis. Gastroenterology 2011;141:358-69.
340. Bosmann M, Grailer JJ, Ruemmler R, et al. Extracellular histones are essential effectors of C5aR- and C5L2-mediated tissue damage and inflammation in acute lung injury. FASEB J 2013;27:5010-21.
341. Saffarzadeh M, Juenemann C, Queisser MA, et al. Neutrophil extracellular traps directly induce epithelial and endothelial cell death: a predominant role of histones. PLoS One 2012;7:e32366.
342. Grailer JJ, Canning BA, Kalbitz M, et al. Critical role for the NLRP3 inflammasome during acute lung injury. J Immunol 2014;192:5974-83.
343. Alhamdi Y, Zi M, Abrams ST, et al. Circulating histone concentrations differentially affect the predominance of left or right ventricular dysfunction in critical illness. Critical Care Med [in-press] 2015.
344. Awla D, Abdulla A, Regner S, et al. TLR4 but not TLR2 regulates inflammation and tissue damage in acute pancreatitis induced by retrograde infusion of taurocholate. Inflamm Res 2011;60:1093-8.

345. Zhang H, Neuhofer P, Song L, et al. IL-6 trans-signaling promotes pancreatitis-associated lung injury and lethality. J Clin Invest 2013;123:1019-31.
346. Martin MA, Saracibar E, Santamaria A, et al. [Interleukin 18 (IL-18) and other immunological parameters as markers of severity in acute pancreatitis]. Rev Esp Enferm Dig 2008;100:768-73.
347. Savchenko AS, Borissoff JI, Martinod K, et al. VWF-mediated leukocyte recruitment with chromatin decondensation by PAD4 increases myocardial ischemia/reperfusion injury in mice. Blood 2014;123:141-8.
348. Ammollo CT, Semeraro F, Xu J, et al. Extracellular histones increase plasma thrombin generation by impairing thrombomodulin-dependent protein C activation. J Thromb Haemost 2011;9:1795-803.
349. Xilong Ou ZC, Tingting Liu, Zhongming Tang, Wei Huang,, Peter Szatmary SZ, Robert Sutton, Cheng Hock Toh,Nan Zhang, and Guozheng Wang. Circulating Histone Levels Reflect Disease Severity in Animal Models of Acute Pancreatitis. Pancreas 2015;44:1089-1095.
350. Alhamdi Y, Abrams ST, Lane S, et al. Histone-Associated Thrombocytopenia in Patients Who Are Critically Ill. JAMA 2016;315:817-9.
351. Alhamdi Y, Zi M, Abrams ST, et al. Circulating Histone Concentrations Differentially Affect the Predominance of Left or Right Ventricular Dysfunction in Critical Illness. Crit Care Med 2016;44:e278-88.
352. Kawai C, Kotani H, Miyao M, et al. Circulating Extracellular Histones Are Clinically Relevant Mediators of Multiple Organ Injury. Am J Pathol 2016;186:829-43.
353. Zois NE, Bartels ED, Hunter I, et al. Natriuretic peptides in cardiometabolic regulation and disease. Nat Rev Cardiol 2014;11:403-12.
354. Sharma S, Jackson PG, Makan J. Cardiac troponins. J Clin Pathol 2004;57:1025-6.
355. Kalbitz M, Grailer JJ, Fattahi F, et al. Role of extracellular histones in the cardiomyopathy of sepsis. FASEB J 2015;29:2185-93.
356. Wu BU, Johannes RS, Sun X, et al. Early changes in blood urea nitrogen predict mortality in acute pancreatitis. Gastroenterology 2009;137:129-35.
357. Wildhagen KC, Wiewel MA, Schultz MJ, et al. Extracellular histone H3 levels are inversely correlated with antithrombin levels and platelet counts and are associated with mortality in sepsis patients. Thromb Res 2015;136:542-7.
358. Huang H, Evankovich J, Yan W, et al. Endogenous histones function as alarmins in sterile inflammatory liver injury through Toll-like receptor 9 in mice. Hepatology 2011;54:999-1008.
359. Brivet FG, Emilie D, Galanaud P. Pro- and anti-inflammatory cytokines during acute severe pancreatitis: an early and sustained response, although unpredictable of death. Parisian Study Group on Acute Pancreatitis. Crit Care Med 1999;27:749-55.
360. Liu ZG, Ni SY, Chen GM, et al. Histones-mediated lymphocyte apoptosis during sepsis is dependent on p38 phosphorylation and mitochondrial permeability transition. PLoS One 2013;8:e77131.
361. Friggeri A, Banerjee S, Xie N, et al. Extracellular histones inhibit efferocytosis. Mol Med 2012;18:825-33.
362. Lam FW, Cruz MA, Leung HC, et al. Histone induced platelet aggregation is inhibited by normal albumin. Thromb Res 2013;132:69-76.

363. Wildhagen KC, Garcia de Frutos P, Reutelingsperger CP, et al. Nonanticoagulant heparin prevents histone-mediated cytotoxicity in vitro and improves survival in sepsis. Blood 2014;123:1098-101.
364. Zhang Y, Zhao Z, Guan L, et al. N-acetyl-heparin attenuates acute lung injury caused by acid aspiration mainly by antagonizing histones in mice. PLoS One 2014;9:e97074.
365. Westman J, Smeds E, Johansson L, et al. Treatment with p33 curtails morbidity and mortality in a histone-induced murine shock model. J Innate Immun 2014;6:819-30.
366. Daigo K, Nakakido M, Ohashi R, et al. Protective effect of the long pentraxin PTX3 against histone-mediated endothelial cell cytotoxicity in sepsis. Sci Signal 2014;7:ra88.
367. Chaaban H, Keshari RS, Silasi-Mansat R, et al. Inter-alpha inhibitor protein and its associated glycosaminoglycans protect against histone-induced injury. Blood 2015;125:2286-96.
368. Westman J, Papareddy P, Dahlgren MW, et al. Extracellular Histones Induce Chemokine Production in Whole Blood Ex Vivo and Leukocyte Recruitment In Vivo. PLoS Pathog 2015;11:e1005319.
369. Wygrecka M, Kosanovic D, Wujak L, et al. Anti-histone Properties of C1 Esterase Inhibitor Protect Against Lung Injury. Am J Respir Crit Care Med 2016.
370. Wen Z, Lei Z, Yao L, et al. Circulating histones are major mediators of systemic inflammation and cellular injury in patients with acute liver failure. Cell Death Dis 2016;7:e2391.
371. Kowalska MA, Zhao G, Zhai L, et al. Modulation of protein C activation by histones, platelet factor 4, and heparinoids: new insights into activated protein C formation. Arterioscler Thromb Vasc Biol 2014;34:120-6.
372. Kumar SV, Kulkarni OP, Mulay SR, et al. Neutrophil Extracellular Trap-Related Extracellular Histones Cause Vascular Necrosis in Severe GN. J Am Soc Nephrol 2015;26:2399-413.
373. Zhang Y, Guan L, Yu J, et al. Pulmonary endothelial activation caused by extracellular histones contributes to neutrophil activation in acute respiratory distress syndrome. Respir Res 2016;17:155.
374. Yang X, Li L, Liu J, et al. Extracellular histones induce tissue factor expression in vascular endothelial cells via TLR and activation of NF-kappaB and AP-1. Thromb Res 2016;137:211-8.
375. Kim JE, Yoo HJ, Gu JY, et al. Histones Induce the Procoagulant Phenotype of Endothelial Cells through Tissue Factor Up-Regulation and Thrombomodulin Down-Regulation. PLoS One 2016;11:e0156763.
376. Lam FW, Cruz MA, Parikh K, et al. Histones stimulate von Willebrand factor release in vitro and in vivo. Haematologica 2016;101:e277-9.
377. Gould TJ, Lysov Z, Swystun LL, et al. Extracellular Histones Increase Tissue Factor Activity and Enhance Thrombin Generation by Human Blood Monocytes. Shock 2016;46:655-662.
378. Ekaney ML, Otto GP, Sossdorf M, et al. Impact of plasma histones in human sepsis and their contribution to cellular injury and inflammation. Crit Care 2014;18:543.
379. Donis-Maturano L, Sanchez-Torres LE, Cerbulo-Vazquez A, et al. Prolonged exposure to neutrophil extracellular traps can induce mitochondrial damage in macrophages and dendritic cells. Springerplus 2015;4:161.

380. Hsu LW, Chen CL, Nakano T, et al. The role of a nuclear protein, histone H1, on signalling pathways for the maturation of dendritic cells. Clin Exp Immunol 2008;152:576-84.
381. Rosenbluh J, Hariton-Gazal E, Dagan A, et al. Translocation of histone proteins across lipid bilayers and Mycoplasma membranes. J Mol Biol 2005;345:387-400.
382. Semeraro F, Ammollo CT, Esmon NL, et al. Histones induce phosphatidylserine exposure and a procoagulant phenotype in human red blood cells. J Thromb Haemost 2014;12:1697-702.
383. Li Y, Liu B, Fukudome EY, et al. Identification of citrullinated histone H3 as a potential serum protein biomarker in a lethal model of lipopolysaccharide-induced shock. Surgery 2011;150:442-51.
384. Iba T, Miki T, Hashiguchi N, et al. Combination of antithrombin and recombinant thrombomodulin modulates neutrophil cell-death and decreases circulating DAMPs levels in endotoxemic rats. Thromb Res 2014;134:169-73.
385. Kusano T, Chiang KC, Inomata M, et al. A novel anti-histone H1 monoclonal antibody, SSV monoclonal antibody, improves lung injury and survival in a mouse model of lipopolysaccharide-induced sepsis-like syndrome. Biomed Res Int 2015;2015:491649.
386. Kolaczkowska E, Jenne CN, Surewaard BG, et al. Molecular mechanisms of NET formation and degradation revealed by intravital imaging in the liver vasculature. Nat Commun 2015;6:6673.
387. Lee SK, Kim SD, Kook M, et al. Phospholipase D2 drives mortality in sepsis by inhibiting neutrophil extracellular trap formation and down-regulating CXCR2. J Exp Med 2015;212:1381-90.
388. Biron BM, Chung CS, O'Brien XM, et al. Cl-Amidine Prevents Histone 3 Citrullination and Neutrophil Extracellular Trap Formation, and Improves Survival in a Murine Sepsis Model. J Innate Immun 2016.
389. Caudrillier A, Kessenbrock K, Gilliss BM, et al. Platelets induce neutrophil extracellular traps in transfusion-related acute lung injury. J Clin Invest 2012;122:2661-71.
390. Zhang Y, Wen Z, Guan L, et al. Extracellular histones play an inflammatory role in acid aspiration-induced acute respiratory distress syndrome. Anesthesiology 2015;122:127-39.
391. Wen Z, Liu Y, Li F, et al. Circulating histones exacerbate inflammation in mice with acute liver failure. J Cell Biochem 2013;114:2384-91.
392. Huang H, Nace GW, McDonald KA, et al. Hepatocyte-specific high-mobility group box 1 deletion worsens the injury in liver ischemia/reperfusion: a role for intracellular high-mobility group box 1 in cellular protection. Hepatology 2014;59:1984-97.
393. De Meyer SF, Suidan GL, Fuchs TA, et al. Extracellular chromatin is an important mediator of ischemic stroke in mice. Arterioscler Thromb Vasc Biol 2012;32:1884-91.
394. Iba T, Hashiguchi N, Nagaoka I, et al. Heparins attenuated histone-mediated cytotoxicity in vitro and improved the survival in a rat model of histone-induced organ dysfunction. Intensive Care Med Exp 2015;3:36.
395. Michels A, Albanez S, Mewburn J, et al. Histones link inflammation and thrombosis through the induction of Weibel-Palade body exocytosis. J Thromb Haemost 2016;14:2274-2286.